AD_____

GRANT NUMBER DAMD17-94-J-4253

TITLE: Molecular Markers for Breast Cancer Susceptibility

PRINCIPAL INVESTIGATOR: Doctor Jeffrey M. Rosen

CONTRACTING ORGANIZATION: Baylor College of Medicine
Houston, Texas 77030

REPORT DATE: September 1998

TYPE OF REPORT: Final

PREPARED FOR: Commander
U.S. Army Medical Research and Materiel Command
Fort Detrick, Frederick, Maryland 21702-5012

REPORT DOCUMENTATION PAGE

Form Approved
OMB No. 0704-0188

1. AGENCY USE ONLY *(Leave blank)*	2. REPORT DATE	3. REPORT TYPE AND DATES COVERED
	September 1998	Final (1 Sep 94 - 31 Aug 98)

4. TITLE AND SUBTITLE
Molecular Markers for Breast Cancer Susceptibility

5. FUNDING NUMBERS
DAMD17-94-J-4253

6. AUTHOR(S)
Doctor Jeffrey M. Rosen

7. PERFORMING ORGANIZATION NAME(S) AND ADDRESS(ES)
Baylor College of Medicine
Houston, Texas 77030

8. PERFORMING ORGANIZATION REPORT NUMBER

9. SPONSORING/MONITORING AGENCY NAME(S) AND ADDRESS(ES)
Commander
U.S. Army Medical Research and Materiel Command
Fort Detrick, Frederick, Maryland 21702-5012

10. SPONSORING/MONITORING AGENCY REPORT NUMBER

11. SUPPLEMENTARY NOTES

19990405 029

12a. DISTRIBUTION / AVAILABILITY STATEMENT
Approved for public release; distribution unlimited

12b. DISTRIBUTION CODE

13. ABSTRACT *(Maximum 200*

A woman's reproductive history is one of the principal determinants of her susceptibility to breast cancer. This study was based upon the hypothesis that the protective effects of an early pregnancy and lactation result from estrogen(E) and progesterone(P)-induced differentiation and the resultant loss of cells susceptible to carcinogenesis. These effects of E and P are mediated by the induction of specific "local mediators", i. e. growth factors that act via autocrine and paracrine mechanisms to influence terminal duct(TD) and end bud(TEB) growth and differentiation. These rapidly proliferating cells are the most susceptible to neoplastic transformation. Thus, the objective of this study was to identify molecular markers for TEB and TD cells in order to follow their fate during mammary development and carcinogenesis. One of the clones identified that was preferentially expressed in the TEB fraction was p190-B a member of the Rho-GAP family of proteins involved in integrin signaling. Higher expression of p190-B was observed in the outer layer of cells of the terminal end bud. In addition, p190-B was highly expressed in approximately 40% of mouse TM and rat NMU-induced mammary tumors. Therefore, p190-B expression may be required for ductal morphogenesis during virgin mammary gland development and its aberrant expression may occur in aggressive tumors. These studies have also resulted in the application of confocal microscopy to study cell cycle kinetics in thick frozen sections derived from the mammary gland at different stages of development. Finally, a chance finding in the course of this study led to the discovery of supernumerary centrosomes in a variety of human breast tumors that correlated with over-expression of a gene known as breast tumor amplified kinase (BTAK) in 12% of human breast tumors. Antibodies raised against the 46 kDa BTAK peptide co-localized with centrosomes. This gene may directly influence genomic instability.

14. SUBJECT TERMS
Breast Cancer , Differential Display PCR, Confocal Microscopy, Terminal End Buds, Centrosomes, p190-B, Rho-GAP

15. NUMBER OF PAGES
117

16. PRICE CODE

17. SECURITY CLASSIFICATION OF REPORT	18. SECURITY CLASSIFICATION OF THIS PAGE	19. SECURITY CLASSIFICATION OF ABSTRACT	20. LIMITATION OF ABSTRACT
Unclassified	Unclassified	Unclassified	Unlimited

NSN 7540-01-280-5500

Standard Form 298 (Rev. 2-89)
Prescribed by ANSI Std. Z39-18
298-102

FOREWORD

Opinions, interpretations, conclusions and recommendations are those of the author and are not necessarily endorsed by the U.S. Army.

____ Where copyrighted material is quoted, permission has been obtained to use such material.

____ Where material from documents designated for limited distribution is quoted, permission has been obtained to use the material.

____ Citations of commercial organizations and trade names in this report do not constitute an official Department of Army endorsement or approval of the products or services of these organizations.

__√__ In conducting research using animals, the investigator(s) adhered to the "Guide for the Care and Use of Laboratory Animals," prepared by the Committee on Care and use of Laboratory Animals of the Institute of Laboratory Resources, national Research Council (NIH Publication No. 86-23, Revised 1985).

____ For the protection of human subjects, the investigator(s) adhered to policies of applicable Federal Law 45 CFR 46.

__√__ In conducting research utilizing recombinant DNA technology, the investigator(s) adhered to current guidelines promulgated by the National Institutes of Health.

__√__ In the conduct of research utilizing recombinant DNA, the investigator(s) adhered to the NIH Guidelines for Research Involving Recombinant DNA Molecules.

__√__ In the conduct of research involving hazardous organisms, the investigator(s) adhered to the CDC-NIH Guide for Biosafety in Microbiological and Biomedical Laboratories.

PI - Signature Date

TABLE OF CONTENTS

INTRODUCTION

A woman's reproductive history is one of the principal determinants of her susceptibility to breast cancer. An early full-term pregnancy is protective and the length of time between menarche and the first full term-pregnancy appears to be critical for the initiation of breast cancer. This study was based upon the hypothesis that the protective effects of an early pregnancy and lactation result from estrogen(E) and progesterone(P)-induced differentiation and the resultant loss of cells susceptible to carcinogenesis. These effects of E and P are mediated by the induction of specific "local mediators", i. e. growth factors that act via autocrine and paracrine mechanisms to influence terminal duct(TD) and end bud(TEB) growth and differentiation. These rapidly proliferating cells are the most susceptible to neoplastic transformation. No molecular markers are available to identify and follow the fate of these susceptible cells, yet this information is required to develop effective diagnostic tools and preventive therapies for breast cancer. Thus, the initial objective of this study was to identify molecular markers for TEB and TD cells in order to follow their fate during mammary development and carcinogenesis. To do so, we attempted to identify genes expressed in the TEBs of the nulliparous rat mammary. These genes could then potentially serve as molecular markers in TEB cell fate studies. In addition, we proposed to define the topology and compare stages of the cell cycle of susceptible and refractory cells, and to identify local mediators of E- and P-treatment in the end buds and surrounding stroma, and characterize the changes in their expression patterns.

BODY

Materials and Methods:

Animals:

Wistar Furth rats with an inbred genetic background were obtained from Harlan Sprague Dawley Inc. USA. Mouse tumors and cell lines were provided by Dr. Daniel Medina, Baylor College of Medicine. All animals were maintained and sacrificed according to IACUC approved guidelines.

Cell lines:

COS 1 cells were obtained from ATCC and cultured as per their recommendations. The TM12, TM2L and TM10 cell lines and TM tumors were provided by Dr. Daniel Medina(Schwartz & Medina, 1987 ; Kittrell et al., 1992)

Probes and antibodies:

A full length p190-B cDNA expression construct was a generous gift of Dr. Peter Burbelo, Laboratory of Developmental Biology, National Institute of Dental Research. The full length adrenomedullin cDNA was the kind gift of Dr. Junichiro Sakata, First Department of Internal Medicine, Miyazaki, Japan. Rabbit polyclonal antibodies for p190-B were raised against two synthetic peptides and were affinity purified. The secondary antibody and peroxidase conjugated antibodies were purchased from Santa Cruz Biotechnology.

Cell culture and transfection:

In order to obtain cells expressing p190-B, 5 μg of plasmid DNA containing a neomycin resistance gene and 5 μg of stuffer plasmid DNA were co-transfected into COS1 cells using the lipofectamine reagent (Boehringer Mannheim). After 5-8 hrs the transfection medium was supplemented with medium containing 20% fetal bovine serum(FBS). The media was replaced after 18 hrs with fresh media containing 10% FBS . Cells were harvested after 24hrs and stored at -80 ^{o}C until analyzed.

Preparation and analysis of RNA:

The fourth inguinal mammary glands from virgin, pregnant and lactating rats were dissected under anesthesia using standard surgical procedures. Tissue was snap frozen in liquid nitrogen and stored at -80^{o}C. Total cellular RNA was prepared using 4M guanidium isothiocynate and CsCl buoyant density centrifugation (Maniatis, 1988). RNA was fractionated on a 1.2% formaldehyde agarose gel and transferred to Hybond N+ (Amersham) membrane with 10X SSC. Hybridization was performed in Hybaid oven at 65^{o}C using procedures recommended by Amersham.

Screening of high density blots by Reverse Northern:

1. **Synthesis of ^{32}P-labeled cDNA probe**: Double stranded ^{32}P-labeled cDNA was synthesized from 5 -6 μg of total RNA from EB (end bud), mid-gland and stromal fractions of the virgin mammary gland using superscript II RT (Gibco BRL) in the presence of 1 μg of oligo dT12- 18mer primers as per manufacturer's instructions. The cDNA was hydrolysed by NaOH treatment and neutralized with HCl treatment. The labeled cDNA was then purified through a G50 column. The efficiency of the reaction was monitored by determining total radioactivity incorporated before and after purification of the probe.

2. **Generation of high density cDNA blots and hybridization**: A total of 15 DD-PCR clones were subjected to PCR amplification. After amplification, a fixed amount of each of the PCR product was loaded onto high density gels in triplicate (Centipede gel electrophoresis chambers: Owl Scientific, Woburn, MA). PCR products were alkali denatured in the gel and blotted onto nylon membranes.. The filters were hybridized under stringent conditions (7% SDS in 0.5 M NaPO4, pH 7.2,) with equivalent amounts of ^{32}P-labeled double stranded cDNA from EB, mid-gland and stromal portions of the virgin mammary gland. The probes were of approximately equal specific activity. The filters were washed under stringent conditions and quantitated using the Phosphorimager. In addition, the filters were exposed to high resolution Kodak Biomax MR films for up to 24 hr at -80°C.

***In situ* Hybridization**:

Probe synthesis: Riboprobes were labeled with ^{33}P (Amersham), using the appropriate T3 or T7 transcription systems from Stratagene. The probe was purified by ammonium acetate precipitation and counted in a scintillation counter.

Pretreatment of slides and hybridization: The fourth inguinal mammary glands from virgin Wistar Furth rats were excised and immediately fixed for 3 hr in ice cold 4% paraformaldehyde in phosphate buffered saline(PBS), dehydrated in a graded series of ethanols to

xylene and embedded in paraffin wax. Sections of 7μm were mounted on ProbeOn Plus slides (Fisher Biotech). Sections were baked overnight at 37°C, dewaxed through xylene and rehydrated through a graded series of ethanols to PBS. Following digestion with proteinase K (20 μg/ml, Sigma) at 50°C for 5 min, the sections were refixed in 4% paraformaldehyde/PBS for 5 min. The sections were then acetylated in 100mM triethanolamine, 25mM acetic anhydride and dehydrated through ethanols. Sections were prehybridised in 2X SSC, 50% formamide, 10% dextran sulfate, 1% SDS and 500 ng/ml denatured herring sperm DNA at 37°C in a sealed humidified chamber. ^{33}P-labeled nucleotide probes were added to 25 μl of hybridization solution and was then added to the solution already covering the section.. The sections were hybridized overnight at 42°C in a sealed humidified chamber.

Preparation of protein extracts and Western blot analysis:

Protein extracts were prepared by lysing the cells in RIPA buffer (Upstate Biotechnology, Lake Placid, NY), followed by pre-cleaning and protein concentration determination (Bio-Rad). For Western blot analysis, 50-100 μg of protein extract from transfected cells or tissue was subjected to electrophoresis through a 6% PAGE-SDS gel. Proteins were electroblotted to PVDF membranes. Filters were blocked with 3%NFDM in TBST and incubated for 1 hr with affinity purified polyclonal antibody for p190-B diluted (1:1000) in blocking buffer. This was followed by incubating the blot with secondary antibody (goat anti rabbit) diluted (1:2000) in blocking buffer. Detection was performed with the enhanced chemiluminescence detection system (Pierce Chemicals).

Cell kinetics:

Mammary glands representing additional positive controls were excised from 104 day old virgin rats. BrdU (50 μg/kg) was injected i.p. at 104 days of age and animals were sacrificed at 4 hr intervals during the following 28 hr period.

An additional 30 rats were subjected to double exposure to MNU at 97 and 104 days and then divided into two subgroups. Subgroup 1 received BrdU injections at 104 days and their mammary glands collected every 4 hrs for 28 hrs. Subgroup 2 received BrdU injections at 109 days and their mammary glands collected every 4 hrs for 28 hrs.

All mammary glands were frozen at -80°C, sectioned on a cryomicrotome at 50 μm thickness, and collected on washed glass slides. The sections were permeabilized by treatment with 0.5% Triton-X 100 in PBS for 4 min at RT. The tissue slices were then fixed in 4% formaldehyde in PBS for 15 min at RT. After treatment with 2.5N HCl at room temperature for 40 min to denature the DNA, the slices were stained with mouse-anti-BrdU antibodies (Boehringer Mannheim) and rabbit anti-keratin 14 (1:500) at 37°C for 3 hrs.

After washing, the samples were incubated with a mixture of three secondary antibodies (FITC-conjugated anti-mouse; a goat-anti-rabbit FITC conjugated anti-K14; and an RITC conjugated goat anti-rabbit antibody). The latter combination of antibodies at a 1:1 mixture produces yellow color in myoepithelial cells. The tissue slices were then stained with propidium iodide (1 μg/ml). This combination of treatments produces a tri-colored histological preparation that enables us to identify and analyze the proliferative compartment of the mammary gland (S-phase cells are green, all other nuclei are red and the myoepithelial cells are stained yellow). The slides were examined by a laser scanning confocal microscope (Molecular Dynamics), operating at an optical section step size of 5 μm thickness. The images are recorded as TIFF or JPG files for cell cycle scoring.

Combination BrdU/Histone H3 staining for mitotic cells:

In order to determine complete cell parameters, it is necessary to score the percentage of BrdU-positive mitotic cells following an earlier pulse with BrdU. Until recently, this was not possible using confocal microscopy. This limitation was overcome by staining cryosections of rat mammary glands with a new mitosis-specific antibody made against the phosphorylated form of the amino terminus of histone H3 (anti-H3) obtained from Dr. C. David Allis (University of Rochester). Following the anti-BrdU step described above, the slides were washed and exposed

to the anti-H3 (1:1000 in PBS plus 1% BSA for 3 hrs). After washing, the samples were treated with Texas Red-labeled goat anti-rabbit IgG. Using this scheme, BrdU-labeled nuclei are green, mitotic cells are red, and BrdU-labeled mitotic cells are yellow.

Centrosome amplification as a marker for genome instability:

Centrosome replication is a useful marker for identifying cells in the cell cycle and for detecting early stages of genome instability (Fukasawa et al., 1996). We adapted this technique for analyzing the cells of the rat mammary gland as well as MNU-induced mammary tumor cells. Cryosections of mammary glands and tumors were obtained as described earlier. In addition to the other antibodies, the sections were incubated with SPJ anti-centrosome serum provided by Dr. Ron Balczon (University of South Alabama) at a dilution of 1:500 for 3 hrs at 37^{o}C, followed by exposure to FITC-goat-anti-human IgG for 3 hrs at 37^{o}C. Scoring was accomplished by counting the number of stained nuclei and the corresponding number of centrosomes in sections of both mammary gland and tumor.

Results and Discussion:

Isolation of TEB specific genes:

The initial objective of this study was to isolate molecular markers that are specific to TEB. A large repertoire of techniques are now available to identify the differential expression pattern of genes between two cell types. Differential display PCR (DD-PCR) is one such method that relies on the use of random primers in conjunction with one of four anchored oligo-dT primers that anneal to a subset of mRNA's . The mRNA population defined by the oligo pairs is amplified by PCR and the resulting products resolved by denaturing polyacrylamide gel electrophoresis. The difference in band intensity of a PCR product between the RNA populations under study, would be a measure of their differential expression.

As described in earlier reports , a total of 14 clones were originally identified by DD-PCR (Table 1). The RNA expression levels of EDD-C3, C6, C11, C14, C15, C18, G5, G6 and G7 were analyzed by RT-PCR to confirm if they were predominantly expressed in the TEB RNA. Four clones; EDD-G5, G6, G7 and C18 were more highly expressed in the TEB RNA.

Interestingly, EDD-G6, G7 and C18 are clones which were originally isolated from a DD-PCR experiment in which two separate RNA pools were used for duplicate PCR runs. These results looked promising, however there were problems with variability of clone expression between the individual RNA preparations and could be attributed to variation in the amount of ductal and stromal contamination in the original pooled dissection fractions used for RNA isolation.

To further confirm these results, we followed the expression of DD-PCR clones by "Reverse Northern" where a fixed amount of each of the amplified DD-PCR clone was run on high density gels and was probed with reverse transcribed radiolabelled cRNA probes. Unlike conventional Northern analysis, in this technique the cDNA clones are blotted onto nylon membranes and probed with reverse transcribed cRNA probes. The abundance of a transcript in the RNA used for reverse transcription should determine the signal intensity on the blot. This method was employed because of the relatively low abundance and the difficulty in obtaining the large amounts of poly A RNA from microdissected TEB fractions required for Northern blot or RNAse protection analyses. The reverse Northern analysis confirmed the overexpression of G-7 (71% homologus to Gene Bank clone KIAA0089) and C-2 (87% homology to p190-B) in the Terminal End Bud fraction as shown earlier by RT-PCR but failed to corroborate the overexpression of EDD clone G-5 (Figure 1). G5 expression instead was higher in mid-gland and stromal RNA samples. EDD-G5, was originally identified as an Expressed Sequence Tag (EST). It has 90% homology to a novel mammalian LDL receptor termed LR11. It is, therefore, likely that its expression may be higher in stromal and glandular regions of the mammary gland. Even using Phosphoimager quantitation some of the clones did not provide a significant signal over background and were still below the level of detection.

While some of the clones identified by DD-PCR may be false positives or potentially less interesting, e.g. cytochrome C oxidase, the three clones G7, G5 and C2 that were preferentially expressed in the TEB fraction were further analyzed by Northern blotting of RNA isolated from the mammary gland at different stages of development and other tissues and tumors. However, when these DD-PCR clones that were only 241 and 108 bp in length were employed as probes for

Northern blot analyses, the signal to noise ratio was not sufficient to detect specific transcripts in total RNA preparations. Although we were previously able to detect expression of these clones in the virgin mammary gland using RT-PCR this technique was not amenable to quantitative studies in the absence of appropriate internal standards. Thus of the 14 clones originally identified and sequenced, two clones with 87% and 98% homology to known genes, were selected for detailed analysis because of their potential importance in mammary gland development. These are discussed in the following sections.

Northern analysis to follow the fate of p190-B gene transcripts during mammary development and carcinogenesis:

One of the clones that was found to be preferentially expressed in TEB fraction was p190-B. p190-B belongs to the Rho-GAP family of proteins and has many cousins, the closest being p190-A. p190-B encodes a protein, which is involved in relaying information from outside of a cell through adhesion molecules called integrins to the inside. The process is mediated by a class of proteins called RhoGTPases. The GTP bound form of Rho is the active form and is responsible for bringing about cytoskeletal reorganization. Since p190Rho-GAPs enhance the conversion of GTPRho to GDPRho, they negatively regulate cytoskeletal assembly and have a role in cell motility and invasion.

The expression of p190-B was analyzed in various adult rat tissues and in mammary glands of Wistar Furth rats at different developmental stages. RNA from p190-B transfected COS 1 cells was used as a positive control. As expected from earlier results (Burbelo, et al., 1995), p190-B was found to be expressed in several adult tissues including lung, liver, kidney, brain and heart. It is expressed at much lower levels in ovary and uterus. Interestingly, p190-B was not only expressed in mammary gland, but was differentially expressed during mammary development. The highest expression was detected in the virgin mammary gland of 45 day and 120 day old rats, the time at which TEB activity is maximal. The mRNA level declined by lactation (Fig 2). Since 20% of the mRNA at this stage of development encodes β-casein , it is likely that p190-B mRNA is decreased due to a dilution effect. However, when the level of p190-B mRNA was compared

relative to keratin 18 (K-18) mRNA, a marker for ductal and alveolar epithelial cells, the relative expression of p190-B was lower than that obtained for virgin or pregnant glands, indicating that it was in fact decreased during late pregnancy and lactation.

Based on our observation that p190-B was expressed at higher levels in the mammary glands at stages representing increased proliferation, i.e. 45-day virgin and early-mid-pregnancy, and was decreased at late pregnancy, we have also performed a preliminary analysis of its expression in a limited number of established mouse mammary hyperplasia outgrowth lines, TM tumors(Kittrell et al., 1992; Schwarz and Medina, 1987) and primary rat nitrosomethylurea(NMU)-induced tumors. p190-B mRNA was overexpressed in both hyperplasias and tumors (Fig 3A & B). p190-B levels in TM tumors were compared to RNA isolated from the mouse mammary gland at day 13 of pregnancy. The level of p190-B expression ranged from 0.5- to 8 -fold. In contrast, the level ranged from 2- to 100-fold in NMU tumors as compared to RNA isolated from the mammary gland of virgin mice at 45 days of age, the time at which the carcinogen was given. The significance of this apparent overexpression in hyperplasias and tumors remains to be determined, but may reflect their increased invasive potential.

Localization of p190-B by *in situ* hybridization:

None of the techniques discussed so far has permitted a conclusive identification of the cell types expressing specific RNA transcripts. Thus both non-radioactive (digoxygenin, DIG) and radioactive *in situ* hybridization techniques were optimized to be used to detect transcripts in the rat mammary gland from virgin mice. The major problem encountered with these techniques is the ability to identify scarce mRNA transcripts at sufficient resolution to localize them at the cellular level. Initially, *in situ* RT-PCR (IS-PCR) of differential display clones was attempted to localize mRNA expression to specific cell types in the virgin gland. However, there was little success in the virgin mammary gland due to high background staining in the nucleus possibly due to DNA and the use of rTth polymerase. We then tried more conventional methods of *in situ* hybridization using ^{35}S-UTP-labeled riboprobes. However, once again there was excessive background, so it was not possible to distinguish the signal for rare transcripts against the noise. This problem was

circumvented with the use of ^{33}P-labeled cRNA probes. Using this technique, the highest concentration of p190-B mRNA was once again localized to the invading terminal end buds (Fig 4 A). The stroma, ducts and alveolar buds were all shown to express p190-B, but at much reduced levels (Fig 4 B &C). Similar results were obtained with the DIG technique (data not shown).

Thus, p190-B gene expression appears to be increased during the proliferating stages of mammary gland development and in rodent tumors and to decrease with progressive differentiation. In addition, *in situ* hybridization has shown that the highly proliferative outer layer of cells in the TEB in particular display the highest expression of this gene. These results suggest that p190-B may normally play a role in mammary gland development by facilitating the invasion of the terminal end buds into the surrounding fat pad. Aberrant expression may occur in different tumor types thus facilitating invasion and potentially metastasis.

Detection of p190-B protein in the mammary gland:

Since p190-B belongs to the family of Rho-GAP proteins and is recruited to the sites of integrin clustering, it was necessary to develop reagents to study the localization and activation of p190-B protein in the virgin mammary gland. In order to detect p190-B expression in the mammary gland extracts of Wistar Furth rats by Western blotting, antisera were generated against two different peptides from the carboxy-terminus (amino acid regions 1018 - 1033, peptide-1 and amino acid 1130 - 1145, peptide-2) of human p190-B. This region is absolutely conserved between rats and human. The antibodies were affinity purified and titrated by ELISA. Of the two antibodies, the rabbit polyclonal antibody against peptide-2 was of higher affinity. Accordingly, only this antibody was employed for further studies.

The specificity of the antibody was determined by assaying p190-B expression in COS 1 cells transiently transfected with a p190-B expression vector. This provided the positive control necessary to characterize these affinity-purified rabbit polyclonal antipeptide antibodies. The peptide-2 antibody recognized the expected 190 kDa protein with an additional 60kDa cross-reactive protein(Fig 5A). The expression of the p190-B protein was also detected in non-transfected cells, although at a decreased level, possibly because COS 1 cells are derived from

kidney cells of African green monkey, a tissue known to highly express p190-B. The specificity of the antibody was demonstrated by competition by peptide-2(Fig. 5B), but not by peptide-1(Fig. 5C). We also detected p190-B expression in extracts of the mammary gland of a rat at day 6 of pregnancy, and of the kidney (data not shown). The protein is expressed in both tissues, although in much lower levels than the transfected COS 1 cells.

Using the same antipeptide antibody we next analyzed the expression of p190-B in virgin mammary gland using both immunohistochemical and immunofluorescence staining. Although, all the ductal structures of the mammary gland exhibit nuclear p190-B staining, the outer layer of Terminal End Bud shows stronger immunostaining. This localization is in agreement with the previous *in situ* results. However, unexpectedly this staining appeared predominantly in the nuclei (Fig 6 A, B, D). The staining could, however, be competed by pre-incubating the antibody with the specific peptide (Fig 6C). Since p190-B expression in fibroblasts has been shown to be predominantly around focal adhesions, the significance of the nuclear localization needs to be confirmed by independent methods. Furthermore, these results need to be interpreted with caution since the antipeptide antibody also detects a cross-reactive band of 60 kDa. We are therefore, currently, trying to modify the p190-B expression construct by including a hemagglutinin(HA) epitope tag that will permit the analysis of the subcellular localization of p190-B in transfected mammary epithelial cells under different culture conditions using a anti-HA antibody.

As the outer layer of terminal end bud is covered by mostly myoepithelial cells, the p190-B expression pattern was also compared with myoepithelial markers keratin-14 (K-14) and maspin, which is expressed in both myoepithelial and luminal epithelial cells. From the staining pattern it appears that the p190-B expressing cells are not the myoepithelial cells (data not shown).

Both the RNA and protein expression data support a role for p190-B in invasion and possibly metastasis. Thus based upon these studies our hypothesis is that p190-B facilitates cell invasion by orchestrating the ECM-mediated integrin signals through Rho proteins. In the future we propose to test this hypothesis both by using an *in vitro* cell culture model where we can study

the effect of gain-of- function and loss-of-function mutants, and most importantly *in vivo* by generating a mammary gland-specific knock out of this gene.

Expression of adrenomedullin mRNA in the mammary gland:

EDD-C12 is rat adrenomedullin, a secreted peptide factor that is expressed in a variety of tissues (lung, heart, kidney, brain and mammary gland) and a potent vasodilator. Polyclonal antiserum and peptide antigen to adrenomedullin were obtained from Dr. Frank Cuttitta at the NIH. The rabbit polyclonal antiserum was generated against the most C-terminal 30 amino acids of the adrenomedullin active peptide (116-146 a.a.). This antiserum reacts with the 18 kDa proprotein, a 14 kDa intermediate form and the 6 kDa active peptide. The polyclonal antiserum was employed to determine the temporal and spatial expression of adrenomedullin in the mammary gland by immunohistochemistry. As reported previously in the year 2 progress report, immunohistochemistry was performed with fixed sections of rat mammary glands from various time points throughout mammary development. Adrenomedullin was localized to the cytoplasm of epithelial and stromal cells of the virgin gland. Staining was most prominent in TEB and ductal epithelium. However, staining was also detected in the alveolar buds, stroma, blood vessels and lymph node. This adrenomedullin staining could be competed with the adrenomedullin peptide but not with a nonspecific peptide. In the mammary gland from mice at day 12 of pregnancy, adrenomedullin expression was pronounced throughout the cytoplasm of alveoli, ducts and stroma. Interestingly, at 18 days of pregnancy adrenomedullin was localized to the nucleus and cytoplasm of alveoli and cells of the stroma. Nuclear staining was also observed in lactating (2 days) and involuting (3 days) tissue but to a lesser extent. The cytoplasmic staining of the epithelium and stroma also continued through lactation and involution. In all cases, adrenomedullin staining could be competed with the specific peptide.

Because adrenomedullin is a secreted growth factor that can act in both a paracrine and autocrine manner we wanted to complement these studies of immunolocalization to determine the levels of adrenomedullin mRNA in the mammary gland at different stages of development. Once again, we were fortunate to obtain a full length cDNA probe from Dr. J. Sakata. As reported

previously, adrenomedullin mRNA was found to be universally expressed with kidney, heart and ovary showing the highest expression(data not shown). Moderate expression was seen in brain and virgin mammary gland, and uterus, lung and liver show low levels of expression. The mRNA appears to be slightly down-regulated during lactation. In order to determine which cell types are synthesizing adrenomedullin mRNA during mammary gland development it will be necessary to complement these studies with *in situ* hybridization analysis. To accomplish this goal the full-length cDNA will be cloned into a vector to generate both sense and antisense ^{33}P-riboprobes for *in situ* hybridization.

Estrogen and Progesterone Regulation of Local Growth Factors:

The regulation of the Wnt and Fgf growth factor families by steroid hormones appears to play an important role in mammary tumorigenesis and breast cancer. We have studied steroid hormone regulation of Wnt gene expression in intact and progesterone-receptor knockout (PRKO) mice. Mouse mammary gland development has also been examined in PRKO mice using reciprocal transplantation experiments to investigate the effects of the stromal and epithelial PRs on ductal and lobuloalveolar development (Humphreys et al., 1997). The absence of PR in transplanted donor epithelium, but not in recipient stroma, prevented normal lobuloalveolar development in response to estrogen and progesterone treatment. Conversely, the presence of PR in the transplanted donor epithelium, but not in the recipient stroma, revealed that PR in the stroma may be necessary for ductal development. Stimulation of ductal development by the progesterone receptor may, therefore, be mediated by a unknown secondary signaling molecule, possibly a growth factor. The continued stimulation of the stromal PR appears to be dependent on reciprocal signal(s) from the epithelium, and in the PRKO mouse this feedback loop is interrupted. Thus, the combination of gene knockout and reciprocal transplantation technologies has provided some new insights into the role of stromal-epithelial interactions and steroid hormones in mammary gland development. Wnt-2 gene expression was maximal in the mammary stroma of 4-6 week old mice and was repressed by estrogen, while Wnt-5b is expressed in lobuloalveolar cells and is dependent upon the presence of intact PR in the epithelium.

Definition of topology and cell cycle analysis by confocal microscopy:

Topology and Cell Cycle. The research completed in this proposal has achieved two major goals regarding this task. We developed and perfected a procedure that enabled us to analyze cell architecture, topology, and cell cycle parameters in thick (25-50 μm) cryosections of rat mammary glands from control and hormone (estrogen plus progesterone) treated animals. Much of our progress was spent working out the technical details, but the procedure we perfected enables the investigator to analyze multiple cell layers within terminal end buds, alveolar buds, and ducts using laser scanning confocal microscopy. Moreover, by including a three-color staining process, we can determine cell cycle parameters in individual cells including duration in S-phase, labeling index (LI), growth fraction (GF) and mitotic index in the mammary gland. Much of this task has been completed as reported in previous progress reports and the procedure will provide three-dimensional analysis of cell-cell interactions and cell kinetic data in various compartments of the TEB and other areas where proliferation is occurring. At the time of this report, we have completed cell cycle analysis on 45- and 104- day old rats and have processed and collected tissues on the following experiments.

Supernumerary Centrosomes in Breast Cancer:

Perhaps one of the most significant achievements in this project evolved from an unexpected finding. We utilized an autoimmune serum containing antibodies directed against the major microtubule organizing center (MTOC) in cells to detect centrosomes in rat mammary gland cells. Our initial aim was to use the centrosome staining technique to determine stages in the cell cycle of individual mammary gland cells *in situ*. From previous studies in our laboratory, we knew that each cell receives one centrosome at the completion of mitosis such that cells in G_1 or G_0 can be expected to contain a single fluorescent spot when examined by fluorescence microscopy. Since centrosomes divide in S-phase, each cell in late S, G_2 and M contains a double centrosome. This approach worked very well in conjunction with BrdU staining to score individual cells, but provided a much more significant finding. While normal mammary gland cells contained the

expected number of centrosomes, we noted that tumor cells generally contained extra centrosomes (supernumerary centrosomes). In addition to our findings, several other laboratories published similar findings *in vitro* and *in vivo* (Fukasawa et al., 1996; Wang et al., 1998; Lingle et al., 1998; and Pihan et al., 1998). Examples of centrosome profiles and fluorescent staining in normal and breast tumors in rats are shown in Fig. 6. Centrosome number is determined by visual scoring of fluorescent spots in tissues in double blind experiments and plotted frequency on a bar graph. Cells with 1-2 centrosomes are normal and those with greater than 2 are supernumerary. Centrosomes correlate with genomic instability in tumor cells because of their role in establishing the mitotic spindle and chromosome segregation. Cells with supernumerary centrosomes arise due to mitotic errors caused by multiple spindle poles. This correlation can be seen in Fig. 7 showing centrosome profiles from a variety of rat mammary tumors as correlated with genomic stability and determined by BrdU incorporation. Animals A-D produced mammary tumors with diploid nuclei, while those represented by E-I were aneuploid. All animals were treated with NMU for 33-36 weeks. Some received E+P while others received no hormone treatment. Another potentially important finding was the appearance of supernumerary centrosomes in TEB epithelial cells from animals treated with NMU many weeks before the appearance of tumors (Fig. 2A) whereas, animals made refractory to NMU after treatment with E+P displayed a normal centrosome profile (Fig. 7B).

Our results in rat tumors, and reports of supernumerary centrosomes in human breast tumors by others, stimulated us to collaborate with Dr. Subrata Sen at The University of Texas M. D. Anderson Cancer Center in Houston to examine human breast cancer cells using the technique worked out here. We not only confirmed the finding of supernumerary centrosomes in a variety of human breast tumors, but discovered that over-expression of a gene known as breast tumor amplified kinase (BTAK) in 12% of human breast cancers was directly involved in centrosome amplification and aneuploidy. Antibodies raised against the 46 kDa BTAK peptide co-localized with centrosomes. Amino acid sequence revealed conservation of twelve kinase-specific domains in BTAK with 40% and 48% sequence identity to a similar serine/threonine kinase in *S. cerevisae*

(Ipl1) and *Drosophila* (aurora). When the BTAK gene was transiently transfected into NIH 3T3 and MCF7 cells, centrosome amplification and subsequent aneuploidy was noted (a manuscript by Zhou et al., 1998 is in press).

CONCLUSIONS

At the time these studies were initiated over four years ago DD-PCR was the method of choice to use to identify candidate genes that might be preferentially expressed in the Terminal End Bud fraction, and may, therefore, have a role in mammary development and cancer. One limitation of this approach was the requirement for manual dissection of TEB, mid-gland and stromal fractions from trypan blue injected mammary glands and the use of pooled tissue from approximately ten rats to isolate sufficient amounts of RNA. Thus, the TEB and mid-gland fractions were always contaminated with stroma and to some extent with each other. If this project were to be initiated today it should possible to use the recently developed technique of laser microdissection to isolate specific cell types without significant cross-contamination. This would be followed by cDNA library generation and sequencing of 10,000 cDNAs similar to the current Cancer Genome Anatomy Project underway at the National Cancer Institute. Using this approach it may be feasible to identify stem cell specific markers, if such cells exist in this population.

Despite this limitation, these studies have identified p190-B as a potentially interesting gene involved in integrin signaling and cell invasion that appears to be expressed preferentially in the TEB. p190-B gene expression was found to be increased in proliferating tissues like virgin mammary gland and was also overexpressed in a subset of rat and mouse mammary tumors. Future studies are designed to determine the function of p190-B in normal mammary gland development and breast cancer.

These studies have also resulted in some technical innovations to permit the detection of RNA transcripts by *in situ* hybridization and most importantly protein localization by confocal microscopy in thick frozen sections derived from the mammary gland at different stages of development. This led to the observation of supernumerary centrosomes in breast tumors. These studies may lead to the discovery of new targets and pathways in the mechanism of carcinogenesis

that may, in turn, lead to new genetic targets and appropriate drugs for the therapy of tumors with chromosomal instability. These findings that have been derived from this basic research project on rat mammary gland development appear to have opened up exciting new vistas for future breast cancer research.

Finally, at the time of the initiation of these studies it was assumed that the protective effect of pregnancy was the net result of pregnancy hormone-induced differentiation with the resultant loss of terminal end buds. However, this hypothesis has been questioned by the recent unpublished results of S. Nandi(personal communication) in which mammary gland differentiation induced by treating rats with perphenazine did not elicit the same protection from carcinogenesis observed with estrogen and progesterone treatment. Thus, the protective effects of pregnancy may be attributed to permanent changes, both systemic and those that may occur in the mammary gland in response to estrogen and progesterone treatment or a full term pregnancy, and not just the loss of the TEB. To address this issue, experiments are in progress to employ subtractive suppressor hybridization in concert with high throughput screening and gene arrays to identify genes that may be differentially expressed in E+P-treated versus their age- matched virgin mice.

FIGURE LEGENDS

Fig. 1. Reverse northern screening of DD-PCR clones. Triplicate filters were hybridized with oligo-dT primed, ^{32}P-labeled reverse transcribed cRNA from TEB, mid-gland and stroma fractions of the virgin mammary gland. The blots were exposed to Phosphorimager overnight. The results were quantitated using the software Image-quant (Molecular Dynamics) and plotted as arbitrary relative volume units/μg RNA. The data have been normalized with respect to their GAPDH expression. (n=4)

Fig. 2. p190-B is differentially expressed during mammary development. Total cellular RNA (20 μg) from the fourth inguinal mammary glands of 45 day virgin, 120 day virgin, 12 day pregnant, 18 day pregnant, 2 day lactating and 10 day lactating rats were probed with p190-B cDNA. The blots were exposed to the Phosphorimager overnight and the results were

quantitated using the software Image-quant (Molecular Dynamics). The data are plotted in arbitrary relative volume units/μg RNA normalized for K18 expression, a marker for epithelial cell proliferation during development.

Fig. 3. Detection of p190-B expression in mouse and rat mammary tumors and cell line A. Total cellular RNA(20 μg) isolated from TM tumors were analyzed for p190-B expression using Northern blotting. Total cellular RNA from a mouse mammary gland at day 13 of pregnancy was used for comparison (lane 1). **B:** Total cellular RNA(20μg) isolated from rat NMU tumors was analysed for p190-B expression using Northern blotting. Total cellular RNA from a virgin rat mammary gland at day 45 was used for comparison.

Fig. 4. *In situ* localization of p190-B gene expression. Paraformaldehyde-fixed paraffin-embedded virgin mammary glands of Wistar Furth rats at 45 days of age were employed. A. Bright field illumination of a Terminal End Bud showing strong hybridization to the antisense probe. B. Mid gland area with only a marginal signal over background using an antisense probe. C. Ducts and alveolar buds also show poor hybridization to the antisense probe. D. A serial section probed with sense probe. All photographs were taken at 20X magnification.

Fig. 5. Western blotting with p190-B antisera. Lysates from nontransfected (NT) and transfected (T) COS-1 cells were resolved on 6% SDS-PAGE and blotted onto PVDF membranes as described in Materials and Methods. Filters were cut into strips and either A) incubated with antibody to p190-B B). incubated with Ab to p190-B that was competed with its specific peptide prior to incubation or C). incubated with Ab to p190-B that was competed with a non-specific peptide.

Fig. 6. Immunohistochemical staining of rat virgin mammary gland with antipeptide Ab against p190-B. A survey photomicrograph of Terminal End Bud (top panels) and alveolar buds (bottom right). Strong staining is observed in the cells lining the end buds and alveolar buds. A. Terminal end bud staining, 20X magnification. B. Same section at 40X. C. staining with peptide competed Ab. D. Alveolar bud staining, 40X magnification.

Fig. 7. Confocal microscopic images of normal stroma, TEB and NMU-tumors. The centrosomes are shown as yellow-green dots adjacent to red nuclei. The myoepithelial cells (green) of the TEBs are stained with anti-keratin to differentiate them from the inner bud cells. The bar graph below shows the quantitative distribution of centrosomes in each of the cell types.

Fig 8. Rat mammary tumor cells showing centrosomes (green dots) adjacent to nuclei. The cells in (a) are mostly diploid while those in (b) are largely aneuploid. Plotted below are centrosome profiles from nine rat mammary tumors. Tumors A-D are near diploid while those from E-I are mostly aneuploid.

Fig. 9. Centrosome alterations correlate with carcinogen-suceptible and refractory states. In A and B are mammary glands from NMU-treated animals that were refractory following E+P treatment and contained one or two centrosomes, while those in C and D are susceptible animals that were treated with NMU alone; note multiple centrosomes in the latter. Centrosome profiles in E show distribution of centrosomes from stromal cells in animals that were refractory (H19-S) and susceptible (A-19S) and from TEB cells from animals that were refractory (H19) and susceptible (A19).

Figure 1

Differential Expression of DD-PCR clones between terminal end buds, mid-gland and fat fractions of the rat virgin mammary gland

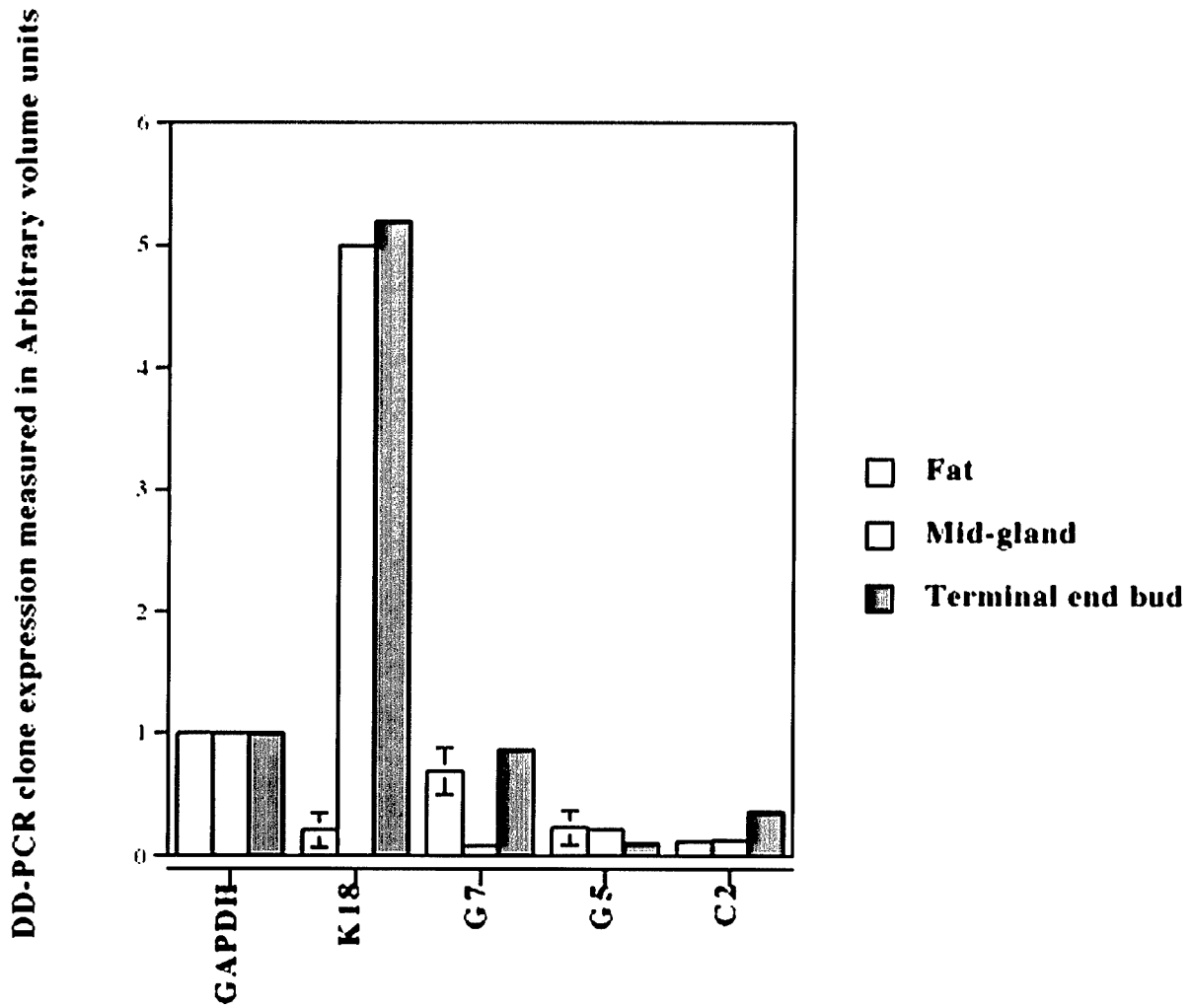

Figure 2

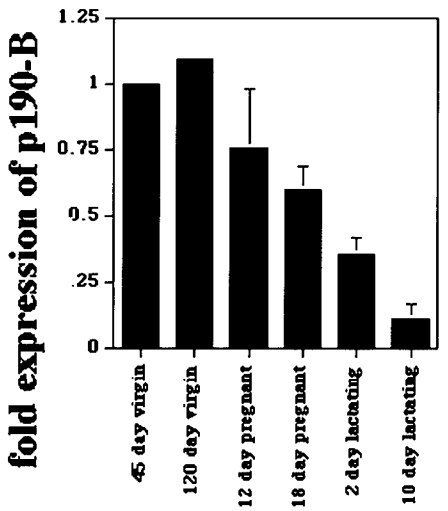

Figure 3

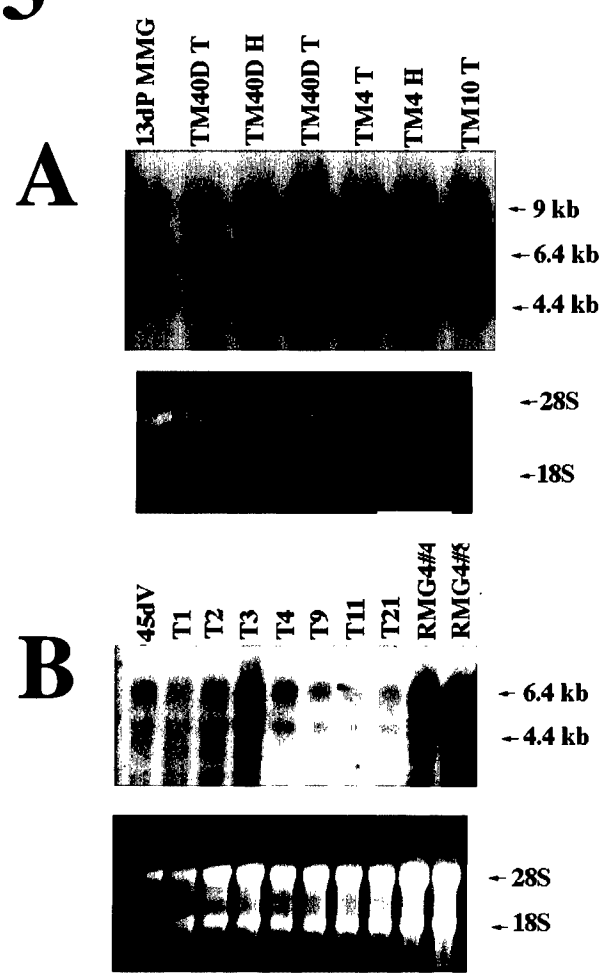

Localization of p190-B mRNA by in situ hybridization

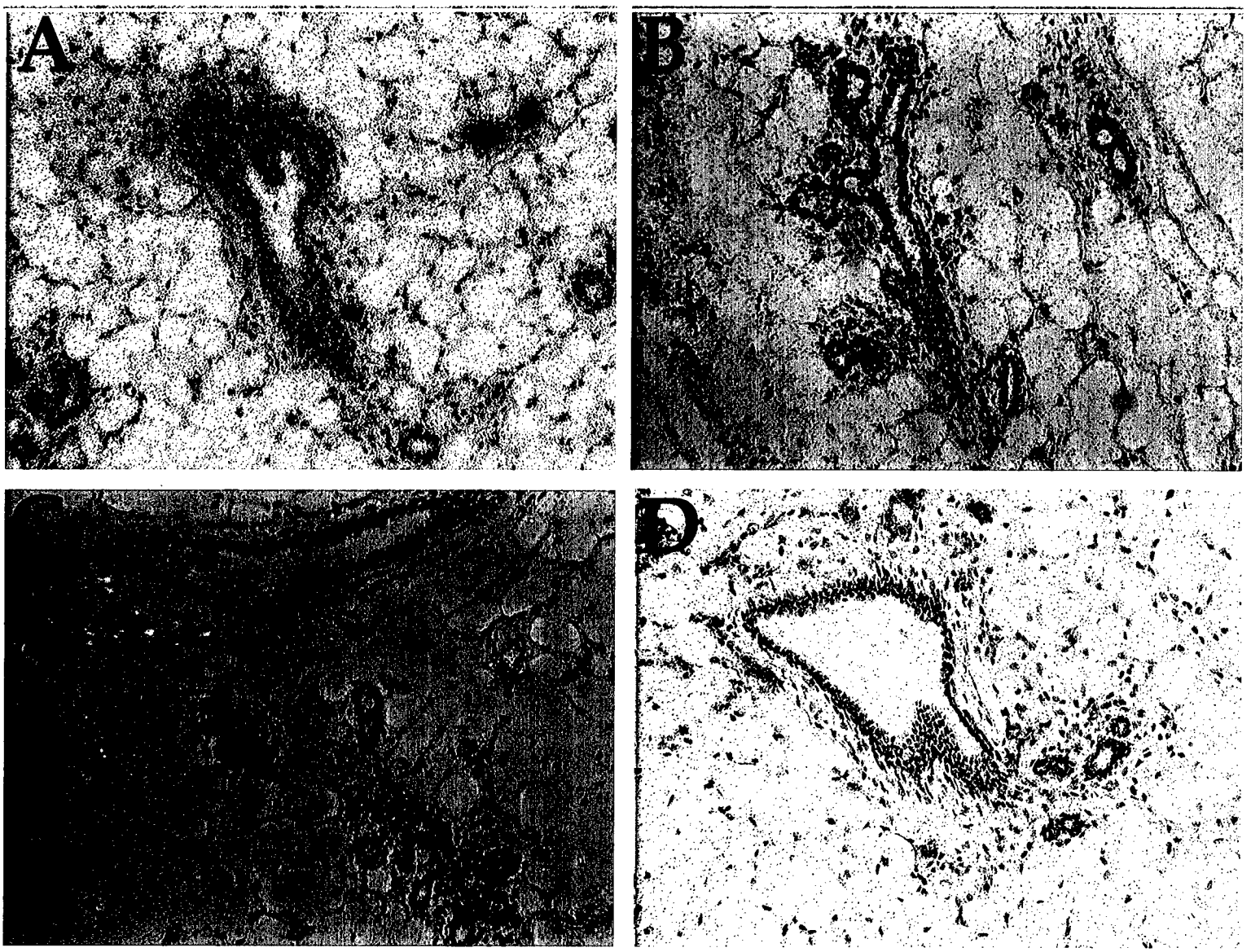

Figure 4

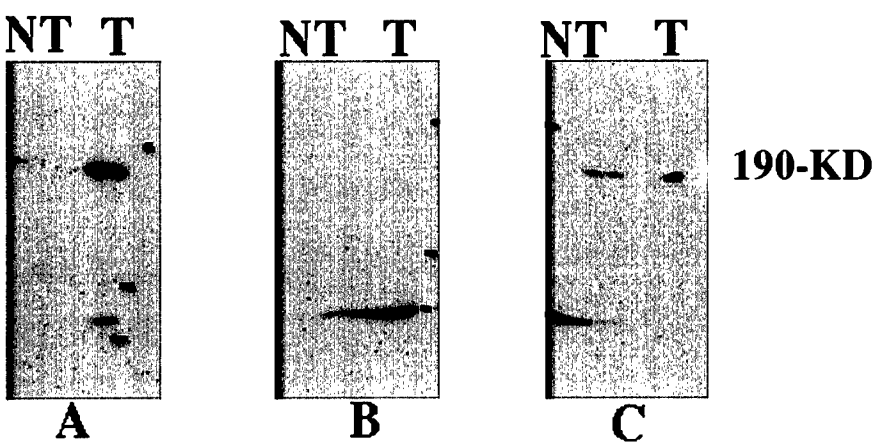

Figure 5

Immunohistochemical localization of p190-B

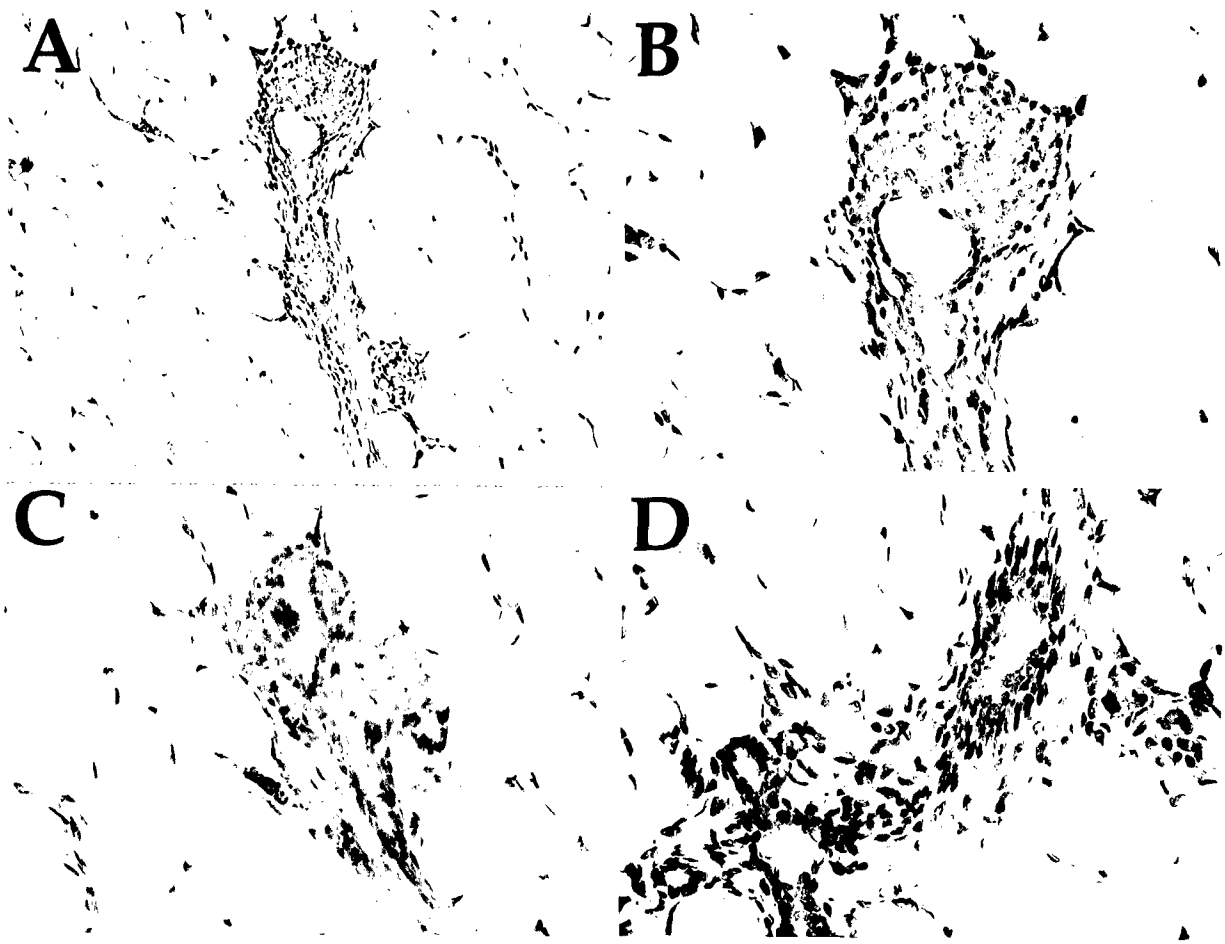

Figure 6

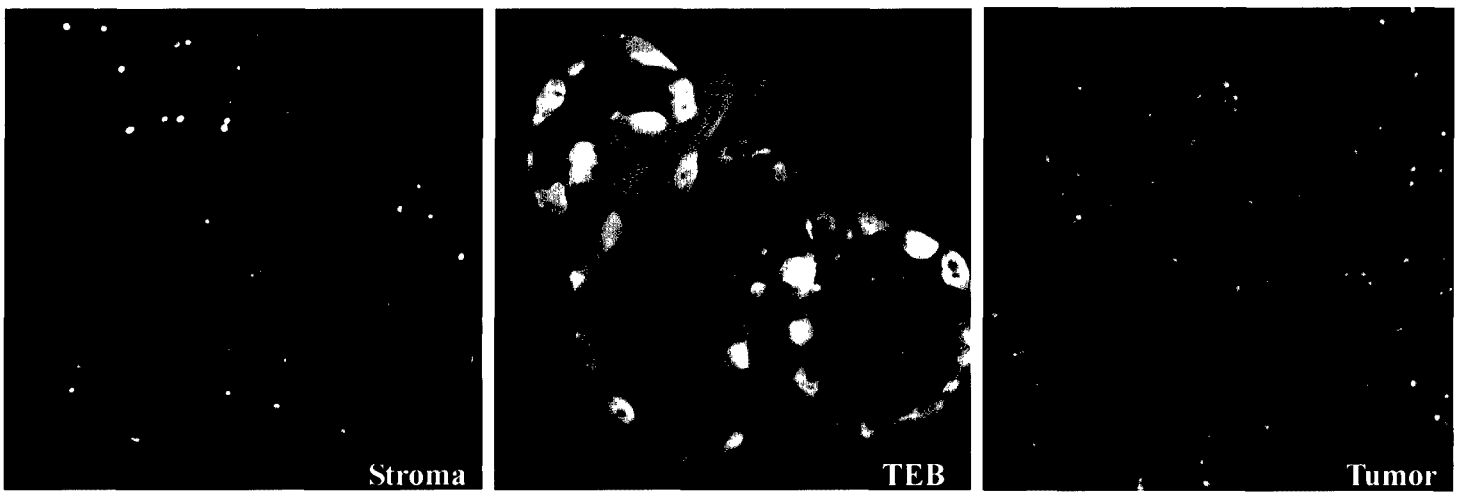
Stroma
TEB
Tumor

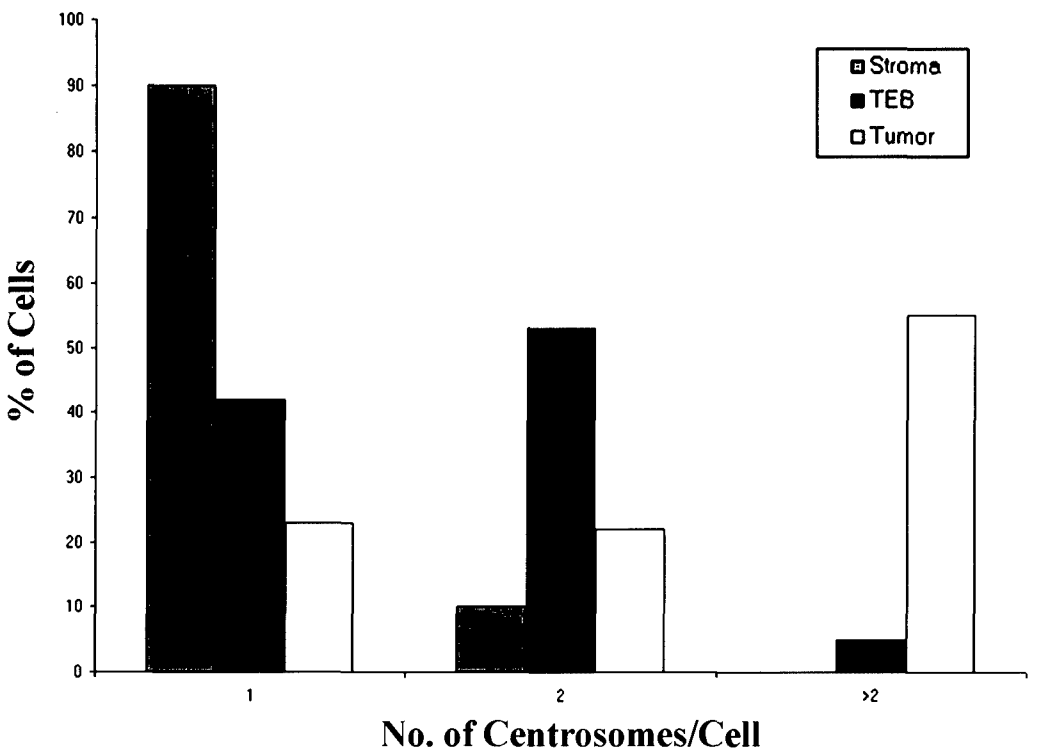
Stroma
TEB
Tumor
% of Cells
100
90
80
70
60
50
40
30
20
10
0
1
2
>2
No. of Centrosomes/Cell

Figure 7

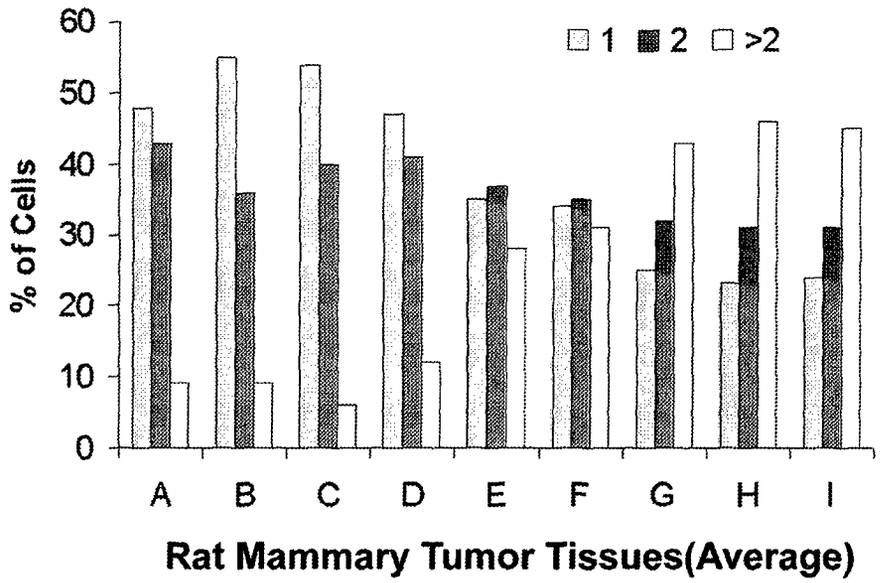
60
50
40
30
20
10
0
% of Cells
1
2
>2
A
B
C
D
E
F
G
H
I
Rat Mammary Tumor Tissues(Average)

Figure 8

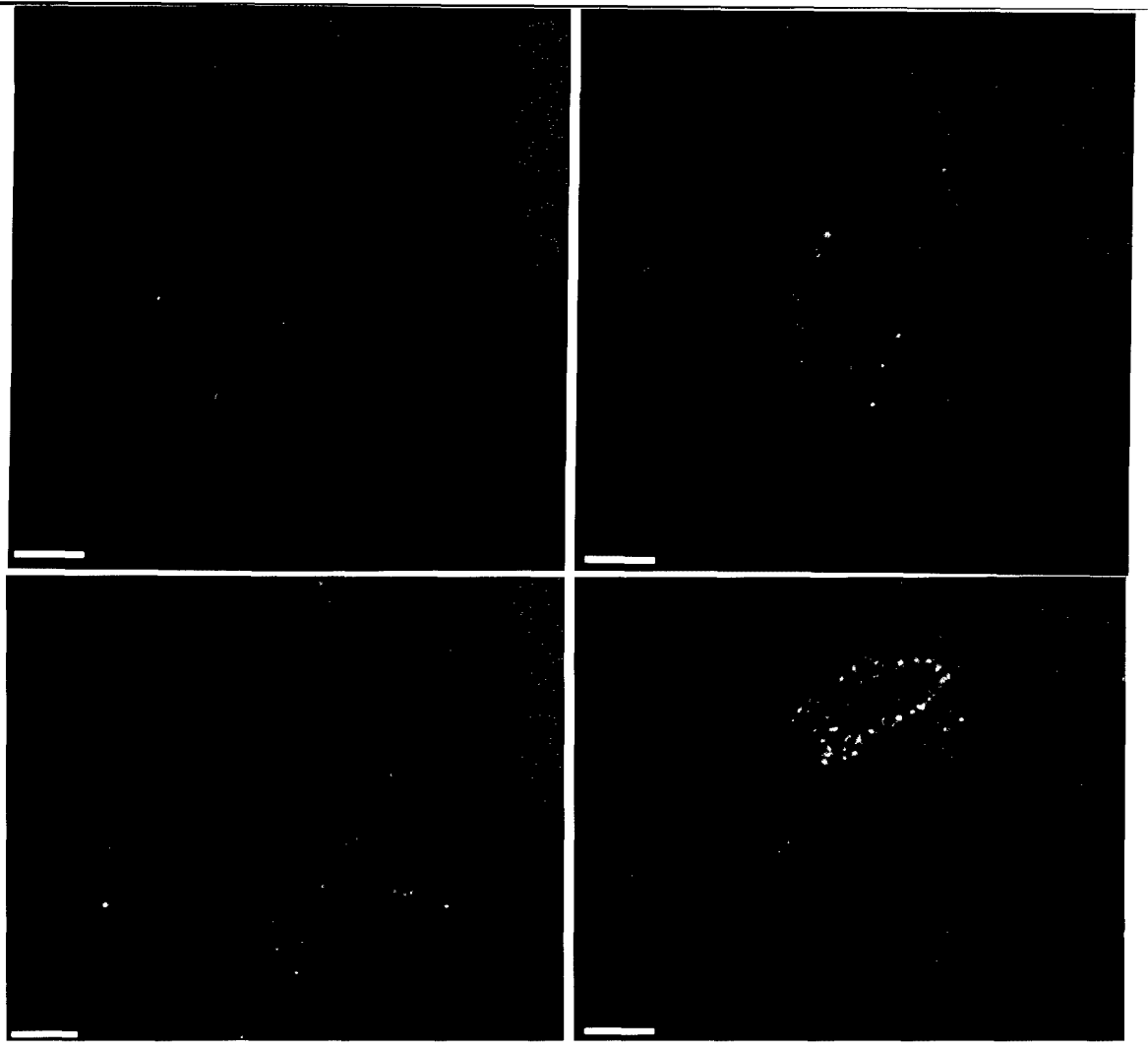

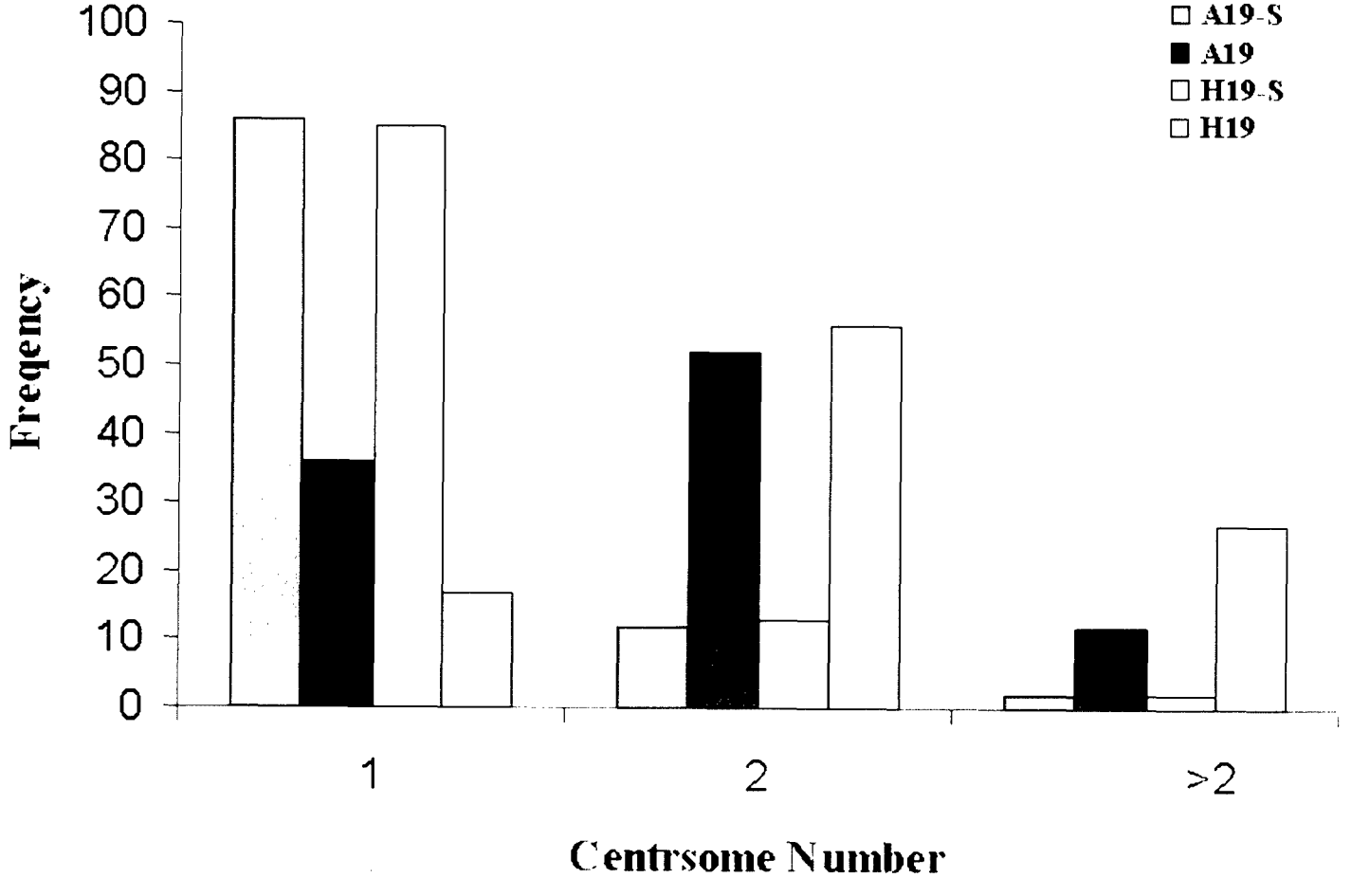
A19-S
A19
H19-S
H19
100
90
80
70
60
50
40
30
20
10
0
Freqency
1
2
>2
Centrsome Number

Figure 9

REFERENCES

1. Balczon, R., Bao, L., Zimmer W. E., Brown, K., Zinkowski, R. P. and Brinkley, B. R., 1995. Dissociation of centrosome replication events from cycles of DNA synthesis and mitotic division in hydroxyurea-arrested Chinese hamster ovary cells. J. Cell Biol. 130:105-115.

2. Burbelo, P.D., Miyamoto, S., Utani, A, Brill, S., Yamada, K.M., Hall, A. and Yamada, Y. 1995 p190-B, a new member of the Rho GAP family, and Rho are induced to cluster after integrin cross-linking. J. Biol. Chem. 270:30919-30926.

3. Fukasawa, K., Choi, T., Kuriyama, R., Rulong, S. and Vande Woude, G. F., 1996. Abnormal centrosome amplification in the absence of p53. Science 271: 1744-1747.

4. He, D. and Brinkley, B.R., 1997. Dynamics of Cell Proliferation in Rat Mammary Glands in 3-D: Analysis by Confocal Microscopy. (in preparation)

5. Hendzel, M. J., Wei, Y., Mancini, M. A., Van Hooser, A., Ranalli, R., Brinkley, B. R., Bazett-Jones, D. P., and Allis, C. D., 1997. Mitosis-specific phosphorylation of histone H3 initiates primarily within pericentromeric heterochromatin during G2 and spreads in an ordered fashion coincident with mitotic chromosome condensation. Chromosoma (in press).

6. Humphreys, R.C., Lydon, J., O'Malley, B.W. and Rosen, J.M. 1997. Mammary gland development is mediated by both stromal and epithelial progesterone receptors. Mol. Endocrinol. 11:801-811.

7. Kittrell, F.S., Oborn, C.J. and Medina, D. 1992. Development of mammary neoplasias in-vivo from mouse mammary epithelial cells in-vitro. Cancer Res. 52 1924 - 1932.

8. Schwartz and Medina, D. Characterization of the DIM series of BALB/C preneoplasms for mouse mammary tumor virus mediated oncogenesis. 1987. Cancer Res. 47 : 5707 - 5714.

9. Lingle, W. L., Lutz, W. H., Ingle, J. N., Maihle, N. J. and Salisbury, J. L. (1998). Centosome hypertrophy in human breast tumors: Implications for genomic stability and cell polarity. Proc. Natl. Acad. Sci. USA. 95:6950-6955.

10. Pihan, G. A., Purohit, A., Wallace, J., Knecht, H., Woda, B., Quesenberry, P. and Doxsey, S. J. (1998). Centrosome defects and genetic instability in malignant tumors. Cancer Res. 58:3974-3985.

11. Wang, X.-J., Greenhalgh, D. A., Jiang, A., He, D., Zhong, L., Medina, D. Brinkley, B. R. and Roop, D. R. (1998). Expression of a p53 mutant in the epidermis of transgenic mice accelerates chemical carcinogenesis. Oncogene 17:35-45.

12. Zhou, H., Kuang, J., Zhong, L., Che, S., Wagh, A., Kuo, W.-L., Gray, J. W., Zhao,S., Sahin, A., Brinkley, B. R., and Sen, S. (1998). Tumor amplified mitotic kinase STK15/BTAK induces centrosome amplification, aneuploidy and transformation. Nature Genetics (in press).

PUBLICATIONS

1. Humphreys, R.C., Rosen, J.M. (1997). Stably transfected HC11 cells provide an *in vitro* and *in vivo* model system for studying Wnt gene function[1]. Cell Growth Diff. 8:839-849.

2. Humphreys, R.C., Lydon J., O'Malley, B.W., Rosen, J.M. (1997). Mammary gland development is mediated by both stromal and epithelial progesterone receptors. Mol. Endocrinol. 11:801-811.

3. Humphreys, R.C., Lydon, J.P., O'Malley, B.W., Rosen, J.M. (1997). Use of PRKO mice to study the role of progesterone in mammary gland development. J. Mammary Gland Biol Neoplasia 2(4):343-354.

4. Hooser, A.V., Brinkley, B.R. (1998). Methods for *in situ* localization of proteins and DNA in the centromere-kinetochore complex. Methods in Cell Biology 61:57-80.

5. Brinkley, B.R., Goepfert, T.M. (1998). Supernumerary centrosomes and cancer: Boveri's hypothesis resurrected. Cell Motility and the Cytoskeleton (in press).

ABSTRACTS

Rosen, J.M., Roy, D., Contreras, A., He, D., Zhong, L., Brinkley, W. (1997). Molecular markers for breast cancer susceptibility. The Department of Defense Breast Cancer Research Program Meeting, Era of Hope. Proceedings, Volume II, 479.

Chakravarty, G., Roy, D., Zhong, L., Rosen, J.M. (1998). Differential expression of p190-B during mammary gland development, involution and carcinogenesis. American Association for Cancer Research Meeting 38, 400.

LIST OF PERSONNEL

Jeffrey Rosen
Deana Roy
Cara D. Boyles
Geetika Chakravarty
Deanna E. Dowlin
Maria Gonzalez-Rimbau
Susanne Krnacik
Rebecca A. Scott
Juddi C. Yeh

William (B.R.) Brinkley
Thea Goepfert
Dacheng He
Ling Zhong
Maureen G. Mancini
Ilia Ouspenski
Almas Papusha

APPENDICES

Humphreys, R.C., Rosen, J.M. (1997). Stably transfected HC11 cells provide an *in vitro* and *in vivo* model system for studying Wnt gene function[1]. Cell Growth Diff. 8:839-849.

Humphreys, R.C., Lydon J., O'Malley, B.W., Rosen, J.M. (1997). Mammary gland development is mediated by both stromal and epithelial progesterone receptors. Mol. Endocrinol. 11:801-811.

Humphreys, R.C., Lydon, J.P., O'Malley, B.W., Rosen, J.M. (1997). Use of PRKO mice to study the role of progesterone in mammary gland development. J. Mammary Gland Biol Neoplasia 2(4):343-354.

Hooser, A.V., Brinkley, B.R. (1998). Methods for *in situ* localization of proteins and DNA in the centromere-kinetochore complex. Methods in Cell Biology 61:57-80.

Brinkley, B.R., Goepfert, T.M. (1998). Supernumerary centrosomes and cancer: Boveri's hypothesis resurrected. Cell Motility and the Cytoskeleton (in press).

Rosen, J.M., Roy, D., Contreras, A., He, D., Zhong, L., Brinkley, W. (1997) Molecular markers for breast cancer susceptibility. The Department of Defense Breast Cancer Research Program Meeting, Era of Hope. Proceedings, Volume II, 479.

Chakravarty, G., Roy, D., Zhong, L., Rosen, J.M. (1998) Differential expression of p190-B during mammary gland development, involution and carcinogenesis. American Association for Cancer Research Meeting 38, 400.

Stably Transfected HC11 Cells Provide an *in Vitro* and *in Vivo* Model System for Studying *Wnt* Gene Function[1]

Robin C. Humphreys and Jeffrey M. Rosen[2]

Department of Cell Biology, Baylor College of Medicine, Houston, Texas 77030

Abstract

The *in vitro* and *in vivo* effects of several Wnt family members have been studied using stably transfected HC11 cells, a clonal mammary epithelial cell line derived from a midpregnant mouse mammary gland capable of hormone-dependent differentiation *in vitro*. Differential effects of Wnt-1, Wnt-2, and Wnt-7B expression were observed both on the morphology of confluent HC11 cells and on the pattern of E-cadherin expression. Wnt-7B had no apparent effect on HC11 cell morphology or E-cadherin expression, as compared to mock-transfected HC11 cells. Injection of stably transfected pools of Wnt-1, Wnt-2, Wnt-7B, and mock-transfected cells into the cleared fat pad of syngeneic BALB/c mice generated reproducible outgrowths after 8 or 12 weeks. Mock-transfected cells produced outgrowths that exhibited some morphologically normal ductal and alveolar-like structures. However, no morphologically normal structures were observed in the fat pads containing Wnt-transfected cells. Instead, these outgrowths were characterized by significant fibrosis, epithelial hyperplasia, and multiple sites of growth. In contrast to the lack of an observed effect *in vitro*, palpable adenocarcinomas were observed 12 weeks after injection of the Wnt-7B-transfected HC11 cells. These tumors contained significant regions of hyperplastic and transformed epithelium and lacked the fibrotic phenotype observed in the Wnt-1 and -2 outgrowths. These results support the hypothesis that different Wnt family members may elicit distinct functional effects and reinforce the need to perform simultaneous comparisons of Wnt function both *in vitro* and *in vivo*. Stably transfected HC11 cells provide a useful model system in which to elucidate the function of different Wnt family members.

Received 11/6/96; revised 1/28/97; accepted 6/2/97.

The costs of publication of this article were defrayed in part by the payment of page charges. This article must therefore be hereby marked *advertisement* in accordance with 18 U.S.C. Section 1734 solely to indicate this fact.

[1] This work was supported by NIH Grant CA16303 and U.S. Army Medical Research and Materiel Command Grant DAMD17-94-J-4253 (to J. M. R.).

[2] To whom requests for reprints should be addressed, at Department of Cell Biology, Baylor College of Medicine, One Baylor Plaza, Houston, TX 77030. Phone: (713) 798-6210; Fax: (713) 798-8012; E-mail: jrosen@bcm.tmc.edu.

Introduction

Both hormonal and developmental status are known to be important factors in the etiology of breast cancer. Such hormonal and developmental cues are often mediated at the molecular level by a combination of systemic hormones and locally acting growth factors. Because of their expression pattern in the mammary gland and their established functions in development, the *Wnt* genes are good candidates for locally acting growth factors. As with other growth factors, aberrant regulation of Wnt-mediated signaling pathways may play an important role in the initiation and progression of breast cancer.

The proto-oncogene *Wnt-1*, first identified as activated by MMTV[3] proviral integration in mammary tumors, is the progenitor of a family of related genes that are highly conserved and expressed in both invertebrates and vertebrates (1–3) The *Wnt* gene family, of which there are at least 15 murine members, has been shown to affect the development and transformation of the mammary gland. In addition to Wnt-1, Wnt-3, Wnt-10B, and several Fgf family members are also activated by MMTV proviral insertion in mammary tumors (4–8). Transgenic mice overexpressing Wnt-1 display epithelial hyperplasia, significant stromal synthesis, and an apparent loss of hormone-dependent growth (9, 10). Primary mammary epithelial cells infected with a retrovirus expressing either Wnt-1 or Wnt-4 exhibit cellular hyperplasia and a pregnancy-like phenotype when transplanted into a cleared mammary fat pad in virgin mice (11, 12). In addition, expression of several *Wnt* genes, including *Wnt-2*, *Wnt-3*, *Wnt-4*, *Wnt-5A*, and *Wnt-7B*, has been found in breast tumors and a number of other human malignancies (13–16).

In vitro studies have revealed that Wnt-1, Wnt-2, Wnt-3A, Wnt-5B, Wnt-7A, and Wnt-7B can morphologically transform C57MG mammary epithelial cells with varying efficiencies (17). These results and direct mRNA injection studies in *Xenopus* (18) have suggested that there are several classes of Wnts possessing separate functional domains. Interestingly, some of the *Wnt* genes that cause transformation *in vitro* and *in vivo*, with the exception of *Wnt-1*, *Wnt-3A*, and *Wnt-7A*, are expressed in unique temporal and spatial patterns during normal mouse mammary gland development (19–21). The function of these endogenous *Wnt* genes during mammary gland development is unknown. Thus, aberrantly expressed Wnts may usurp the signaling pathways normally regulated by Wnts during mammary gland development, resulting in transformation. Unfortunately, no correlation has been demonstrated between *in vitro* "morphological" transformation efficiency and transformed phenotypes in the mammary gland.

[3] The abbreviations used are: MMTV, mouse mammary tumor virus; Fgf, fibroblast growth factor.

The Wnt signaling pathway has been elucidated primarily by epistasis experiments in *Drosophila* (22). A candidate Wnt receptor, (Dfz2) frizzled, has been recently identified (23). Dfz2 is epistatic to dishevelled (*dsh*), zeste white-3 (*zw3*), a serine threonine kinase, and armadillo (*arm*), the homologue to the mammalian β-catenin. β-Catenin is known to interact with the intercellular adhesion molecule E-cadherin (24–26). Biochemical experiments have demonstrated that one of the consequences of Wnt action is an increase in the pool of free β-catenin and the alteration of intercellular adhesion. Aberrant E-cadherin expression may facilitate increased tumor invasiveness, providing a possible mechanism for the transforming action of the *Wnt* genes. In addition, another role for β-catenin in the nucleus has been recently identified (27, 28). Lef-1, an HMG box transcription factor with DNA bending activity, has been shown to interact with β-catenin in the cytoplasm and to "piggyback" β-catenin into the nucleus, where it may modify transcription of a number of genes, including decreasing that of E-cadherin to provide an autoregulatory feedback system (29).

HC11 is a clonal mammary epithelial cell line that is derived from spontaneously immortalized COMMA-D epithelial cells, isolated from the mammary gland of midpregnant BALB/c mice (30). HC11 cells have been used extensively to study the hormonal regulation of mammary epithelial cell differentiation and *casein* gene expression (31–33). When grown at confluence for several days after exposure to certain growth factors, such as epidermal growth factor, and then treated with the lactogenic hormones, prolactin, hydrocortisone, and insulin, HC11 cells can be induced to express the milk protein, β-casein. In addition, these cells have been used to study the effects of oncogene expression on the mammary epithelial cell differentiation *in vitro* (34–40). Transplantation of HC11 cells transfected with certain oncogenes, such as *erbB-2*, has resulted in tumors in nude mice, but successful transplantation and growth of stably transfected HC11 cells into the cleared fat pad of syngeneic mice has not been reported.

This study reports the outgrowth of stably transfected HC11 cells *in vivo* in the fat pads of syngeneic mice, permitting a correlation of the *in vitro* and *in vivo* effects of *Wnt* gene expression. Several different Wnts were studied: Wnt-1, which is not normally expressed in the mammary gland except as a function of MMTV proviral activation, and two other Wnts, Wnt-2 and Wnt-7B, which are expressed primarily in virgin BALB/c mice during normal mammary gland development but not in HC11 cells. These experiments demonstrated that E-cadherin expression and cellular morphology were affected by Wnt-1 and Wnt-2 (but not Wnt-7B) expression *in vitro* but that all three Wnts can generate fibrotic outgrowths after transplantation of HC11 cells stably transfected with Wnt expression constructs into the cleared fat pad of BALB/c mice. Surprisingly, transplanted HC11 cells expressing Wnt-7B developed palpable tumors after 12 weeks.

Results

Wnt-1 and Wnt-2 Alter the Three-Dimensional Morphology of Hyperconfluent HC11 Cells. HC11 cells were chosen for studies of Wnt function because it has been demonstrated previously that stably transfected HC11 cells respond to lactogenic hormones when grown at confluence for several days, during which time they secrete laminin and interact with extracellular matrix (30, 31, 35). Therefore, HC11 cells represent one of the few nontransformed, clonal mammary epithelial cell lines. When grown at confluence for more than 16 days, HC11 cells form spherical structures that are evenly spaced and of a consistent size (Fig. 1*D*) and are somewhat reminiscent of the mammospheres formed by primary mouse mammary epithelial cells when they are grown at appropriate densities on an extracellular matrix. These structures were not observed in HC11 cells containing Wnt-1 or Wnt-2 expression constructs (Fig. 1, *A* and *B*). Wnt-1 transfectants failed to form any spherical structures; instead, they generated disorganized piles of cells that often exhibited elongated attachments between cells (Fig. 1*A*). Wnt-2-transfected HC11 cells formed enlarged and distorted clumps of cells, as seen in Fig. 1*B*. Wnt-7B transfectants did not disrupt the ability of HC11 cells to form three-dimensional structures, as illustrated in Fig. 1*C*. No obvious changes in cellular morphology were observed in subconfluent HC11 cells or in cells maintained at confluence for less than 7 days.

Wnt-1 and Wnt-2 Transfected HC11 Cells Have Altered E-Cadherin Staining Patterns. Wnt signaling is known to affect the stability of the E-cadherin-β-catenin complex and adhesion between adjacent epithelial cells (41), primarily through E-cadherin. To determine whether the inability to form higher-order structures in Wnt-1- and Wnt-2-expressing HC11 cells was reflected by the loss of E-cadherin at the adherens junctions, the pattern of E-cadherin staining was examined in Wnt- and pBKCMVneo (mock)-transfected cells using an specific antibody to E-cadherin and indirect immunofluorescence. Wnt-1-transfected HC11 cells, as shown in Fig. 2*A* (*top right panel*), exhibited a disrupted pattern of E-cadherin staining reflected by a significantly lower level of E-cadherin staining at the junctions between adjacent cells. In Wnt-2 transfected cells, E-cadherin staining at cell junctions was still evident, but the uniform staining pattern was disrupted; instead, a stellate pattern was observed (Fig. 2*A, bottom right panel*). Wnt-7B-transfected cells did not exhibit any obvious disruption of E-cadherin staining, as compared to the mock-transfected controls in Fig. 2*A* (*bottom left* and *top left panels*, respectively).

An antibody to the myc epitope, present at the COOH termini of each Wnt expression construct, detected punctate Wnt expression, primarily in the cytoplasm of the stably transfected HC11 cells, possibly reflecting the sorting of the protein into vesicles, which is consistent with their role as secreted growth factors (Fig. 2*B*: *top*, Wnt-1; *bottom*, Wnt-2; Ref. 42). Expression was observed in all of the cells stably transfected with the Wnt expression constructs, both at confluence and during exponential growth. A similar pattern was observed for Wnt-7B-transfected cells, and no expression was detected in the mock-trans-

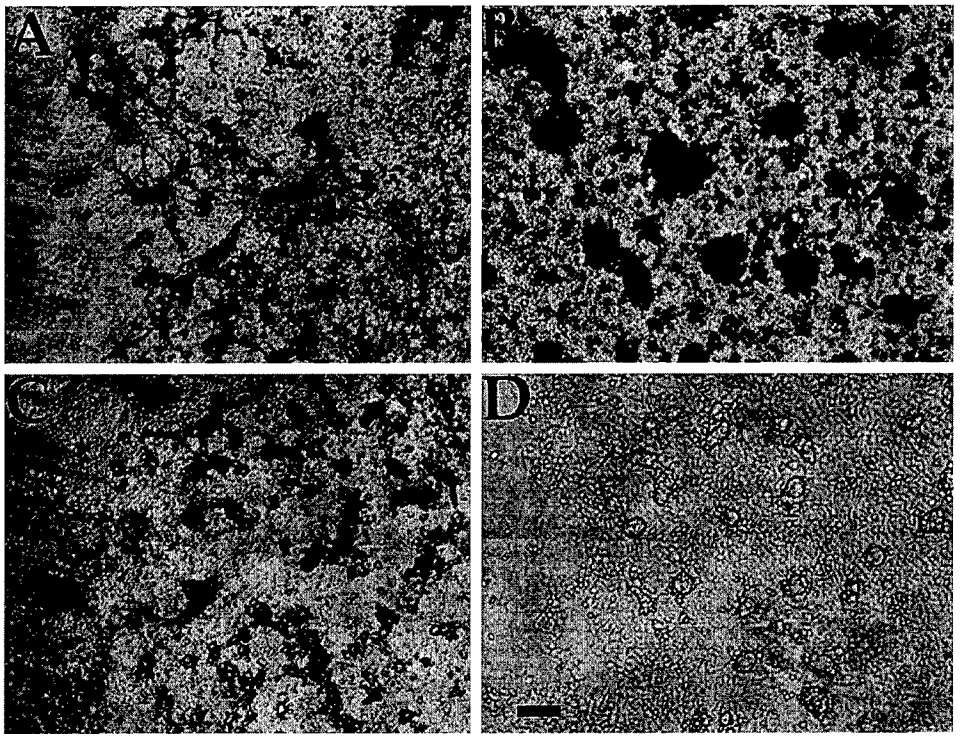

Fig. 1. Wnt transfection of HC11 cells affects three-dimensional morphology. Wnt-transfected HC11 cells were grown at confluence for 18 days under G418 selection. Unfixed, Wnt-1-, Wnt-2-, Wnt-7B-, and mock-transfected HC11 cells (*A*, *B*, *C*, and *D*, respectively) were photographed with phase contrast *in vitro*. *Scale bar*, 2 mm.

fected HC11 cells (data not shown). These results suggested that transfection of HC11 cells with Wnt-1 or Wnt-2 expression constructs may disrupt three-dimensional cellular morphology by modifying the pattern of E-cadherin expression at the adherens junctions. Examination of the E-cadherin staining pattern in hyperconfluent transfected cells was unsuccessful because the three-dimensional structures prevented a clear definition of intercellular junctions.

Wnt-Transfected HC11 Cells Generate Fibrotic Outgrowths *in Vivo*. Murine mammary epithelium has the unique ability to recapitulate the entire mammary ductal structure from a fragment of epithelium or from immortalized epithelial cell lines when transplanted or injected, respectively, into the cleared fat pad of a syngeneic host (43). This capability was used to examine the effects of Wnt transfection on mammary gland development. Freshly harvested pools of Wnt- and mock-transfected HC11 cells (5×10^5 cells/10 μl) were injected into the cleared fat pad of number 4 mammary glands of syngeneic BALB/c mice and allowed to grow for 8 weeks. At 8 weeks, 10 of 10 injected mammary glands produced outgrowths of different sizes in the Wnt-1-, Wnt-7B-, and mock-transfected cells (Table 1). Additionally, in the fat pads injected with Wnt-2 transfected cells, 8 of 10 glands generated outgrowths. A second set of animals that were injected with a subsequent passage of cells and allowed to grow for 12 weeks replicated this high proportion of successful outgrowths. This is the first report of HC11 cells being transplanted back into the fat pad of a syngeneic host generating epithelial growth, although there have been anecdotal reports of transplanted HC11 cells producing outgrowth and tumors in the fat pad.[4]

Whole mount staining of these outgrowths with hematoxylin revealed that the fat pads injected with Wnt-transfected HC11 cells contained outgrowths that were distributed throughout the mammary glands in various locations distal to the injection site (Fig. 3). This was not observed in the fat pads injected with mock-transfected HC11 cells. The outgrowths in these fat pads were usually centered around the injection site and did not fill the fat pad, as is usually observed in transplantation experiments with normal mammary epithelium. The mock-transfected outgrowths, however, possessed some morphologically normal structures. In Fig. 3*D*, ductal- (arrow) and alveolar-like structures can be observed. This result was not unexpected because HC11 cells are derived from a midpregnant gland. No morphologically normal structures were observed, however, in the fat pads containing Wnt-transfected cells. These outgrowths had a generally feathery appearance and lacked any obvious normal morphological structures (Fig. 3, *A–C*).

Examination of Masson's trichrome-stained sections revealed that outgrowths derived from Wnt-transfected cells were composed of hyperplastic epithelium encased in a thick, collagenous fibrosis (Fig. 4). Collagen was the major component of these outgrowths, as evidenced by the bright blue staining in all of the sections (Fig. 4, *C–H*). Fat pads with Wnt-7B-transfected cells produced the largest outgrowths with the densest collagen. HC11 cells are a spontaneously

[4] G. Smith, personal communication.

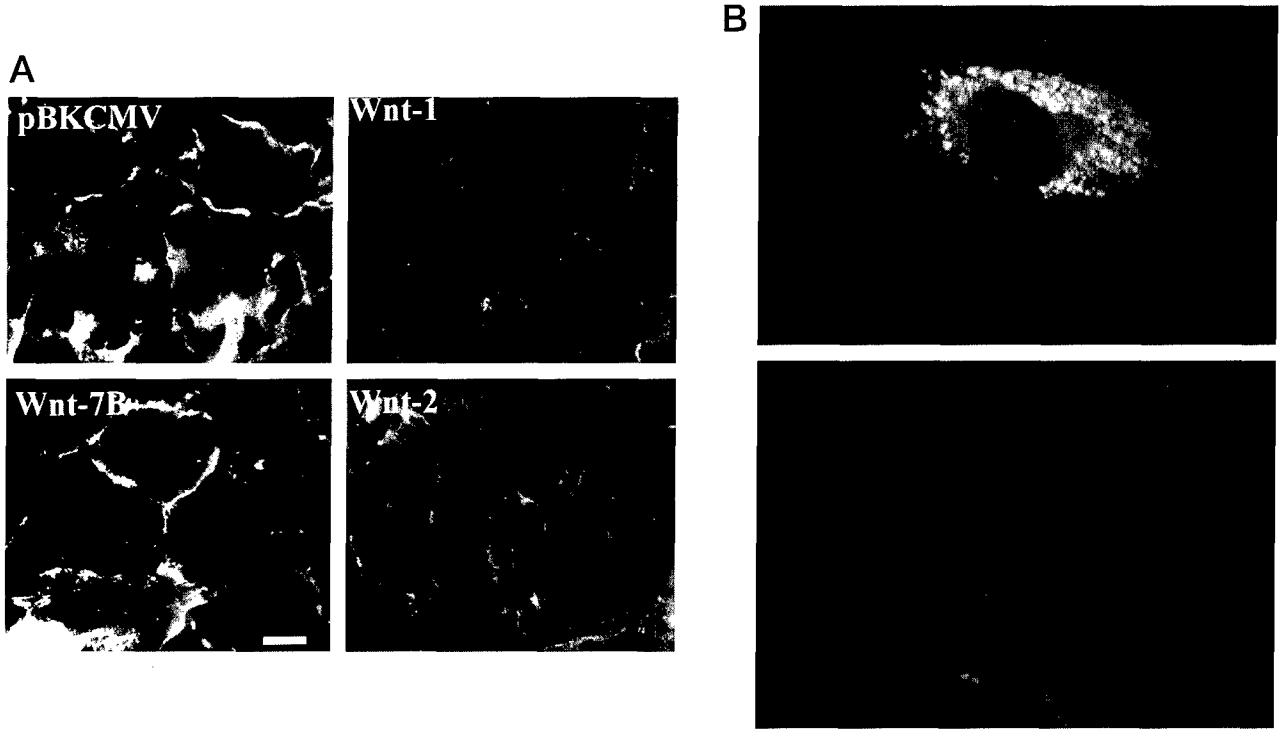

Fig. 2. *A*, Wnt transfection of HC11 cells alters the pattern of E-cadherin at the cell surface. Representative immunofluorescence of Wnt and mock-transfected cells at confluence with E-cadherin antibodies. Note that E-cadherin staining in the mock control is located at the intercellular junctions. Compare to the pattern detected in Wnt-1- and Wnt-2-transfected cells. *Bar*, 2 μm. *B*, immunofluorescent detection of Myc-epitope tagged *Wnt* genes in transfected HC11 cells. The myc epitope is detected by indirect immunofluorescence in the cytoplasm of Wnt-1- and Wnt-2-transfected HC11 cells (*top* and *bottom*, respectively). Individual cells rather than confluent cells are shown to better illustrate the cytoplasmic localization, but expression was observed in all of the stably transfected cells, both at confluence and during exponential growth. A similar pattern was observed for Wnt-7B-transfected cells (data not shown). Magnification, ×400.

Table 1 Frequency of outgrowth and phenotype of stably transfected HC11 cells in vivo

Gene	No. outgrowths/ no. injected glands	% tumors	Fibrosis
8 weeks			
Wnt-1	10/10	0	++
Wnt-2	8/10	0	++
Wnt-7B	10/10	0	+++
Mock	6/6	0	–
12 weeks			
Wnt-1	10/10	0	++
Wnt-2	10/10	0	++
Wnt-7B	10/10	60	++
Mock	8/8	0	–/+

immortalized cell line that express a mutant p53 and display characteristics that are reminiscent of hyperplastic epithelium (37). In the mock-transfected outgrowths, this hyperplasia is evident in the seminormal ductal-like structures that are filled with cells (Fig. 4, *A* and *E*). Interestingly, the mock-transfected cells are able to form structures reminiscent of ducts in a pregnant gland. The mock-transfected cells are not transformed, as evidenced by the regular and even appearance of these duct-like structures. In addition to the large distal sites of growth, the Wnt transfected cells displayed regions of limited growth (5–10 cells) associated with small blood vessels, suggesting the migration of transfected cells through the mammary gland was accomplished through the vasculature (data not shown). In a Wnt-1 and Wnt-7B outgrowth, corruption of the lymph node was observed, with epithelial cells and fibrosis penetrating the capsule of the lymph node (Fig. 4*B*). Interestingly, in some glands in regions distal to the outgrowths, there was an obvious increase in collagen synthesis in the stroma (Fig. 4, *B* and *C*, and data not shown).

Immunohistochemical analysis of mock and Wnt-1 outgrowths for E-cadherin revealed a significant disruption in the E-cadherin pattern in Wnt-1 outgrowths. No signal was observed at the junctions between cells, and staining was diffused across the whole cell (Fig. 5*A*). A similar result was observed for the Wnt-2 outgrowths (Fig. 5*B*). In comparison, the mock-transfected HC11 outgrowth (Fig. 5*C*), while still atypical as compared to the normal pattern of E-cadherin staining observed in a midpregnant mammary gland (Fig. 5*D*), do exhibit E-cadherin staining that is localized to the junctions between cells.

Tumor Formation in Wnt-transfected HC11 Cells. A second set of animals was injected with Wnt-transfected HC11 cells and allowed to grow for an additional 4 weeks, for a total of 12 weeks (Table 1). Three mice that were injected with Wnt-7B-transfected HC11 cells produced large, palpable tumors (Fig. 6). In addition, histologically evident tumors,

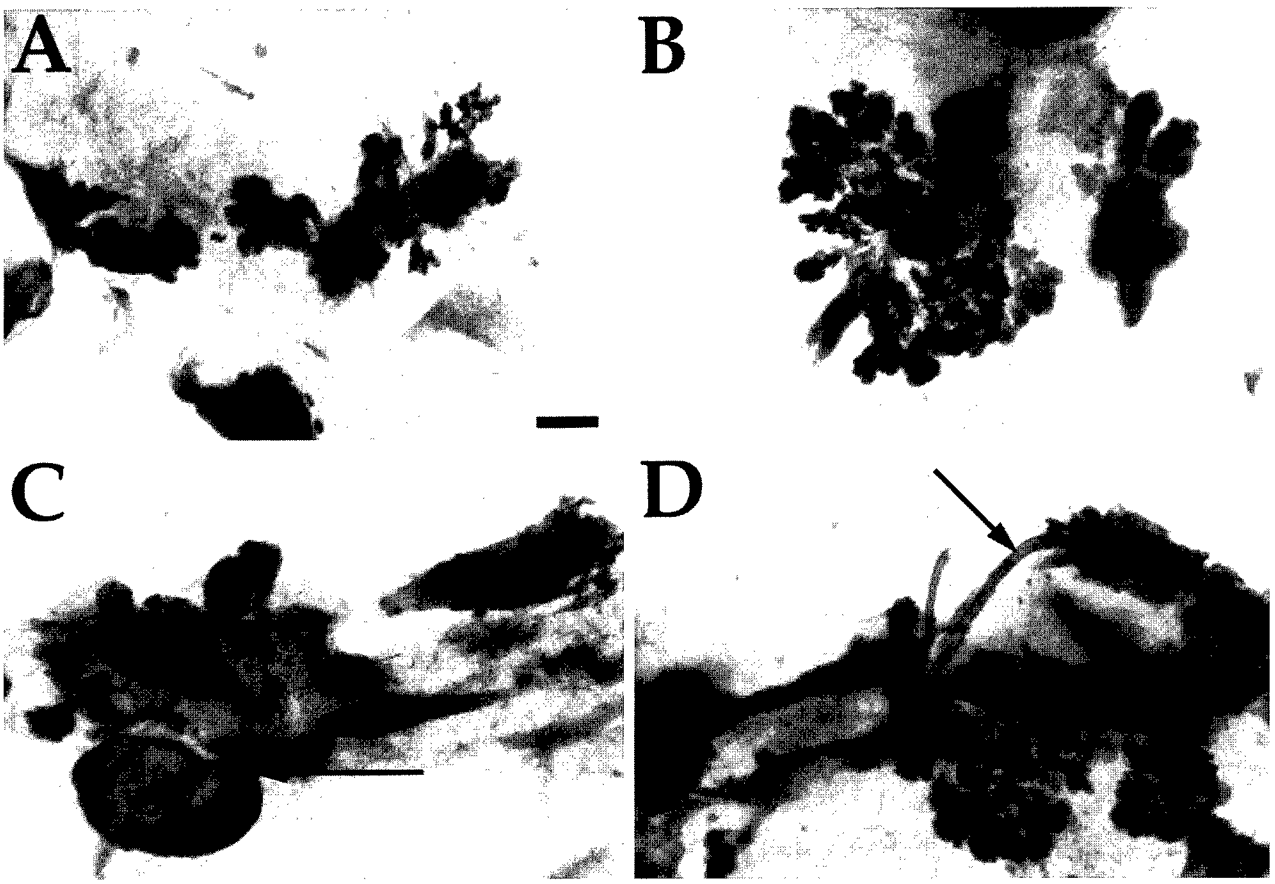

Fig. 3. Wnt-1-, Wnt-2-, Wnt-7B-, and mock-transfected HC11 cells produce outgrowths *in vivo*. Mammary glands injected with Wnt-transfected HC11 cells and grown for 8 weeks *in vivo* were stained with hematoxylin as described in "Materials and Methods." Note the ductal-like structure in the mock-transfected (*D*) outgrowth (*arrow*). Wnt-1 (*A*), Wnt-2 (*B*), and Wnt-7B (*C*) outgrowths appear at several locations throughout the mammary fat pad. *Arrow* (*C*), a potential site of lymph node corruption. *Scale bar*, 1 mm.

characterized as undifferentiated mammary adenocarcinomas, were produced in 6 of 10 mammary glands injected with Wnt-7B-transfected HC11 cells (Table 1). No tumors were observed in any of the other Wnt- or mock-transfected HC11 cells. Histological examination of the Masson's trichrome-stained tumors revealed extensive epithelial hyperplasia and minimal fibrosis. Three of six tumors occupied the entire fat pad within 12 weeks, reflecting a significant growth rate. The tumors had the phenotype of undifferentiated adenocarcinoma, with large areas of hyperplastic, columnar glandular epithelium reminiscent of myc-induced mammary tumors, and metastatic characteristics, as evidenced by the invasion of muscle (Fig. 6, *A* and *B*) and skin. All of the Wnt-7B-induced tumors had central areas of necrosis (Fig. 6*C*, *arrow*) and displayed extensive angiogenesis.

Discussion

***Wnt* Gene Expression Elicits Distinct *in Vitro* Phenotypes.** These experiments demonstrate that the effects of different *Wnt* genes can be studied in HC11 cells stably transfected with different Wnt expression constructs both in *vitro* and after their transplantation into the clear mammary fat pad. The *in vitro* data demonstrate that transfection of *Wnt* genes into a mammary epithelial cell line can affect the intercellular adhesion, as demonstrated by the disruption of E-cadherin pattern and three-dimensional morphology. Each transfected *Wnt* gene generated distinct *in vitro* phenotypes, with an apparent correlation between the E-cadherin pattern and degree of morphological disruption. Thus, the most dramatic disruption in three-dimensional architecture occurred in the cells that had the most significant alteration in E-cadherin pattern. These results suggest that the disruption in patterning of this intercellular adhesion molecule affects the ability of these cells to form these higher-order structures. There was no obvious difference in the two-dimensional morphology of the cells at confluence, suggesting that the disruption of intercellular adhesion was not manifested until the cells required more sophisticated organization.

Previous studies have shown Wnt-1 expression regulates the free pool of β-catenin and increases cell adhesion, as measured by a cell trituration assay in AtT20 and C57MG cells (41, 44). Conversely, Wnt-1 transfection of MDCK cells did not increase cellular adhesion, suggesting that the effects of Wnt-1 on cell adhesion are cell type-dependent. The pattern of cadherin at the cell surface was not examined in these studies. Consequently, a direct comparison between

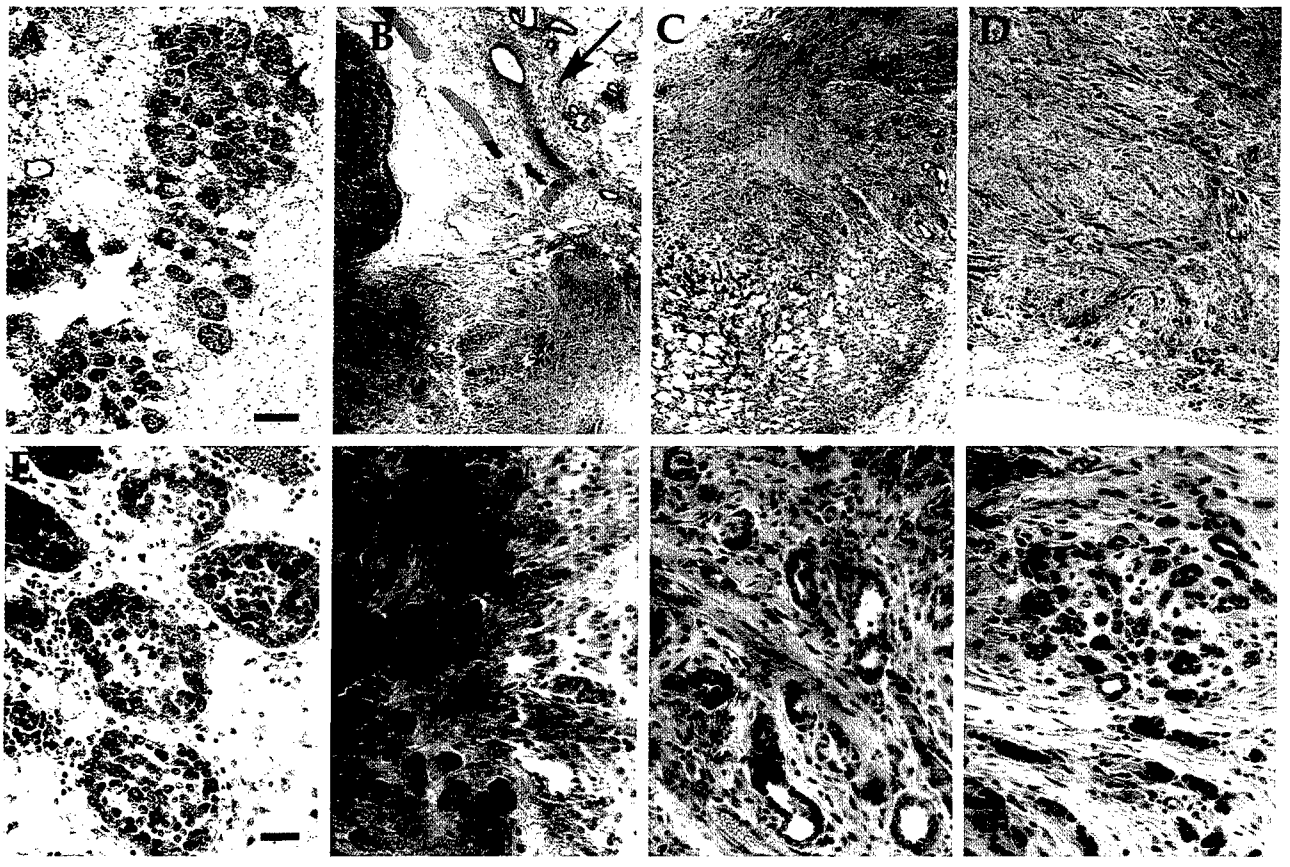

Fig. 4. Wnt-transfected HC11 cells generate fibrotic outgrowths *in vivo*. Mock (*A* and *E*), Wnt-1 (*B* and *F*), Wnt-2 (*C* and *G*), and Wnt-7B (*D* and *H*) outgrowths stained with Masson's trichrome at high (*E–H*) and low (*A–D*) magnification. Note the absence of regular ductal structures and the significant fibrosis in the Wnt-transfected outgrowths (*B–D*) compared to the mock-transfected outgrowths (*A*). In *B*: *L*, lymph node; *arrow*, region of stromal collagen synthesis distal to outgrowth site. *Scale bar* (*A*), 100 μm (applies to *A–D*); scale bar (*E*), 20 μm (applies to *E–H*).

the observed phenotypes in HC11 and C57MG cells cannot be made. It is unclear how much of an alteration in the E-cadherin pattern is required to elicit a change in the adhesive properties of the cell. The results of these studies in HC11 cells are consistent with the reported decrease in E-cadherin expression observed in breast cancer and a concomitant increase in the metastatic potential of these tumors (45). In addition, recent data have suggested that the Wnt-1-mediated increase in the β-catenin pool could have multiple biochemical consequences (27).

Surprisingly, a new role for β-catenin as a transcriptional coactivator has been demonstrated by its ability to activate transcription in association with the Tcf/LEF-1 transcription factors (reviewed in Ref. 46). This nuclear signaling complex is activated in colon carcinoma, where mutation of the *APC* gene, which normally complexes with and degrades the β-catenin protein, permits increased levels of β-catenin and the resulting transcriptional activity of Tcf/β-catenin complex (47, 48). The target genes of this transcriptional complex are unknown, but presumably, this new nuclear function may provide an additional mechanism for β-catenin to stimulate the proliferative and differentiative changes induced by the Wnt pathway.

The effect of transfecting Wnt expression constructs on the morphology of mammary epithelial cells has been reported in several previous studies (49–51). These studies have been performed primarily in C57MG cells, either following direct transfection or coculture with transfected Rat-2 or quail fibroblasts (52), and have relied on a semiquantitative assessment of morphological transformation of these cells that is characterized by an elongated, refractile morphology and a loss of contact-inhibited growth. It has not been possible to compare the extent of morphological transformation *in vitro* of the C57MG transfectants with their growth or tumorigenic properties *in vivo* either after s.c. inoculation in nude mice or after transplantation into the cleared mammary fat pad. Studies in 10T1/2 fibroblasts have also been used to assess the biochemical properties of several Wnts and to help elucidate the *wg* signal transduction pathway (53). In addition, studies of the biochemical and proliferative properties primarily of Wnt-1 and, to a lesser extent, Wnt-2 have been performed in a number of different cell types, including CHO (51), P19 mouse embryo carcinoma cells (26, 54), AtT20 mouse pituitary cells (24, 51), and RAC311, cuboidal mammary tumor cells (50). Because many of these cells are tumorigenic in the absence of Wnt transfection, *in vivo* studies of Wnt function have not usually been performed, with the exception of the RAC311 cells, which were isolated from int-2/Fgf-3 mammary tumors. More recently, expression of Wnt-5A has been reported to inhibit the tumorigenic prop-

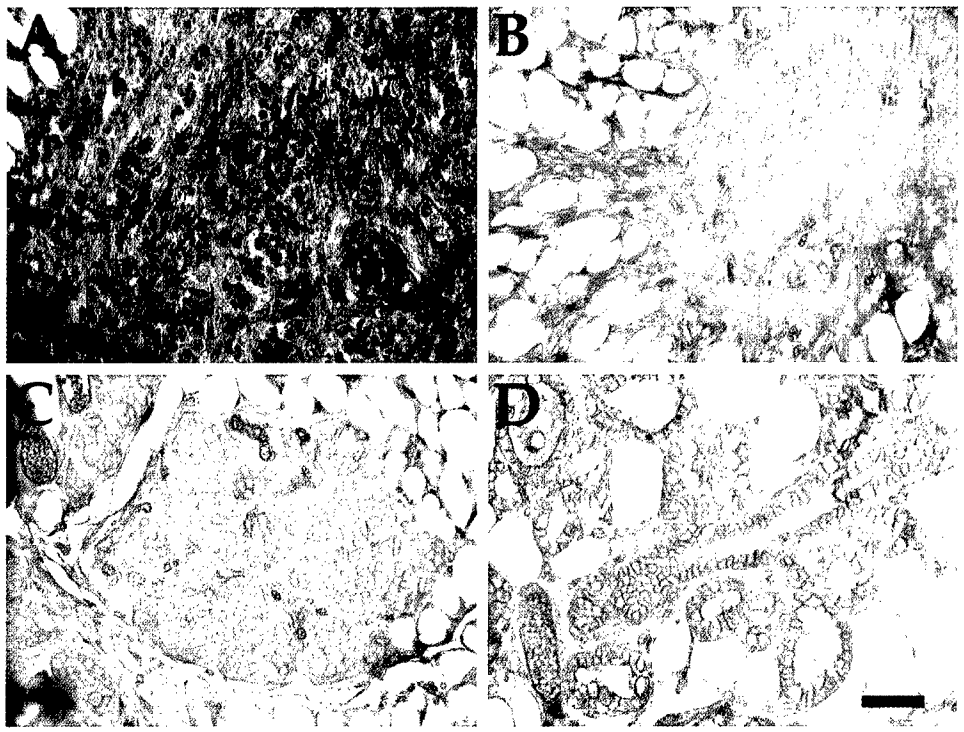

Fig. 5. E-cadherin expression is altered in Wnt-transfected outgrowths. Immunohistochemical localization of E-cadherin expression in Wnt-1-, Wnt-2-, and mock-transfected HC11 cell outgrowths (*A*, *B*, and *C*, respectively) and in 10-day pregnant mammary gland (*D*). Note the pattern of staining at the intercellular junctions in the mock-transfected outgrowths and 10-day pregnant gland. *Scale bar*, 20 μm.

erties of a uroepithelial carcinoma cell line, leading to the suggestion that Wnt-5A may actually act as a tumor suppressor (55). In addition, Wnt-11 has been demonstrated to induce differentiation of a quail mesoderm cell line (56). Thus, the classification of *Wnt* genes into separate functional groups, which has received strong support from studies in *Xenopus* (18), may require reevaluation when the properties of individual Wnts are studied in different mammalian cell types *in vivo*.

The discovery of the wingless receptor (Dfz2) frizzled (23) and the revelation that it is a member of a large family of related receptor proteins (57) suggest that the specificity for Wnt signaling may also be determined in part by the expression of individual receptor family members. Each *Wnt* gene or class of genes may have a distinct receptor, and the presence or absence of a particular receptor may facilitate or decrease the activity of a specific Wnt. Evidence for the restriction of Wnt activity due to the absence of a specific receptor has been demonstrated in recent experiments in *Xenopus*, where a specific frizzled receptor, hFz5, permitted a new functional activity, *i.e.*, axis duplication from Wnt-5A, when Wnt-5A does not normally possess this activity (58). Thus, differences in the Wnt receptors may in part be related to the cell-specific effects observed in mammalian cells, and additional studies will be required to examine which members of the *frizzled* gene family are expressed in HC11, as compared to C57MG cells. It is of interest that Wnt-7B appeared to have little effect on the morphology and E-cadherin staining pattern in HC11 cells and has been reported to exhibit a moderate transformation potential in C57MG cells (17). However, Wnt-7B expression has been reported to be 30-fold higher in 10% of human breast carcinomas when compared to normal breast tissue (13), and it appeared to be more tumorigenic in HC11 cells (see below).

One caveat that must be considered in interpreting these results is the undetermined effect of the level of expression of the individual Wnt proteins. Unfortunately, because of a lack of good immunological reagents, the precise level of expression of the individual Wnt proteins expressed in the HC11 cells could not be determined. Most previous studies have relied on analyzing the expression levels of the individual Wnt mRNAs but have not measured protein expression, with the notable exception of one recent report on Wnt-11 (56). The use of the myc epitope tag permitted the detection of the Wnts in stably transfected HC11 cells by indirect immunofluorescence but was not useful in quantitating the relative levels of Wnt expression in Western blots. The use of alternative epitope tags may circumvent this problem in the future. It is, therefore, conceivable that variable expression levels are responsible for the observed differences in E-cadherin staining and morphology. However, the reproducible phenotypes observed using replicate pools of Wnt-transfected HC11 cells argues that the different effects observed were not due to variable expression levels.

***In Vivo* Outgrowths Are Similar but May Reflect Functional Differences between the *Wnt* Genes.** The dramatic levels of fibrosis observed in all of the Wnt-transfected outgrowths is consistent with the phenotype observed in the mammary glands of transgenic mice expressing Wnt-1. Histologically, the outgrowths generated in this study are very similar to those described in outgrowths from the Wnt-1 transgenic mice (9–11). The Wnt-1 transgenic mammary glands have hyperproliferative, pregnant-like epithelium surrounded by a thick sheath of stroma. This provides strong

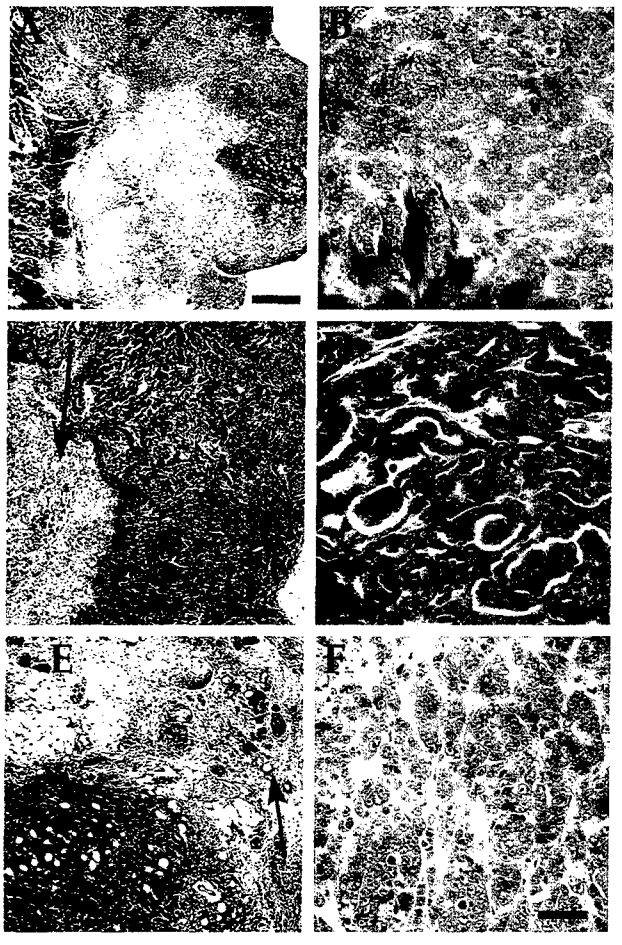

Fig. 6. HC11 cells can generate tumors *in vivo*. Masson's trichrome stain of sections of three separate tumors at low (*A*, *C*, and *E*) and high (*B*, *D*, and *F*) power from fat pads injected with Wnt-7B-transfected HC11 cells and grown *in vivo* for 12 weeks. *Arrow* (*C*), central area of necrosis. *A* and *B*, invasive epithelial cells penetrating muscle (*M*). *Arrow* (*E*), region of fibrotic outgrowth adjacent to a tumor. *Scale bar* (*C*), 100 μm (applies to *C* and *E*); *scale bar* (*F*), 20 μm (applies to *B*, *D*, and *F*); *scale bar* (*A*), 0.5 mm.

correlative evidence that the formation of this hyperplasia and fibrosis is, in fact, due to the expression of Wnt-1. Many of the HC11-injected mammary glands demonstrated a fibrotic stromal response that was distant from the nearest site of transplanted epithelium (see Fig. 4). This suggests that *Wnt* gene products, in general, may have a stimulatory effect on the stromal fibroblasts in the mammary gland. Similar tumor cell-stromal interactions have been observed in human breast cancer (59). *Wnt* gene products are secreted growth factors that act through a paracrine mechanism and, therefore, could affect the stromal fibroblasts. The only reproducible difference between the phenotypes of the Wnt-transfected HC11 outgrowths was that the outgrowths from the Wnt-7B-transfected cells were significantly larger and more fibrotic.

The appearance of tumors exclusively in the Wnt-7B-transfected fat pads suggested that there maybe some increase in tumorigenicity in these cells, when compared to Wnt-1 and Wnt-2. Unfortunately, this study does not analyze the long-term tumorigenicity of the different *Wnt* genes. Previous studies with Wnt-1 transgenic mice revealed that, despite the presence of extensive hyperplasia in virgin female mice, the earliest mammary carcinomas were detected after only 3 months, and by 8 months of age, only 80% of the transgenic animals had developed tumors (10). Thus, it is not unexpected that tumors were not detected in the Wnt-1 HC11 outgrowths after 12 weeks.

Comparison of the histological characteristics of the outgrowths to the tumors indicates that the tumors lack the significant fibrosis observed in the outgrowths. It is likely that the tumors are, in fact, derived from the outgrowths but require additional mutational events to produce a highly proliferative cell, which then overwhelms the fibrotic nature of the outgrowth. For example, cooperativity between Wnt and Fgf family members, resulting in increased tumorigenicity, has been demonstrated in bitransgenic mice expressing both Wnt-1 and Fgf-3 (60). Hyperinfection of Wnt-1 or Fgf-3 transgenic mice with MMTV has also resulted in mammary tumors with secondary MMTV insertions, activating additional Fgf or Wnt family members, respectively (6–8).

A New Method for Analysis of Wnt Function *in Vivo*. The reproducible generation of outgrowths in the cleared fat pad with stably transfected HC11 cells was surprising because similar reported experiments had not been successful (34). This most likely reflects the use of early-passage cells, the inclusion of sufficient pooled transfectants, and the method of reinjection back into the fat pad. The use of pooled transfectants may have allowed cells that have lost certain critical survival characteristics to proliferate because of the presence of adjacent cells that still secrete these locally acting factors. This method complements the two other approaches used to study Wnt function in the mammary gland: the generation of transgenic mice, in which Wnt expression has been targeted to the mammary gland using MMTV-based constructs (10), and the use of retroviral expression vectors to infect primary mammary epithelial cells and the reintroduction of these cells into the mammary fat pad (11, 12). To date, both of these approaches have had limited success, most likely due to the inefficient expression of the transgenic cDNA constructs and the inability to infect a sufficient number of clonigenic cells necessary to repopulate the mammary gland. The HC11 cells should permit a direct evaluation of the effects of different Wnt family members on both the *in vitro* properties and *in vivo* characteristics of mammary epithelial cells.

Materials and Methods

Animals. BALB/c and C3H mice were acquired from Charles River Labs (Wilmington, MA) or from a breeding colony at Baylor College of Medicine, courtesy of Dr. Daniel Medina. All animals were maintained according to IACUC-approved guidelines.

Whole Mount Staining and Sectioning. The whole gland staining was carried out essentially as described (61), except that glands were stained for only 2 h in hematoxylin. Fixed and stained glands were embedded in paraffin and sectioned (5 μm) onto Probe-on plus slides (Fisher Scientific, Pittsburgh, PA).

cDNA Constructs. Wnt-1, Wnt-2, and Wnt-7B cDNAs, isolated by PCR from mammary cDNA (53), were excised from the vector pYES, purified, and subcloned into the modified pBKCMV expression vector (Stratagene, La Jolla, CA). The pBKCMV vector was modified by deletion

of sequences between the *Nhe*I-*Spe*I sites to remove the transcription start site of the *lacP* gene. Each cDNA contained a myc epitope tag inserted at their COOH termini (sequence, EQKLISEEDL) to permit detection of the expressed protein. Cell culture studies in 10T1/2 fibroblasts have shown that, for Wnt-1 and Wnt-7B, the myc epitope does not interfere with the function.[5] After blue-white selection, subclones were isolated, purified on a Qiagen column, and sequenced.

Transfection of *Wnt* Genes. Each Qiagen-purified Wnt construct (20 μg), including a mock control (pBKCMVneo), was mixed with 50 μl of lipofectamine (Life Technologies, Inc.) and incubated with semiconfluent HC11 cells, according to the manufacturer's protocol. After a 5-h incubation at 37°C, the lipofectamine-DNA mixture was replaced with normal growth medium. Twenty-four h after transfection, selection with 200 μg/ml G418 was begun. Transfected cells were maintained for 40 days under selection before injection into the fat pad. The optimal amount of DNA (30 μg) produced 1–15 colonies per μg of DNA for each construct.

Growth Conditions of HC11 Cells. The HC11 cell line, a COMMA-D-derived cell line from the mammary gland of midpregnant BALB/c mice, was kindly provided by Dr. Bernd Groner (30). HC11 cells (passage 8) were maintained in 10% bovine calf serum in RPMI 1640 (JRL Bioscience) with 10 ng/ml insulin, 10 ng/ml epidermal growth factor, and 1 mM glutamine at 37°C in a 5% CO_2 incubator. For transfection, the cells were grown in normal medium without serum for 3 h. For analysis of cellular morphology, cells were grown past confluence for 18 days, and the medium was changed every two days. There was no significant loss of viability when the cells were maintained in normal growth medium past confluence.

Photography of Transfected HC11 Cells. Hyperconfluent, unfixed HC11 cells were photographed with a Nikon inverted, phase-contrast tissue culture microscope with Ecktachrome 400ASA film (Kodak, Rochester, NY).

Immunofluorescence Analysis of E-Cadherin and Myc in Transfected HC11 Cells. E-cadherin antibodies were purchased from Zymed (San Francisco, CA). Anti-myc epitope antibodies were purchased from Santa Cruz Biotechnology (Santa Cruz, CA). Nontransfected and Wnt-transfected HC11 cells were trypsinized and placed in a 100-ml plastic Petri dish with several sterile glass coverslips. A set of coverslips was removed from each dish after 2 days, during exponential growth, and 2 days after the cells had grown to confluence. Coverslips were removed from the Petri dish, rinsed in PBS twice at 24°C, and fixed in −20°C 100% methanol and −20°C 100% acetone for 5 min each. Coverslips were then rinsed in PBS twice, placed cell side up in a glass Petri dish, and incubated with primary antibody at 1:100 for 60 min at 37°C. Goat antirat secondary antibody (Oncogene Science) to the anti-E-cadherin primary antibody was applied at a dilution of 1:500. Rabbit antimouse secondary antibody (Molecular Probes, Eugene, OR) to the anti-myc primary antibody was applied at 1:500. Secondary antibodies were incubated at 37°C for 1 h, and then the coverslips were rinsed in 1× PBS for 3 min three times. Coverslips were then inverted and mounted onto glass slides with Permafluor, a semipermanent antifading agent. Slides were analyzed under fluorescence with a fluorescent Nikon microscope.

Transplantation of Wnt Transfected HC11 Cells *in Vivo*. Each plate of transfected cells was passaged once after 40 days of selection and split 1:1. These pools were allowed to grow to confluence in 100-mm Petri dishes. Pools of HC11 clones (representing 20–30 colonies per construct), transfected with Wnt-1, Wnt-2, Wnt-7B, or the mock construct, were collected from 100-ml dishes after cells had grown to confluence by a standard trypsin treatment. Briefly, cells were rinsed twice in 1× Hanks' solution and incubated with 0.1× trypsin in Hanks' solution for 15 min at 37°C or until the cells were lightly adherent. Cells were gently removed by pipetting with growth medium, pelleted in a clinical centrifuge at low speed, and resuspended in 100 μl of normal growth medium with serum to give a final concentration of 5×10^5 cells/10 μl. Endogenous epithelium from mammary glands was removed according to surgical techniques described by DeOme *et al.* (43). Using a beveled Hamilton syringe, the resuspended HC11 cells were injected into the cleared fat pad of 3-week-old BALB/c virgin recipient mice, just above the lymph node, in a volume of 10 μl. Each mouse had the same construct injected into both number 4 fat pads. Mock-transfected HC11 cells were also collected and injected in the same manner. The transplants were allowed to proliferate and fill the fat pad for 8–12 weeks (see Table 1) when the glands were surgically removed and stained with hematoxylin, as described previously. The injections were carried out at 12 weeks with cells that were left over after the injection process and replated for an additional 2 weeks until they had reached confluence.

[5] M. S. Naylor and T. C. Dale, personal communication.

Acknowledgments

We gratefully acknowledge Drs. Stuart Naylor and Trevor Dale (Institute of Cancer Research, Surrey, United Kingdom) for providing the myc-Wnt constructs. We acknowledge the excellent technical support of Frances Kittrell, Jason Gay, and Liz Hopkins. We also acknowledge Drs. Mike Mancini for assistance with the immunofluorescence and Ron Morton for the immunohistochemical staining of E-cadherin.

References

1. van Ooyen, A., and Nusse, R. Structure and nucleotide sequence of the putative mammary oncogene int-1: proviral insertions leave the protein-encoding domain intact. Cell, *39:* 233–240, 1984.

2. Nusse, R., van Ooyen, A., Cox, D., Fung, Y. K., and Varmus, H. Mode of proviral activation of a putative mammary oncogene (int-1) on mouse chromosome 15. Nature (Lond.), *307:* 131–136, 1984.

3. Nusse, R., and Varmus, H. E. *Wnt* genes. Cell, *69:* 1073–1087, 1992.

4. Roelink, H., Wagenaar, E., Lopes da Silva, S., and Nusse, R. *Wnt-3*, a gene activated by proviral insertion in mouse mammary tumors, is homologous to int-1/Wnt-1 and is normally expressed in mouse embryos and adult brain. Proc. Natl. Acad. Sci. USA, *87:* 4519–4523, 1990.

5. Roelink, H., Wagenaar, E., and Nusse, R. Amplification and proviral activation of several *wnt* genes during progression and clonal variation of mouse mammary tumors. Oncogene, *7:* 487–492, 1992.

6. Shackleford, G. M., MacArthur, C. A., Kwan, H. C., and Varmus, H. E. Mouse mammary tumor virus infection accelerates mammary carcinogenesis in Wnt-1 transgenic mice by insertional activation of int-2/Fgf-3 and hst/Fgf-4. Proc. Natl. Acad. Sci. USA, *90:* 740–744, 1993.

7. Lee, F. S., Lane, T. F., Kuo, A., Shackleford, G. M., and Leder, P. Insertional mutagenesis identifies a member of the *Wnt* gene family as a candidate oncogene in the mammary epithelium of int-2/Fgf-3 transgenic mice. Proc. Natl. Acad. Sci. USA, *92:* 2268–2272, 1995.

8. MacArthur, C. A., Shankar, D. B., and Shackleford, G. M. Fgf-8, activated by proviral insertion, cooperates with the Wnt-1 transgene in murine mammary tumorigenesis. J. Virol., *69:* 2501–2507, 1995.

9. Lin, T. P., Guzman, R. C., Osborn, R. C., Thordarson, G., and Nandi, S. Role of endocrine, autocrine, and paracrine interactions in the development of mammary hyperplasia in Wnt-1 transgenic mice. Cancer Res., *52:* 4413–4419, 1992.

10. Tsukamoto, A. S., Grosschedl, R., Guzman, R. C., Parslow, T., and Varmus, H. E. Expression of the int-1 gene in transgenic mice is associated with mammary gland hyperplasia and adenocarcinomas in male and female mice. Cell, *55:* 619–625, 1988.

11. Edwards, P. A., Hiby, S. E., Papkoff, J., and Bradbury, J. M. Hyperplasia of mouse mammary epithelium induced by expression of the *Wnt-1* (*int-1*) oncogene in reconstituted mammary gland. Oncogene, *7:* 2041–2051, 1992.

12. Bradbury, J. M., Edwards, P. A., Niemeyer, C. C., and Dale, T. C. Wnt-4 expression induces a pregnancy-like growth pattern in reconstituted mammary glands in virgin mice. Dev. Biol., *170:* 553–563, 1995.

13. Huguet, E. L., McMahon, J. A., McMahon, A. P., Bicknell, R., and Harris, A. L. Differential expression of human *Wnt* genes *2*, *3*, *4*, and *7B* in human breast cell lines and normal and disease states of human breast tissue. Cancer Res., *54:* 2615–2621, 1994.

14. Iozzo, R. V., Eichstetter, I., and Danielson, K. G. Aberrant expression of the growth factor Wnt-5A in human malignancy. Cancer Res., *55:* 3495–3499, 1995.

15. Lejeune, S., Huguet, E. L., Hamby, A., Poulsom, R., and Harris, A. L. Wnt5a cloning, expression, and upregulation in human primary breast cancers. Clin. Cancer Res., *1:* 215–222, 1995.

16. Vider, B. Z., Zimber, A., Chastre, E., Prevot, S., Gespach, C., Estlein, D., Wolloch, Y., Tronick, S. R., Gazit, A., and Yaniv, A. Evidence for the involvement of the *Wnt 2* gene in human colorectal cancer. Oncogene, *12:* 153–158, 1996.

17. Wong, G. T., Gavin, B. J., and McMahon, A. P. Differential transformation of mammary epithelial cells by *Wnt* genes. Mol. Cell. Biol., *14:* 6278–6286, 1994.

18. Du, S. J., Purcell, S. M., Christian, J. L., McGrew, L. L., and Moon, R. T. Identification of distinct classes and functional domains of Wnts through expression of wild-type and chimeric proteins in *Xenopus* embryos. Mol. Cell. Biol., *15:* 2625–2634, 1995.

19. Bühler, T. A., Dale, T. C., Kieback, C., Humphreys, R. C., and Rosen, J. M. Localization and quantification of *Wnt-2* gene expression in mouse mammary development. Dev. Biol., *155:* 87–96, 1993.

20. Gavin, B. J., and McMahon, A. P. Differential regulation of the *wnt* gene family during pregnancy and lactation suggests a role in postnatal development of the mammary gland. Mol. Cell. Biol., *12:* 2418–2423, 1992.

21. Weber-Hall, S. J., Phippard, D. J., Niemeyer, C. C., and Dale, T. C. Developmental and hormonal regulation of *Wnt* gene expression in the mouse mammary gland. Differentiation, *57:* 205–214, 1994.

22. Klingensmith, J., and Nusse, R. Signaling by wingless in *Drosophila*. Dev. Biol., *166:* 396–414, 1994.

23. Bhanot, P., Brink, M., Samos, C. H., Hsieh, J-C., Wang, Y., Macke, J. P., Andrew, D., Nathans, J., and Nusse, R. A new member of the *frizzled* family from *Drosophila* functions as a wingless receptor. Nature (Lond.), *382:* 225–230, 1996.

24. Smolich, B. D., McMahon, J. A., McMahon, A. P., and Papkoff, J. Wnt family proteins are secreted and associated with the cell surface. Mol. Biol. Cell, *4:* 1267–1275, 1993.

25. Peifer, M., Pai, L. M., and Casey, M. Phosphorylation of the *Drosophila* adherens junction protein Armadillo: roles for wingless signal and zeste-white 3 kinase. Dev. Biol., *166:* 543–556, 1994.

26. Papkoff, J. Identification and biochemical characterization of secreted Wnt-1 protein from P19 embryonal carcinoma cells induced to differentiate along the neuroectodermal lineage. Oncogene, *9:* 313–317, 1994.

27. Behrens, J., von Kries, J. P., Kühl, M., Bruhn, L., Wedlich, D., Grosschedl, R., and Birchmeier, W. Functional interaction of β-catenin with transcription factor LEF-1. Nature (Lond.), *383:* 638–642, 1996.

28. Molenaar, M., van de Wetering, M., Oosterwegel, M., Peterson-Maduro, J., Godsave, S., Korinek, V., Roose, J., Destrée, O., and Clevers, H. XTcf-3 transcription factor mediates β-catenin-induced axis formation in *Xenopus* embryos. Cell, *86:* 391–399, 1996.

29. Peifer, M. *β-catenin* as oncogene: the smoking gun. Science (Washington DC), *275:* 1752–1753, 1997.

30. Ball, R. K., Friis, R. R., Schoenenberger, C. A., Doppler, W., and Groner, B. Prolactin regulation of *β-casein* gene expression and of a cytosolic 120-kd protein in a cloned mouse mammary epithelial cell line. EMBO J., *7:* 2089–2095, 1988.

31. Chammas, R., Taverna, D., Cella, N., Santos, C., and Hynes, N. E. Laminin and tenascin assembly and expression regulate HC11 mouse mammary cell differentiation. J. Cell Sci., *107:* 1031–1040, 1994.

32. Doppler, W., Groner, B., and Ball, R. K. Prolactin and glucocorticoid hormones synergistically induce expression of transfected rat *β-casein* gene promoter constructs in a mammary epithelial cell line. Proc. Natl. Acad. Sci. USA, *86:* 104–108, 1989.

33. Doppler, W., Hock, W., Hofer, P., Groner, B., and Ball, R. K. Prolactin and glucocorticoid hormones control transcription of the β-casein gene by kinetically distinct mechanisms. Mol. Endocrinol., *4:* 912–919, 1990.

34. Hynes, N. E., Taverna, D., Harwerth, I. M., Ciardiello, F., Salomon, D. S., Yamamoto, T., and Groner, B. Epidermal growth factor receptor, but not c-erbB-2, activation prevents lactogenic hormone induction of the beta-casein gene in mouse mammary epithelial cells. Mol. Cell. Biol., *10:* 4027–4034, 1990.

35. Doppler, W., Villunger, A., Jennewein, P., Brduscha, K., Groner, B., and Ball, R. K. Lactogenic hormone and cell type-specific control of the whey acidic protein gene promoter in transfected mouse cells. Mol. Endocrinol., *5:* 1624–1632, 1991.

36. Happ, B., Hynes, N. E., and Groner, B. Ha-*ras* and v-*raf* oncogenes, but not *int-2* and c-*myc*, interfere with the lactogenic hormone dependent activation of the mammary gland specific transcription factor. Cell Growth & Differ., *4:* 9–15, 1993.

37. Merlo, G. R., Venesio, T., Taverna, D., Marte, B. M., Callahan, R., and Hynes, N. E. Growth suppression of normal mammary epithelial cells by wild-type p53. Oncogene, *9:* 443–453, 1994.

38. Uberall, F., Kampfer, S., Doppler, W., and Grunicke, H. H. Activation of c-*fos* expression by transforming Ha-*ras* in HC11 mouse mammary epithelial cells is PKC-dependent and mediated by the serum response element. Cell. Signalling, *6:* 285–297, 1994.

39. Marte, B. M., Jeschke, M., Graus, P. D., Taverna, D., Hofer, P., Groner, B., Yarden, Y., and Hynes, N. E. Neu differentiation factor/heregulin modulates growth and differentiation of HC11 mammary epithelial cells. Mol. Endocrinol., *9:* 14–23, 1995.

40. Sgambato, A., Han, E. K., Zhou, P., Schieren, I., and Weinstein, I. B. Overexpression of cyclin E in the HC11 mouse mammary epithelial cell line is associated with growth inhibition and increased expression of p27(Kip1). Cancer Res., *56:* 1389–1399, 1996.

41. Hinck, L., Nelson, W. J., and Papkoff, J. Wnt-1 modulates cell-cell adhesion in mammalian cells by stabilizing β-catenin binding to the cell adhesion protein cadherin. J. Cell Biol., *124:* 729–741, 1994.

42. Papkoff, J., Brown, A. M., and Varmus, H. E. The *int-1* proto-oncogene products are glycoproteins that appear to enter the secretory pathway. Mol. Cell. Biol., *7:* 3978–3984, 1987.

43. DeOme, K. B., Faulkin, L. J., Bern, H. A., and Blair, P. B. Development of mammary tumors from hyperplastic alveolar nodules transplanted into gland-free mammary pads of female C3H mice. Cancer Res., *19:* 515–519, 1958.

44. Bradley, R. S., Cowin, P., and Brown, A. M. Expression of Wnt-1 in PC12 cells results in modulation of plakoglobin and E-cadherin and increased cellular adhesion. J. Cell Biol., *123:* 1857–1865, 1993.

45. Berx, G., Cleton, J. A., Nollet, F., de Leeuw, W. J., van de Vijver, M., Cornelisse, C., and van Roy, F. E-cadherin is a tumour/invasion suppressor gene mutated in human lobular breast cancers. EMBO J., *14:* 6107–6115, 1995.

46. van Leeuwen, F., Samos, C. H., and Nusse, R. Biological activity of soluble wingless protein in cultured *Drosophila* imaginal disc cells. Nature (Lond.), *368:* 342–344, 1994.

47. Korinek, V., Barker, N., Morin, P. J., van Wichen, D., de Weger, R., Kinzler, K. W., Vogelstein, B., and Clevers, H. Constitutive transcriptional activation by a β-catenin-Tcf complex in APC−/− colon carcinoma. Science (Washington DC), *275:* 1784–1787, 1997.

48. Morin, P. J., Sparks, A. B., Korinek, V., Barker, N., Clevers, H., Vogelstein, B., and Kinzler, K. W. Activation of β-catenin-Tcf signaling in colon cancer by mutations in β-catenin or APC. Science (Washington DC), *275:* 1787–1790, 1997.

49. Brown, A. M., Papkoff, J., Fung, Y. K., Shackleford, G. M., and Varmus, H. E. Identification of protein products encoded by the proto-oncogene *int-1*. Mol. Cell. Biol., *7:* 3971–3977, 1987.

50. Rijsewijk, F., van Deemter, L., Wagenaar, E., Sonnenberg, A., and Nusse, R. Transfection of the *int-1* mammary oncogene in cuboidal RAC mammary cell line results in morphological transformation and tumorigenicity. EMBO J., *6:* 127–131, 1987.

51. Blasband, A., Schryver, B., and Papkoff, J. The biochemical properties and transforming potential of human wnt-2 are similar to wnt-1. Oncogene, *7:* 153–161, 1992.

52. Jue, S. F., Bradley, R. S., Rudnicki, J. A., Varmus, H. E., and Brown, A. M. The mouse wnt-1 gene can act via a paracrine mechanism in transformation of mammary epithelial cells. Mol. Cell. Biol., *12:* 321–328, 1992.

53. Bradbury, J. M., Niemeyer, C. C., Dale, T. C., and Edwards, P. A. Alterations of the growth characteristics of the fibroblast cell line C3H 10T1/2 by members of the *Wnt* gene family. Oncogene, *9:* 2597–2603, 1994.

54. Schuuring, E., van Deemter, L., Roelink, H., and Nusse, R. Transient expression of the proto-oncogene *int-1* during differentiation of P19 embryonal carcinoma cells. Mol. Cell. Biol., *9:* 1357–1361, 1989.

55. Olson, D. J., Gibo, D. M., Saggers, G., Debinski, W., and Kumar, R. Reversion of uroepithelial cell tumorigenesis by the ectopic expression of human wnt-5a. Cell Growth & Differ., *8:* 417–423, 1997.

56. Eisenberg, C. A., Gourdie, R. G., and Eisenberg, L. M. Wnt-11 is expressed in early avian mesoderm and required for the differentiation of the quail mesoderm cell line QCE-6. Development (Camb.), *124:* 525–536, 1997.

57. Wang, Y., Macke, J. P., Abella, B. S., Andreasson, K., Worley, P., Gilbert, D. J., Copeland, N. G., Jenkins, N. A., and Nathans, J. A large family of putative transmembrane receptors homologous to the product of the *Drosophila* tissue polarity gene frizzled. J. Biol. Chem., *271:* 4468–4476, 1996.

58. He, X., Saint-Jeannet, J-P., Wang, Y., Nathans, J., Dawid, I., and Varmus, H. A member of the frizzled protein family mediating axis induction by wnt-5A. Science (Washington DC), *275:* 1652–1654, 1997.

59. Ronnov, J. L., Petersen, O. W., and Bissell, M. J. Cellular changes involved in conversion of normal to malignant breast: importance of the stromal reaction. Physiol. Rev., *76:* 69–125, 1996.

60. Kwan, H., Pecenka, V., Tsukamoto, A., Parslow, T. G., Guzman, R., Lin, T. P., Muller, W. J., Lee, F. S., Leder, P., and Varmus, H. E. Transgenes expressing the *wnt-1* and *int-2* proto-oncogenes cooperate during mammary carcinogenesis in doubly transgenic mice. Mol. Cell. Biol., *12:* 147–154, 1992.

61. Williams, J. M., and Daniel, C. W. Mammary ductal elongation: differentiation of myoepithelium and basal lamina during branching morphogenesis. Dev. Biol., *97:* 274–290, 1983.

Mammary Gland Development Is Mediated by Both Stromal and Epithelial Progesterone Receptors

Robin C. Humphreys, John Lydon, Bert W. O'Malley, and Jeffrey M. Rosen

Department of Cell Biology
Baylor College of Medicine
Houston, Texas 77030

A combination of a knockout mouse model, tissue transplantation, and gene expression analysis has been used to investigate the role of steroid hormones in mammary gland development. Mouse mammary gland development was examined in progesterone receptor knockout (PRKO) mice using reciprocal transplantation experiments to investigate the effects of the stromal and epithelial PRs on ductal and lobuloalveolar development. The absence of PR in transplanted donor epithelium, but not in recipient stroma, prevented normal lobuloalveolar development in response to estrogen (E) and progesterone (P) treatment. Conversely, the presence of PR in the transplanted donor epithelium, but not in the recipient stroma, revealed that PR in the stroma may be necessary for ductal development. Members of the Wnt growth factor family, Wnt-2 and Wnt-5B, were employed as molecular markers of steroid hormone action in the mammary gland stroma and epithelium, respectively, to investigate the systemic effects of E and P. Hormonal treatment of intact, ovariectomized, and $PR^{-/-}$ mice and mice after transplantation of $PR^{-/-}$ epithelium into wild type ($PR^{+/+}$) stroma demonstrated that these two locally acting growth factors are regulated by independent mechanisms. Wnt-2 is acutely repressed by E alone, while Wnt-5B gene expression is induced only after chronic treatment with both E and P. Wnt 5B appears to be one of the few molecular markers of P action in the mammary epithelium. This study suggests that the regulation of mammary gland development by steroid hormones is mediated by distinct effects of the stromal and epithelial PR and differential growth factor expression. (Molecular Endocrinology 11: 801–811, 1997)

0888-8809/97/$3.00/0
Molecular Endocrinology

INTRODUCTION

Aberrant regulation of normal developmental pathways plays an important role in initiating and supporting mammary gland transformation. Both hormonal and developmental status are known to be important factors in the etiology of breast cancer. These hormonal and developmental cues are often mediated at the molecular level by a combination of systemic hormones and locally acting growth factors. Synergism among locally acting growth factors enhances and augments the diversity of potential signals transmitted to the epithelial and stromal components of the gland. This synergism can be stimulatory or inhibitory and can affect gene expression in the epithelium and mesenchyme.

Estrogen (E) and progesterone (P), in cooperation with pituitary hormones, are the primary systemic hormones required for the induction of proliferation and differentiation of epithelial and stromal cells leading ultimately to the formation of ductal and alveolar structures during mammary gland development. The interaction of E and P with GH, PRL, and insulin in regulating this differentiative process has been well documented (1). Steroid hormones also regulate the expression of a number of different locally acting growth factors, including members of the epidermal growth factor, insulin-like growth factor, and fibroblast growth factor (FGF) families (2, 3). Most of these growth factors exhibit localized effects due to protein stability, adhesion and residence in extracellular matrix, transport and secretion, and availability of receptor molecules. For this reason they are believed to act as local mediators of the differentiative and proliferative signals of the systemic hormones. Systemic regulation of locally acting growth factor activity allows for fine regulation of large-scale developmentally associated proliferative and differentiative functions.

Mammary gland development is dependent on physical, molecular, and often reciprocal, interactions between the stromal and epithelial compartments (4). The ability to recapitulate fully differentiated structures from a fragment of syngeneic parenchyma, and to

separate and recombine epithelial and stromal compartments *in vivo*, makes the mammary gland an excellent model system in which to study these interactions. Evidence for this reciprocal dependence has been demonstrated in classic recombination experiments between the epithelial and stromal androgen receptor pathways (4). The specific role of the epithelial and stromal PR in the development and differentiation of the mammary gland is unclear (5, 6).

Wnt-1, the progenitor of a family of related growth factors, was discovered in mouse mammary tumors as a result of proviral activation (7). Members of the Wnt gene family are expressed in invertebrates and vertebrates where they regulate cell fate and pattern formation (8). Wnt genes, other than Wnt-1, are expressed in the mammary glands of mice in a developmentally specific pattern (9–11). The function of these endogenous Wnt genes during mammary gland development is unknown. From these studies it is apparent that Wnt gene expression is tightly regulated and is dependent on the developmental state of the mammary gland. In BALB/c mice, Wnt-2 is expressed primarily during early ductal development, 5–8 weeks postnatally, coincident with time of PR induction by E, and is markedly down-regulated at the onset of pregnancy. Conversely, Wnt-5B transcripts are detectable in the late virgin gland at 6–12 weeks of age but increase markedly during pregnancy, reaching a peak at day 18. Wnt-5B expression is localized primarily in the ductal and lobuloalveolar cells, while Wnt-2 expression is detected in the stroma (9, 11). These results suggest that E and P may play a role in regulating Wnt-2 and Wnt-5B gene expression in both the stroma and epithelium. This restricted pattern of gene expression is indicative of molecules that may be involved in the developmental processes of the gland.

In this study the progesterone receptor knockout (PRKO) mouse (12) has been used for reciprocal transplantation experiments in syngeneic mice to investigate the distinct roles of the stromal and epithelial PR in mammary ductal and alveolar development. Wnt-2 and -5B provided specific molecular markers of steroid hormone action in the mammary gland stroma and epithelium, respectively. The PRKO mouse permitted definition of the unique effects of P distinct from those mediated by E on Wnt gene expression. This experimental approach should facilitate the identification of other steroid-mediated local growth factors on mammary gland development.

RESULTS

Epithelial and Stromal PRs Have Separate Roles in Mammary Gland Development

The mammary gland has the unique ability to recapitulate the complete ductal and alveolar structures from a transplanted fragment of syngeneic mammary epithelium (13). This characteristic allows the analysis of interactions between epithelium and stroma *in vivo*. The PR is present in both epithelial and stromal compartments of the murine mammary gland (5, 14). To establish the role of the PR in each of these compartments, reciprocal transplantation experiments were performed using epithelium and stroma derived from syngeneic 129SvEv $PR^{-/-}$ and $PR^{+/+}$ mice, respectively. $PR^{-/-}$ epithelium transplanted into the cleared fat pads of $PR^{+/+}$ mice penetrated and filled the stroma with ductal structures (Fig. 1A). Interestingly, the $PR^{-/-}$ epithelium failed to develop alveoli and to display an increase in the number of secondary ductal branches in response to steroid hormone treatment (Fig. 1B). The control ipsilateral glands from the host animal responded as expected to steroid hormone treatment with alveolar proliferation (Fig. 1, D *vs.* C). This result demonstrates that the PR in the epithelium is required for normal lobuloalveolar formation and differentiation of the epithelium. In addition, the presence of PR-regulated signaling pathway in the stroma cannot compensate for the lack of PR in the epithelium. In contrast, $PR^{+/+}$ epithelium transplanted into the cleared fat pad of $PR^{-/-}$ hosts and treated with E and P exhibited lobuloalveolar development (Fig. 2D). An increase in secondary branching in these E- and P-treated transplants can be clearly seen under higher magnification (Fig. 2F, *arrow*). However, an unexpected, marked reduction in the extent of ductal outgrowth was observed in these transplants after

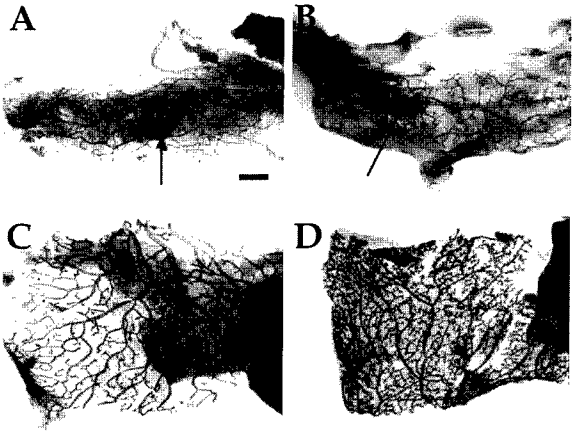

Fig. 1. Absence of Lobuloalveolar Development in Transplanted $PR^{-/-}$ Epithelium

$PR^{-/-}$ epithelium was transplanted into cleared fat pads of $PR^{+/+}$ 129SvEv mice. After 10 weeks of growth, the mice were injected subcutaneously daily with E and P, and the mammary glands were collected at day 0 (A and C) and day 8 (B and D). The *arrows* in panels A and B denote the site of transplantation. Note that in panel A the fat pad has been penetrated with ductal epithelium after 10 weeks of growth *in vivo*. Also note the increase in alveolar development in the ipsilateral $PR^{+/+}$ glands (C and D) after hormonal stimulation (compare panels C and D). *Bar* = 1.4 mm.

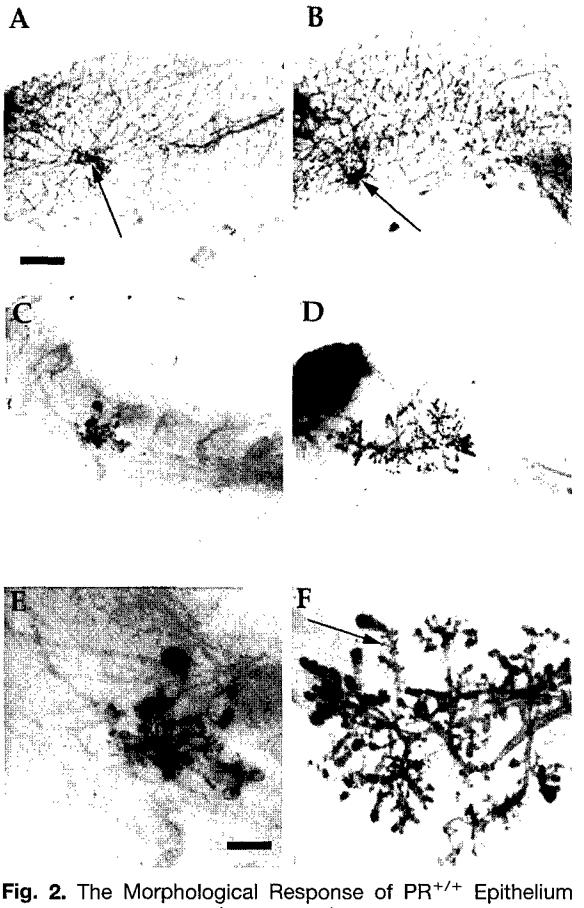

Fig. 2. The Morphological Response of $PR^{+/+}$ Epithelium Transplanted into $PR^{-/-}$ and $PR^{+/+}$ Stroma to Steroid Hormone Treatment

$PR^{+/+}$ epithelium was transplanted into $PR^{+/+}$ (A and B) and $PR^{-/-}$ (C, D, E, and F) stroma. After 10 weeks of growth, the mice were injected daily with E and P subcutaneously, and the mammary glands were collected at day 0 (A, C, and E) and day 8 (B, D, and F). Alveolar formation is evident in $PR^{+/+}$ (epithelium) $PR^{-/-}$ (stroma) after 8 days of E and P treatment (*arrow* in F). Note the reduction in ductal development in $PR^{-/-}/PR^{+/+}$ (D) compared with both $PR^{+/+}$ (B) and $PR^{-/-}$ epithelium (Fig. 1, A and B). $PR^{+/+}$ epithelium in $PR^{+/+}$ stroma responds to steroid hormone treatment with extensive alveolar growth and an increase in secondary branching (B). The *arrows* in A and B define the site of transplantation. Magnification in panels A, B, C, and D is defined by *bar* in A = 2 mm. Magnification in panels E and F is defined by *bar* in E = 0.75 mm. ($PR^{-/-}/PR^{+/+}$, n = 4 and $PR^{+/+}/PR^{+/+}$, n = 4).

10 weeks of growth (Fig. 2C), as compared with the $PR^{+/+}$ (Fig. 2, A and B) and the $PR^{-/-}$ (Fig. 1A) epithelium transplanted into the $PR^{+/+}$ stroma. The same $PR^{+/+}$ epithelium transplanted in $PR^{+/+}$ stroma responded as expected to steroid hormone treatment with extensive alveolar growth and an increase in secondary branching (Fig. 2B). The outgrowths from the $PR^{+/+}$ epithelium transplanted into the $PR^{-/-}$ stroma also displayed unusual terminal endbuds (Fig. 2, C and E).

E and P Treatment Represses Wnt-2 Gene Expression in the Mammary Glands of Ovariectomized (ovx) and Intact Mice

The role of E and P in regulating Wnt gene expression has been implied from the pattern of Wnt gene expression observed in normal mammary gland development (9–11). In particular, Wnt-2 and Wnt-5B display dramatic and inverse changes in gene expression levels at the onset of pregnancy. Wnt-2 appears to be expressed primarily in the mammary gland stroma, and Wnt-2 transcripts have been detected in the cleared mammary fat pad (9, 11), whereas Wnt-5B is expressed specifically in ductal and lobuloalveolar cells (11). Thus, these locally acting growth factors provide excellent molecular markers to investigate the role of steroid receptors on ductal and lobuloalveolar development. First, however, it was necessary to establish whether E and P either alone or in combination could regulate the expression of Wnt-2 and Wnt-5B in a manner analogous to that observed during mammary gland development. BALB/c mice were treated with E and P to mimic the onset of pregnancy. RNA from the mammary glands of hormonally treated and untreated, ovx, and intact mice were examined for changes in gene expression using a quantitative, RT-PCR method (9). A decrease of approximately 4-fold relative to the untreated (time zero) group in Wnt-2 gene expression was observed after E and P treatment of intact BALB/c mice ($n = 3$, $P < 0.001$, Fig. 3A). A 2-fold decrease ($P < 0.002$) in Wnt-2 gene expression is observed after only 2 days of E and P treatment. Wnt-2 gene expression decreased progressively with daily E and P treatment and remained low to day 12 (data not shown). This decrease in gene expression of Wnt-2 is not, however, as dramatic (20-fold) as that observed after the onset of pregnancy (9).

Circulating E and P can cause cyclical repression and induction of PR expression levels and possibly attenuate the molecular effects of pharmacological doses of E and P. To eliminate the effects of endogenous ovarian hormones, three groups of ovx mice were implanted subcutaneously for 14 days with beeswax pellets that contained E and P together, E alone, or carrier. The thoracic mammary glands were collected from three animals at each time point within each treatment group at 1, 3, and 14 days after implantation of the pellets. A 3-fold decrease relative to the day 1 E and P treatment group was observed in Wnt-2 expression after 3 days, increasing to 5-fold at 14 days compared with control ($n = 3$, $P < 0.001$, Fig. 2B). Interestingly, mice treated with E alone showed the same 5-fold decrease relative to day 1 E alone mice in Wnt-2 gene expression after 14 days ($n = 3$, $P < 0.001$).

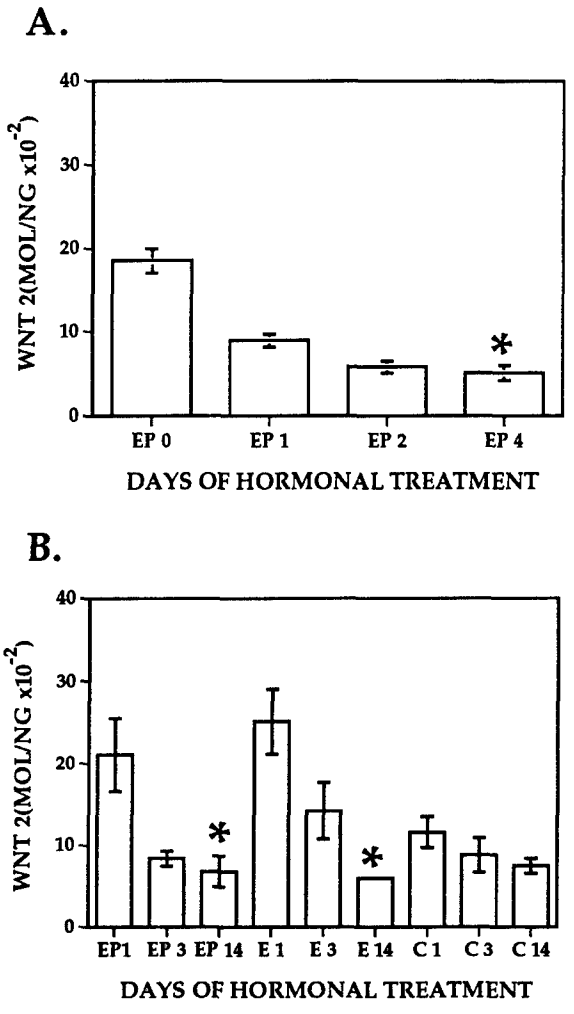

Fig. 3. The Response of Wnt-2 Gene Expression in Intact (A) and ovx (B) BALB/c Mice to E and P Treatment

A, Quantitative RT-PCR analysis of RNA from mammary glands of BALB/c mice injected daily with E and P, subcutaneously, for 8 days. EP refers to treatment with E and P for the number of days designated. Values: Molecules/nanogram RNA(MOL/NG) represent the mean ± SEM. The *star* denotes that EP 4 is statistically different from EP 0, $P < 0.001$, n = 3. B, Quantitative RT-PCR analysis of RNA from mammary glands of BALB/c mice treated with E and P, E, and vehicle beeswax implants for 1, 3, and 14 days. E refers to treatment with E alone for the number of days designated. The absolute values for the entire control group (C) were low in this experiment, possibly due to an effect of the vehicle, but did not change significantly with time. Values represent the mean ± SEM. The *stars* denote that EP 14 and E 14 are statistically different from EP 1 and E 1, respectively; $P < 0.001$, n = 3.

Wnt-5B Expression Is Induced by E and P in ovx and Intact Mice

During normal mammary gland development, Wnt-5B expression is observed initially at 6–8 weeks in the virgin mouse and increases at the onset of pregnancy with maximal expression observed at day 16–18 of pregnancy (9–11). Wnt-5B expression increased 4-fold by day 8 of E and P treatment of intact mice as compared with the untreated (time zero) mice and was maximally induced by day 16 ($P < 0.004$, n = 3) as illustrated in Fig. 4A. Thus, the increase in Wnt-5B gene expression, which parallels that observed during midpregnancy, requires chronic E and P treatment. The pattern of Wnt-5B expression in the ovx mice (Fig. 4B) was similar to that observed in the intact animal but displayed a more dramatic response. Wnt-5B expression remained low at day 1 and day 3 but increased 9-fold at day 14 relative to the day 1 E- and P-treated group ($P < 0.001$, n = 3). In contrast to the regulation of Wnt-2, there was no significant effect of E alone on Wnt-5B expression in ovx mice. The large increase observed in Wnt-5B expression in ovx mice

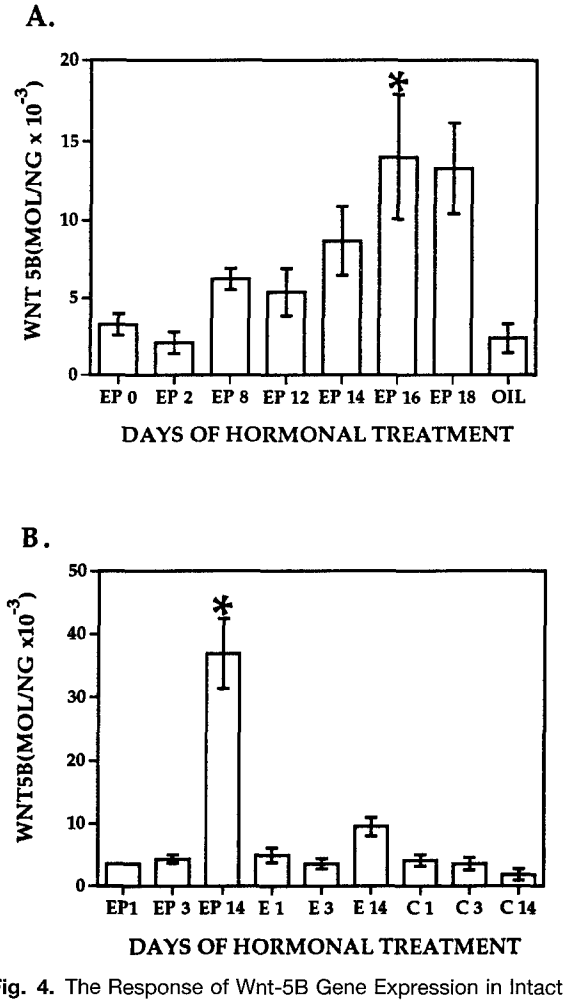

Fig. 4. The Response of Wnt-5B Gene Expression in Intact (A) and ovx (B) BALB/c Mice to E and P Treatment

A, Quantitative RT-PCR analysis of RNA from mammary glands of BALB/c mice injected daily with E and P, subcutaneously, for 18 days. Values represent mean ± SEM. The *star* denotes that EP 16 is statistically different from EP 0, $P < 0.004$, n = 3. B, Quantitative RT-PCR analysis of RNA from mammary glands of BALB/c mice treated with E and P beeswax implants for 1, 3, and 14 days. Values represent mean ± SEM. The *star* denotes that EP 14 is statistically different from EP 1; $P < 0.001$, n = 3.

may reflect the sensitization of the gland to P due to the absence of endogenous hormones and a rapid induction of PR gene expression.

Morphological Changes in Normal and Steroid Hormone-Treated Mice Correlate with the Changes in Wnt Gene Expression

Changes in Wnt-2 and Wnt-5B gene expression are coincident with morphological changes observed in the mammary gland in response to E and P treatment (Fig. 5). Mammary glands of 12-day E- and P-treated BALB/c mice (Fig. 5H) exhibit a morphology similar to that observed in an 8-day pregnant mouse. Several differences were observed, however, between the steroid hormone-treated glands and those from the normal midpregnant mouse, especially when comparing the first few days after hormone administration. For example, on the second day of treatment, transient alveolar proliferation was observed (Fig. 5F). However, by the fourth day these alveoli were no longer detectable, and a decrease in the amount of secondary branches was observed (Fig. 5). This transient alveolar budding has not been reported in mice treated with pharmacological doses of E and P but is similar to the effect observed in some strains of mice who respond to ovarian cycling by producing a transient alveolar proliferation in the mature virgin gland. This phenomena has, however, not been observed in BALB/c mice (1, 15). Surprisingly, at day 8 some major ducts displayed a ductal hypertrophy (Fig. 5G, *arrow*). This hypertrophy has been observed in mammary glands of mice implanted with hepatocyte-growth factor (HGF) and treated with E and P (16). Unlike the alveolar budding, this ductal hypertrophy was not transient and was still detectable in some glands at day 12–16 (Fig. 5H). Permanent alveoli appeared at day 12 and increased in number and density throughout the remainder of the treatment. This progression of morphological changes can be compared with the normal gland (1). During pregnancy, alveoli and secondary branching appear by day 4 and increase in density and number with the progression of pregnancy (Fig. 5, C and D).

These morphological alterations observed in hormonally treated and normal mammary glands can be correlated with the E- and P-induced changes in Wnt-2 and Wnt-5B gene expression. The appearance of transient alveoli at day 2 coincides with the decrease in Wnt-2 expression observed in E- and P-treated and normal glands. Conversely, permanent and functionally capable alveoli appear after 4–8 days of E and P treatment, preceding the increase in Wnt-5B expression. P concentrations increase gradually during pregnancy, affecting the formation of alveoli and the induction of the differentiated alveolar phenotype (6, 17). Appropriately, the increase in Wnt-5B expression in the E- and P-treated mouse requires

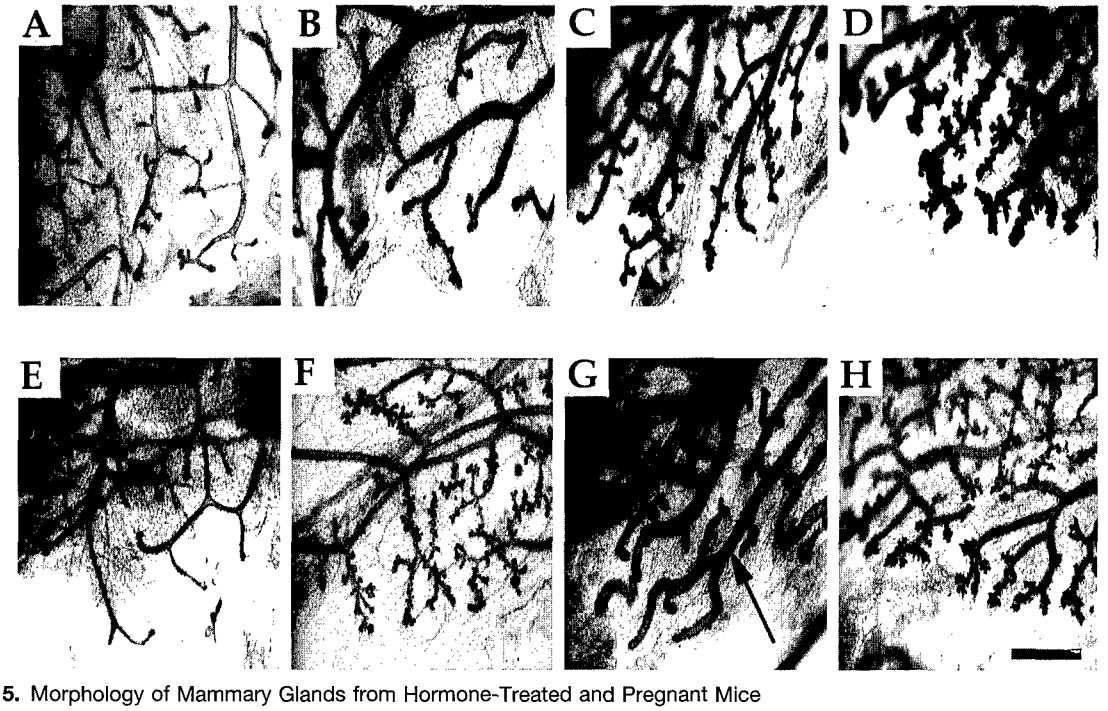

Fig. 5. Morphology of Mammary Glands from Hormone-Treated and Pregnant Mice

The progression of morphological changes in control mammary glands in response to the onset of pregnancy (panel A, 10-week virgin; B, day 2 pregnancy; C, day 4 pregnancy; D, day 12 pregnancy) and in E- and P-treated (panel E, untreated; panel F, E + P, 2 days of treatment; panel G, E + P, 4 days of treatment; panel H, E + P, 12 days of treatment). Mammary glands isolated from control and hormonally treated mice were stained with hematoxylin as described in *Materials and Methods*. Note the transient alveoli in panel F. The *arrow* in panel G denotes the hypertrophic duct. *Bar* = 100 μm.

long-term treatment of steroid hormones mimicking the pattern of morphological and gene expression changes, observed in the pregnant gland.

Differential Regulation of Wnt-2 and Wnt-5B Gene Expression in $PR^{-/-}$ Mammary Glands and in $PR^{-/-}$ Epithelium Transplanted into $PR^{+/+}$ Stroma after E and P Treatment

The response of Wnt-2 and Wnt-5B gene expression to the onset of pregnancy and exogenous E and P suggested that the P-signaling pathway might play a primary role in regulating Wnt gene expression in the mammary gland. To examine the role of the PR in Wnt gene regulation, Wnt gene expression levels were determined in $PR^{-/-}$ mice (12) after treatment with E and P. Wnt-5B gene expression did not change in response to E and P treatment in $PR^{-/-}$ mice (n = 3, Fig. 6A). However, the E and P repression of Wnt-2 expression was still observed but was not significant until day 8 of hormone treatment ($P < 0.003$, n = 3, Fig. 6B). This E-induced decrease in Wnt-2 gene ex-

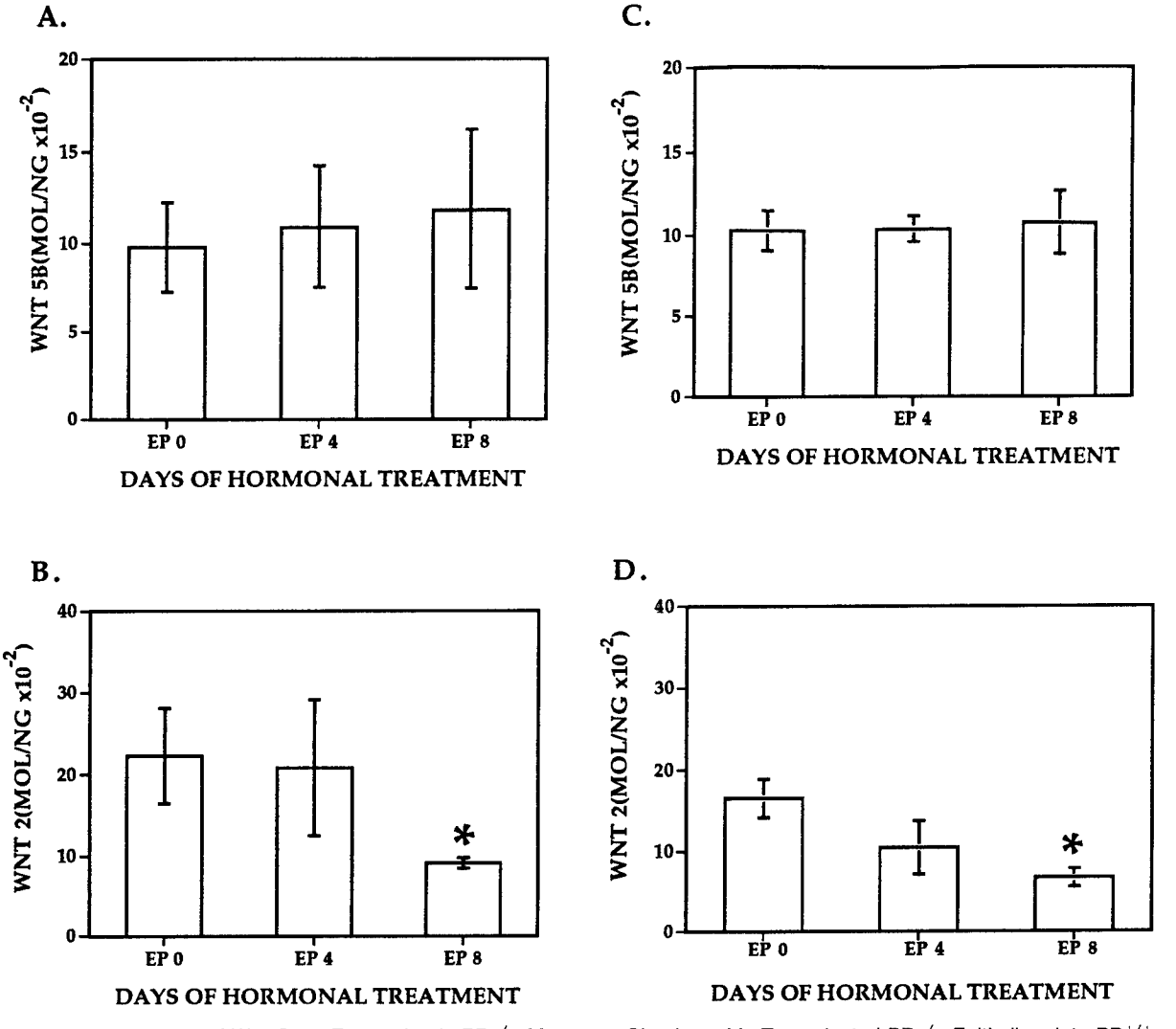

Fig. 6. The Response of Wnt Gene Expression in $PR^{-/-}$ Mammary Glands and in Transplanted $PR^{-/-}$ Epithelium into $PR^{+/+}$ Stroma to Steroid Hormone Treatment

A, Quantitative RT-PCR analysis of Wnt-5B gene expression from $PR^{-/-}$ mammary glands after daily injections with E and P, subcutaneously, for 0, 4, and 8 days (n = 3). B, Quantitative RT-PCR analysis of Wnt-2 gene expression from $PR^{-/-}$ mammary glands after daily injections with E and P, subcutaneously, for 0, 4, and 8 days. The *star* denotes that EP 8 is statistically different from EP 0; $P < 0.001$, n = 3. C and D, $PR^{-/-}$ epithelium was transplanted into cleared fat pads of $PR^{+/+}$ 129SvEv mice. After 10 weeks of growth, the mice were treated with E and P. C, Quantitative RT-PCR analysis of Wnt-5B gene expression in transplanted mammary glands after daily injections with E and P, subcutaneously, for 0, 4, and 8 days. Values represent the mean ± SEM (n = 6). D, Quantitative RT-PCR analysis of Wnt-2 gene expression in transplanted mammary glands after daily injections with E and P, subcutaneously., for 0, 4, and 8 days. Values represent the mean ± SEM. The *star* denotes that EP 8 is statistically different from EP 0; $P < 0.013$, n = 6.

pression was observed in the absence of any detectable changes in mammary gland morphology in the $PR^{-/-}$ mice.

To determine whether stromal or epithelial PRs were involved in differential Wnt gene response, the levels of Wnt transcripts were quantitated in RNA isolated from the previously described transplants. The role of the epithelium in the induction of Wnt-2 and Wnt-5B gene regulation was examined using $PR^{-/-}$ epithelium, transplanted into the stromal fat pad of cleared $PR^{+/+}$ hosts. In these transplants no increase in the level of P-dependent Wnt-5B expression was observed after 8 days of E and P treatment ($n = 6$, Fig. 6C). To confirm that the low level of Wnt-5B expression seen in the different samples was due to the response in the epithelium and not due to absence or degradation of RNA, the expression of glyceraldehyde-3-phosphate dehydrogenase (G3PDH) was also analyzed by RT-PCR. G3PDH transcripts are readily detectable and constant throughout the treatment period (data not shown). The same 129SvEv mice containing transplanted $PR^{-/-}$ epithelium and treated with E and P for 8 days still possessed the ability to repress Wnt-2 expression when subjected to steroid hormone treatment ($P < 0.013$, $n = 3$, Fig. 6D). Interestingly, the reduction of Wnt-2 gene expression was again delayed requiring 8 days of steroid hormone treatment as observed previously in $PR^{-/-}$ mice.

DISCUSSION

PR Deficiency in the Stroma and Epithelium Has Distinct Effects on Mammary Gland Development

The absence of lobuloalveolar development in the $PR^{-/-}$ transplants into the $PR^{+/+}$ fat pad after steroid hormone treatment indicates that the PR in the epithelium is required for this stage of mammary gland development. These results are consistent with previous studies showing that the absence of the PR influences lobuloalveolar development (12). Furthermore, in the reciprocal transplants, $PR^{+/+}$ epithelium into $PR^{-/-}$ stroma (Fig. 2, D and E), lobuloalveolar development was observed in response to E and P, indicating that the absence of the PR in the stroma does not significantly impair the ability of the epithelium to undergo alveolar differentiation. However, ductal growth was impaired, as the $PR^{+/+}$ epithelium failed to fill the $PR^{-/-}$ fat pad. In addition to the limited ductal development, unusual distended endbuds were present in these outgrowths. This restricted ductal growth may be due to disruption of reciprocal interactions between the stromal and epithelial compartments required for this stage of development. Less dramatic effects on ductal morphogenesis have been observed in the $PR^{-/-}$ mouse (12). This suggests that the $PR^{-/-}$ stroma, when recombined with $PR^{+/+}$ epithelium *in vivo*, lacks the mechanism to correctly interact with and stimulate growth in the epithelium and that the stroma fails to generate signals upon which the ductal growth of the epithelium is dependent. In contrast, in the $PR^{-/-}$ mouse, the $PR^{-/-}$ epithelium, in the presence of $PR^{-/-}$ stroma, has adapted to the absence of reciprocal signals, and the epithelium has become independent of these inputs required for ductal growth. This hormone-dependent reciprocity of growth regulation has been observed previously in recombination experiments with wild type and TfM androgen-insensitive mammary glands. These experiments revealed that the epithelium can induce the expression of mesenchymal androgen receptors. In turn, the mesenchyme condenses around the epithelium and causes an epithelial regression (18, 19).

The PR in the stroma is expressed in a temporally distinct pattern from the epithelial receptor, has a different signaling mechanism, and affects a separate group of target genes (5). Therefore, these data support the theory of two separate functional effects of mammary gland PR based on their compartmentalization and roles in development. The unexpected results observed in transplants of $PR^{+/+}$ epithelium in the $PR^{-/-}$ stroma suggest that there is a P-dependent stromal signal for ductal development. Recent *in vivo* studies of murine mammary glands treated with HGF in the presence of E and P suggest that HGF is a potential candidate second messenger for ductal growth in the mammary gland (16, 20). HGF-treated mammary glands respond to E and P by stimulating ductal growth. Interestingly, this growth factor has also been shown to regulate Wnt-5A expression (21). If this hypothesis is valid, it may be possible to rescue the $PR^{-/-}$ stroma defect by the direct addition of HGF. Unfortunately, because HGF knockouts are embryonic lethal and die before E16.5, no information has been obtained to date on mammary ductal development in these knockout mice (22).

Wnt-2 and Wnt-5B Gene Expression Are Regulated Independently by Steroid Hormones

This study demonstrates that two developmentally regulated Wnt genes are regulated by distinct mechanisms. The unique temporal and spatial patterns of expression of Wnt-2 and Wnt-5B suggest that these genes may play some role in the development of the mammary gland. The response of Wnt-2 and Wnt-5B to E and P treatment indicates that these genes are useful markers for the action of E in the virgin mammary gland, and for P during pregnancy, respectively. Wnt-2 gene expression is highest in the immature virgin gland of BALB/c mice and declines rapidly at the onset of pregnancy (9). In ovx and intact BALB/c mice this effect can be mimicked with the addition of pharmacological doses of E. This acute repression of Wnt-2 gene expression is correlated with the appearance of lobuloalveolar structures and the termination of ductal development. Conversely, an increase in Wnt-5B gene expression in ovx and intact mice requires chronic

treatment with E and P. Ovariectomy enhances the magnitude of this response. Without the stimulation from the ovaries, the basal levels of Wnt-5B expression are probably significantly reduced, thereby allowing an enhanced response. Wnt 5B provides one of the few molecular endpoints for the action of P, and changes in Wnt 5B are coincident with lobuloalveolar development.

The results from the $PR^{-/-}$ studies demonstrate that Wnt-5B gene expression is induced by P and dependent on the presence of PR specifically in the epithelial compartment. E alone has no effect on Wnt-5B expression. Interestingly, the PR present in the stroma cannot compensate for the absence of PR in the epithelium for lobuloalveolar development or for induction of Wnt 5B gene expression. This result implies that P acts directly on the epithelium to induce lobuloalveolar development and, either directly or indirectly, to activate Wnt-5B gene expression. E is required for induction and maintenance of PR expression in the mammary gland (6). Therefore, it is unlikely that the regulation of Wnt-5B expression is independent of E.

Wnt-2 gene expression was inhibited by administration of E in both $PR^{-/-}$ mice and in transplanted $PR^{-/-}$ epithelium. These results suggest that Wnt-2 gene expression is not primarily regulated by PR signaling. In the $PR^{-/-}$ studies there was a delay in the kinetics of the Wnt-2 response. The absence of the PR may have restricted the development of the gland in these mice and slowed the appearance of the ER, which normally appears at 4 weeks of age (23, 24). Alternatively, the absence of the PR could influence reciprocal interactions between the stroma and the epithelium, thereby preventing proper induction of ERs. ER gene expression is affected by feedback controls between E and other hormones including P (14).

Previous studies performed in Parks mice demonstrated Wnt-2 expression through midpregnancy and a repression of Wnt-2 and Wnt-5B expression after ovariectomy (11). Parks mice possess virgin lobuloalveolar development, which is absent in BALB/c mice, and it is possible that this epithelial sensitivity to estrous-associated hormones alters the regulation of Wnt-2 and Wnt-5B gene expression.

The rapid repression of Wnt-2 expression suggests the ER may be directly regulating Wnt-2. The ER is expressed in both the stroma and epithelium including the endbud (5, 14, 23–25). Interestingly, PR is induced by the ER-signaling pathway in the epithelial compartment 48 h after initial addition of E (26). This temporal delay in receptor response coincides exactly with the initial decrease observed in Wnt-2 gene expression after hormonal treatment. Therefore, the timing of this E-induced gene expression and localization of some Wnt-2 transcripts in the epithelium suggests that Wnt-2 could be regulated directly by E.

The Wnts Are Growth Factors with Pleiotropic Effects on Development

The development of the mammary gland is dependent on the interaction and cooperation of growth factors and hormones functioning through the stromal and epithelial compartments. Studies of PRL, epidermal growth factor, FGF, TGFα and β, insulin-like growth factor, and HGF action reveal that they are regulated in specific spatial and temporal patterns and have effects on proliferation and differentiation in mammary gland development (1, 27–30). The developmentally associated expression pattern, their role in the development of other organisms, biochemical characteristics, and hormonal regulation of the Wnts suggest that they are members of this complex family of locally acting growth factors.

The function of the Wnt genes in the development of the mammary gland can only be inferred from limited expression studies *in vivo* and *in vitro* and functional studies in other organisms. Wingless, the *Drosophila* homolog of Wnt-1, has proliferative, inductive, and cell fate determination functions (8). In addition, Wnt genes have demonstrated functional roles in *Xenopus*, mouse, and chicken (31–36). These diverse studies revealed that Wnt genes can possess inductive, growth-stimulatory, and growth-restrictive functions all within a single organism.

In the mammary gland, overexpression of Wnt-1 influences the proliferation of mammary epithelium (37). The expression of Wnt-4 and Wnt-5A has been inversely correlated with proliferation in mammary epithelial cells (38). Because of its localization both within and around the highly proliferative terminal endbud, it is possible that Wnt-2 has a role in regulating proliferation in the virgin gland. The pattern of Wnt-5B expression and its dependence on the PR suggests that it interacts with cells in a more differentiated state. Interestingly, proliferation is high in the pregnant gland coincident with the increase in Wnt-5B expression. Localization of Wnt-5B transcripts to the ductal epithelium reveals it is expressed in the proper cellular location to be involved in regulating proliferation in these cells. The localization of Wnt-5B and Wnt-2 transcripts to the ductal epithelial and stromal compartments of the mammary gland (9, 11), respectively, suggest that although these two genes may have separate or even overlapping functional roles, their temporal and spatial expression patterns restrict their activity to specific stages of development. Therefore, it is probable that the expression of these Wnt genes is regulated in a specific manner to restrict their functional activities to particular developmental stages in the mammary gland.

Alteration of Wnt Gene Expression Can Transform Mammary Epithelium

In the mammary gland, ectopic expression of the Wnt genes has dramatic consequences on the transforma-

tion and development of the gland. Inappropriate expression of Wnts either temporally or spatially may result in mammary tumorigenesis. For example, Wnt-1 and Wnt-4 have been demonstrated to affect the development and transformation of the gland *in vivo* (37, 39, 40). Numerous other Wnts, including Wnt-2 and Wnt-5B, have *in vitro* transforming effects (41, 42). These *in vitro* transfection experiments have revealed that separate classes of Wnts exist that are distinguished by their transforming ability (43), although the properties defined in these *in vitro* assays do not always correspond to their effects *in vivo* (R. C. Humphreys and J. M. Rosen, submitted for publication).

In addition, overexpression of Wnt genes, including Wnt-2 and Wnt-5B, has been found associated with tumors in the breast and intestinal epithelium (44–47). Thus, loss of regulatory control on these two Wnt genes, as with other growth factor molecules like TGF-β and FGF (48, 49), has deleterious consequences for the development of the mammary gland. Interestingly, compartment switching of Wnt-2 expression from breast fibroblasts to tumor epithelium has been observed recently in human breast tumors (50). Therefore, there is evidence for a critical role of Wnt-2, and possibly Wnt-5B, in the transformation of the gland. Since most of the Wnt knockouts are embryonic lethals resulting in neural or kidney defects, the precise functional roles of these and other Wnt family members on normal mammary gland development will require the use of tissue-specific or regulated knockouts.

To summarize, the Wnt genes act in a cell-autonomous manner in cooperation with other growth factors and have pleuripotent effects on various developmental processes within the same organism (8). Wnt gene expression can be differentially regulated by steroid hormones in the mammary stroma and epithelium where they may act as locally acting growth factors to influence ductal and lobuloalveolar development. Hopefully, with the recent discovery of the Wnt receptor in *Drosophila* (51), the mechanism of Wnt action and the function of the individual Wnt family members in mammary gland development will begin to be illuminated.

MATERIALS AND METHODS

Animals

BALB/c mice were acquired from Charles River Laboratories (Wilmington, MA) or from a breeding colony at Baylor College of Medicine, courtesy of Dr. Daniel Medina. Mice carrying the PRKO mutation in the 129SvEv inbred genetic background were used in these studies. All animals were maintained according to IACUC approved guidelines.

Isolation of Mammary Glands and RNA

Number 4 (thoracic) mammary glands were removed from aged matched 6- and 8-week-old virgin BALB/c and C3H mice using standard surgical techniques. The thoracic and inguinal mammary glands from 11-week-old wild type control mice, 6-week-old 129SvEv $PR^{-/-}$ mice, 129SvEv $PR^{+/+}$, and 129SvEv $PR^{-/-}$ mice with transplanted PR-deficient epithelium or wild type epithelium, respectively, were removed using standard surgical techniques. For morphological analysis, mammary glands were fixed in Tellyesniczky's solution for 5 h and stained with hematoxylin as described previously (52). For isolation of RNA, mammary glands were homogenized in a PT2000 Polytron (Brinkmann, Westbury, NY) with RNazol (Biotecx, Houston, TX) as described by the manufacturer or homogenized in 4 M guanididium isothiocynate (Sigma, St. Louis MO) and isolated by CsCl centrifugation method. RNA was quantitated spectrophotometrically and stored at −20 C in 70% ethanol.

Construction and Transcription of cRNA Templates

Quantitative noncompetitive RT-PCR was performed as previously described (9). Complementary DNAs from Wnt-5B and Wnt-2 were prepared according to standard bacterial plasmid isolation protocols, and the DNA was purified on Qiagen (Qiagen, Chatsworth, CA) columns according to the manufacturer and isolated from the vector using unique restriction enzymes. To construct the Wnt-2 cDNA deletion template, *Sty*I (New England Biolabs, Beverly, MA) was used to excise a fragment from bases 493–580. Digestion products were separated from the small internal fragment, religated, and subcloned into the vector pBKSII (Stratagene, La Jolla, CA). Clones were analyzed for a size difference and sequenced to confirm the location of the deletion. The Wnt-5B template was constructed in the same manner with an *Ava*I (New England Biolabs, Beverly MA) deletion of bases 501–576. Both templates were sequenced to confirm the orientation in the vector and the presence of an internal deletion. These constructs were used as templates for *in vitro* transcription reactions as described in Promega Protocols and Applications Guide, ed 2 (Promega, Madison WI). The cRNA reactions were treated with 1 U of ribonuclease-free RQ1 deoxyribonuclease in deoxyribonuclease buffer (Promega) for 60 min at 37 C and then extracted with phenol-chloroform twice and precipitated with 3 M NaAc and 100% ethanol at −20 C. The cRNA was resuspended in Tris-EDTA, quantitated spectrophotometrically, and stored at −20 C in 70% ethanol. Each template was assayed by PCR to confirm the absence of contaminating cDNA template. Optimum RT-PCR conditions for each of the templates were developed that allowed a linear response with respect to the RNA input and exhibited noncompetitive PCR.

Quantitative RT-PCR

Isolated RNA was transcribed in a reaction consisting of 1× *Taq* polymerase buffer (Promega), 3 mM $MgCl_2$, 100 pmol hexanucleotide random primers (Boehringer Mannheim, Indianapolis, IN) 1.25 U of RT (GIBCO BRL, Gaithersburg MD), 1 mM of each of four deoxynucleoside triphosphates (Pharmacia, Milwaukee WI), and 20 U of RNasin (Pharmacia, Milwaukee WI) in a final reaction volume of 20 μl. Fifty nanograms, 100 ng, and 150 ng of sample RNA were added to separate RT reactions. A constant amount of cRNA template (~10,000 molecules) was added to each RT reaction as an internal standard to control for differences in RT and PCR reaction efficiency.

The primer sequences for the Wnt-2 and Wnt-5B amplifications, respectively, were:

forward: 5′-AGTCGGGAATCGGCCTTTGTTTACG-3′ and reverse: 5′-AAAGTTCTTCGCGAAATGTCGGAAG-3′; forward: 5′-GACAGCGCCGCGGCCATGCGC-3′ and reverse: 5′-CATTTGCAGGCGACATCAGC-3′. PCR conditions were 94 C for 1 min, 60 C for 2 min, and 72 C for 3 min, for 30 cycles and 94 C for 1 min, 65 C for 2 min, and 72 C for 3 min

for 32 cycles for Wnt-2 and Wnt-5B, respectively. Primers for G3PDH were: forward: 5′-AGAGGCCTTTGCTCGAACTG-GAAAG-3′ and reverse: 5′-CACCAAGACGTCTGTCGC-CTACTTA-3. PCR conditions were 94 C for 1 min, 60 C for 2 min, and 72 C for 3 min, for 30 cycles. All PCRs were followed by an extension at 72 C for 5 min. PCR was performed with 10 μl of each RT reaction, 2 mM magnesium chloride, 1×PCR buffer (Promega), 0.1 μCi [α-^{32}P]dCTP (NEN DuPont, Boston, MA), 1 U of *Taq* polymerase (Promega, Madison WI) in a final reaction volume of 50 μl. Ten microliters of the RT-PCR products were separated on a 2% Nusieve agarose (FMC Bioproducts, Rockland, ME) gel and transferred overnight in 0.4 M NaOH to Hybond N^+ nylon membrane (Amersham, Buckinghamshire, UK), and the radioactive signal was quantitated with 4–8 h exposure on a PhosphoImager (Molecular Dynamics, Sunnyvale, CA).

Steroid Hormone Treatment of Mice

All groups of mice were treated with 1 mg of P (Steris, Phoenix, AZ) and 1 μg of 17 β-estradiol (Sigma) per day in 60 μl of sesame seed oil (Sigma) subcutaneously. Mammary glands were collected at days 0, 1, 2, 4, 8, 12, and 18. Animals were ovariectomized and allowed to regress for 4 weeks before hormone treatments were begun. Beeswax implants containing 20 μg of E and/or 20 mg of P were synthesized by adding the powdered form of the hormones to melted beeswax. The suspended hormone mixture was dropped onto dry ice to form pellets. The pellets, synthesized to deliver 1 mg P and 1 μg E/day, respectively, were implanted subcutaneously in the neck of the mice for 2 weeks. Inguinal mammary glands were collected at days 1, 3, and 14 and analyzed as described.

Transplantation Studies

Tissue fragments of 10-week-old virgin $PR^{-/-}$ mammary epithelium were isolated and implanted into six PR-positive 129SvEv hosts using the technique described by DeOme *et al.* (13). Epithelium from 129SvEv hosts was removed as described (13). In addition, tissue fragments from a 10-day pregnant 129SvEv $PR^{+/+}$ mammary epithelium were isolated and implanted into four $PR^{-/-}$ 129SvEv hosts. Due to the limited number of $PR^{-/-}$ homozygote recipients and the limited extent of ductal outgrowth, these glands could not be examined for changes in Wnt gene expression. Mammary gland epithelial transplants were allowed to proliferate and penetrate the stromal fat pad for 10 weeks and then treated with steroid hormones as described above. Control experiments with wild type 129SvEv $PR^{+/+}$ epithelium into cleared fat pads of three wild type 129SvEv $PR^{+/+}$ mice were performed in the same manner.

Whole Mount Staining and Sectioning

The whole gland staining was carried out essentially as described (25) except that glands were stained for only 2 h in hematoxylin.

Acknowledgments

The authors thank Dr. Susanne Krnacik for providing the RNA for the ovariectomy experiments and for critical reading of the manuscript.

Received September 9, 1996. Revision received November 14, 1996. Accepted November 21, 1996.

Address requests for reprints to: Jeffrey M. Rosen, Baylor College of Medicine, Houston, Texas 77030.

This work was supported by NIH Grant CA-64255 and Grant DAMD17-94-J-4253 from the Department of Defense (to J.M.R.).

REFERENCES

1. Imagawa W, Yang J, Guzman R, Nandi S 1994 Control of Mammary Gland Development. In: Knobrl E, Neill JD (eds) The Physiology of Reproduction. Raven Press, New York, pp 1033–1063
2. Daniel CW, Silberstein GB 1987 Postnatal development of the rodent mammary gland. In: Neville MC, Daniel CW (eds) The Mammary Gland. Plenum Press, New York, pp 3–36
3. Vonderhaar BK 1988 Regulation of development of the normal mammary gland by hormones and growth factors. Cancer Treat Res 40:251–266
4. Cunha GR, Hom YK 1996 Role of mesenchymal-epithelial interactions in mammary gland development. J Mammary Gland Biol Neoplasia 1:21–35
5. Haslam SZ, Shyamala G 1981 Relative distribution of estrogen and progesterone receptors among the epithelial, adipose, and connective tissue components of the normal mammary gland. Endocrinology 108:825–830
6. Haslam SZ 1988 Acquisition of estrogen-dependent progesterone receptors by normal mouse mammary gland. Ontogeny of mammary progesterone receptors. J Steroid Biochem 31:9–13
7. Nusse R, van OA, Cox D, Fung YK, Varmus H 1984 Mode of proviral activation of a putative mammary oncogene (int-1) on mouse chromosome 15. Nature 307:131–136
8. Klingensmith J, Nusse R 1994 Signaling by wingless in *Drosophila*. Dev Biol 166:396–414
9. Bühler TA, Dale TC, Kieback C, Humphreys RC, Rosen JM 1993 Localization and quantification of Wnt-2 gene expression in mouse mammary development. Dev Biol 155:87–96
10. Gavin BJ, McMahon AP 1992 Differential regulation of the wnt gene family during pregnancy and lactation suggests a role in postnatal development of the mammary gland. Mol Cell Biol 12:2418–2423
11. Weber-Hall SJ, Phippard DJ, Niemeyer CC, Dale TC 1994 Developmental and hormonal regulation of Wnt gene expression in the mouse mammary gland. Differentiation 57:205–214
12. Lydon JP, DeMayo FJ, Funk CR, Mani SK, Hughes AR, Montgomery CJ, Shyamala G, Conneely OM, O'Malley BW 1995 Mice lacking progesterone receptor exhibit pleiotropic reproductive abnormalities. Genes Dev 9:2266–2278
13. DeOme KB, Faulkin LJ, Bern HA, Blair PB 1958 Development of mammary tumors from hyperplastic alveolar nodules transplanted into gland-free mammary pads of female C3H mice. Cancer Res 19:515–519
14. Haslam SZ 1989 The ontogeny of mouse mammary gland responsiveness to ovarian steroid hormones. Endocrinology 125:2766–2772
15. Vonderhaar BK 1984 Hormone and growth factors in mammary gland development. In: Veneziale CM (ed) Control of Cell Growth and Proliferation. Van Nostrand-Reinhold, Princeton, NJ, pp 11–33
16. Jones FE, Jerry JJ, Guarino BC, Andrews GC, Stern DF 1996 Heregulin induces *in vivo* proliferation and differentiation of mammary epithelium into secretory lobuloalveoli. Cell Growth Differ 7:1031–1038
17. Murr SM, Stabenfeldt GH, Bradford GE, Geschwind II 1974 Plasma progesterone during pregnancy in the mouse. Endocrinology 94:1209–1211
18. Heuberger B, Fitzka I, Wasner G, Kratochwil K 1982 Induction of androgen receptor formation by epithelium-mesenchyme interaction in embryonic mouse mammary

gland. Proc Natl Acad Sci USA 79:2957–2961
19. Kratochwil K 1987 Tissue combination and organ culture studies in the development of the embryonic mammary gland. In: Gwatkin RBL (ed) Developmental Biology: A Comprehensive Synthesis. Plenum Press, New York, pp 315–334
20. Yang Y, Spitzer E, Meyer D, Sachs M, Niemann C, Hartmann G, Weidner KM, Birchmeier C, Birchmeier W 1995 Sequential requirement of hepatocyte growth factor and neuregulin in the morphogenesis and differentiation of the mammary gland. J Cell Biol 131:215–226
21. Huguet EL, Smith K, Bicknell R, Harris AL 1995 Regulation of Wnt5a mRNA expression in human mammary epithelial cells by cell shape, confluence, and hepatocyte growth factor. J Biol Chem 270:12851–12856
22. Schmidt C, Bladt F, Goedecke S, Brinkmann V, Zschlesche W, Sharpe M, Gherardi E, Birchmeier C 1995 Scatter factor/hepatocyte growth factor is essential for liver development. Nature 373:699–702
23. Muldoon TG 1978 Characterization of mouse mammary tissue estrogen receptors under conditions of differing hormonal backgrounds. J Steroid Biochem 9:485–494
24. Hunt ME, Muldoon TG 1977 Factors controlling estrogen receptor levels in normal mouse mammary tissue. J Steroid Biochem 8:181–186
25. Daniel CW, Silberstein GB, Strickland P 1987 Direct action of 17 beta-estradiol on mouse mammary ducts analyzed by sustained release implants and steroid autoradiography. Cancer Res 47:6052–6057
26. Shyamala G, Ferenczy A 1984 Mammary fat pad may be a potential site for initiation of estrogen action in normal mouse mammary glands. Endocrinology 115:1078–1081
27. Knight CH, Peaker M 1982 Development of the mammary gland. J Reprod Fertil 65:521–536
28. Nandi S 1959 Hormonal control of mammogenesis and lactogenesis in the C3H/He Crgl mouse. In: Stern C, Benson S, Quay W (eds) University of California Berkeley Publications in Zoology. University of California Press, Berkeley, pp 1–128
29. Topper YJ, Freeman CS 1980 Multiple hormone interactions in the developmental biology of the mammary gland. Physiol Rev 60:1049–1106
30. Plaut K, Ikeda M, Vonderhaar BK 1993 Role of growth hormone and insulin-like growth factor-I in mammary development. Endocrinology 133:1843–1848
31. Cui Y, Brown JD, Moon RT, Christian JL 1995 Xwnt-8b: a maternally expressed Xenopus Wnt gene with a potential role in establishing the dorsoventral axis. Development 121:2177–2186
32. Du SJ, Purcell SM, Christian JL, McGrew LL, Moon RT 1995 Identification of distinct classes and functional domains of Wnts through expression of wild-type and chimeric proteins in Xenopus embryos. Mol Cell Biol 15:2625–2634
33. Augustine KA, Liu ET, Sadler TW 1995 Interactions of Wnt-1 and Wnt-3a are essential for neural tube patterning. Teratology 51:107–119
34. Hollyday M, McMahon JA, McMahon AP 1995 Wnt expression patterns in chick embryo nervous system. Mech Dev 52:9–25
35. Yoshioka H, Ohuchi H, Nohno T, Fujiwara A, Tanda N, Kawakami Y, Noji S 1994 Regional expression of the Cwnt-4 gene in developing chick central nervous system in relationship to the diencephalic neuromere D2 and a dorsal domain of the spinal cord. Biochem Biophys Res Commun 203:1581–1588
36. McMahon AP, Bradley A 1990 The wnt-1 (int-1) proto-oncogene is required for development of a large region of the mouse brain. Cell 62:1073–1085
37. Edwards PA, Hiby SE, Papkoff J, Bradbury JM 1992 Hyperplasia of mouse mammary epithelium induced by expression of the Wnt-1 (int-1) oncogene in reconstituted mammary gland. Oncogene 7:2041–2051
38. Olson DJ, Papkoff J 1994 Regulated expression of Wnt family members during proliferation of C57mg mammary cells. Cell Growth Differ 5:197–206
39. Lin TP, Guzman RC, Osborn RC, Thordarson G, Nandi S 1992 Role of endocrine, autocrine, and paracrine interactions in the development of mammary hyperplasia in Wnt-1 transgenic mice. Cancer Res 52:4413–4419
40. Bradbury JM, Edwards PA, Niemeyer CC, Dale TC 1995 Wnt-4 expression induces a pregnancy-like growth pattern in reconstituted mammary glands in virgin mice. Dev Biol 170:553–563
41. Bradley RS, Brown AM 1995 A soluble form of Wnt-1 protein with mitogenic activity on mammary epithelial cells. Mol Cell Biol 15:4616–4622
42. Blasband A, Schryver B, Papkoff J 1992 The biochemical properties and transforming potential of human wnt-2 are similar to wnt-1. Oncogene 7:153–161
43. Wong GT, Gavin BJ, McMahon AP 1994 Differential transformation of mammary epithelial cells by Wnt genes. Mol Cell Biol 14:6278–6286
44. Huguet EL, McMahon JA, McMahon AP, Bicknell R, Harris AL 1994 Differential expression of human Wnt genes 2, 3, 4, and 7B in human breast cell lines and normal and disease states of human breast tissue. Cancer Res 54:2615–2621
45. Iozzo RV, Eichstetter I, Danielson KG 1995 Aberrant expression of the growth factor Wnt-5A in human malignancy. Cancer Res 55:3495–3499
46. Lejeune S, Huguet EL, Hamby A, Poulsom R, Harris AL 1995 Wnt5a cloning, expression, and upregulation in human primary breast cancers. Clin Cancer Res 1:215–222
47. Vider BZ, Zimber A, Chastre E, Prevot S, Gespach C, Estlein D, Wolloch Y, Tronick SR, Gazit A, Yaniv A 1996 Evidence for the involvement of the Wnt 2 gene in human colorectal cancer. Oncogene 12:153–158
48. MacArthur CA, Shankar DB, Shackleford GM 1995 Fgf-8, activated by proviral insertion, cooperates with the Wnt-1 transgene in murine mammary tumorigenesis. J Virol 69:2501–2507
49. Shackleford GM, MacArthur CA, Kwan HC, Varmus HE 1993 Mouse mammary tumor virus infection accelerates mammary carcinogenesis in Wnt-1 transgenic mice by insertional activation of int-2/Fgf-3 and hst/Fgf-4. Proc Natl Acad Sci USA 90:740–744
50. Dale TC, Weber-Hall SJ, KS, Huguet EL, Jayatilake H, Gusterson BA, Shuttleworth G, O'Hare M, Harris AL 1996 Compartment switching of WNT-2 expression in human breast tumors. Cancer Res 56:4320–4323
51. Bhanot P, Brink M, Samos CH, Hsieh J-C, Wang Y, Macke JP, Andrew D, Nathans J, Nusse R 1996 The new member of the *frizzled* family from *Drosophila* functions as a wingless receptor. Nature 382:225–230
52. Humphreys RC, Krajewska M, Krnacik S, Jaeger R, Weiher H, Krajewski S, Reed JC, Rosen JM 1996 Apoptosis in the terminal endbud of the murine mammary gland: a mechanism of ductal morphogenesis. Development 122:4013–4022

Journal of Mammary Gland Biology and Neoplasia, Vol. 2, No. 4, 1997

Use of PRKO Mice to Study the Role of Progesterone in Mammary Gland Development

Robin C. Humphreys,[1] John P. Lydon,[2] Bert W. O'Malley,[2] and Jeffrey M. Rosen[2,3]

To better understand the distinct physiological roles played by progesterone and estrogen receptors (PR amd ER)[4] as well as to study directly PR function in an *in vivo* context, a novel mutant mouse strain, the PR knockout (PRKO) mouse, was generated carrying a germline loss of function mutation at the PR locus. Mouse mammary gland development has been examined in PRKO mice using reciprocal transplantation experiments to investigate the effects of the stromal and epithelial PRs on ductal and lobuloalveolar development. The absence of PR in transplanted donor epithelium, but not in recipient stroma, prevented normal lobuloalveolar development in response to estrogen and progesterone treatment. Conversely, the presence of PR in the transplanted donor epithelium, but not in the recipient stroma, revealed that PR in the stroma may be necessary for ductal development. Stimulation of ductal development by the PR may, therefore, be mediated by an unknown secondary signaling molecule, possibly a growth factor. The continued stimulation of the stromal PR appears to be dependent on reciprocal signal(s) from the epithelium. Thus, the combination of gene knockout and reciprocal transplantation technologies has provided some new insights into the role of stromal-epithelial interactions and steroid hormones in mammary gland development.

KEY WORDS: Progesterone receptor; gene knockout; reciprocal transplantation; ductal and lobuloalveolar development; stromal-epithelial interactions.

INTRODUCTION

The development of the murine mammary gland is dependent upon and regulated by systemic steroid hormones and locally-acting growth factors (1–3). These competing and complementary, growth and differentiation signals modulate the physical and molecular characteristics of the stromal and epithelial compartments. In turn, the interaction between the stroma and epithelium regulates molecular signaling pathways that are critical for the proper morphological and functional development of the gland. Elucidating these complex interactions, which regulate mammary gland development, is facilitated by the mammary gland's intrinsic ability to recapitulate all of the ductal and lobular structures from a fragment of syngenic epithelium. This regenerative characteristic has been exploited by separating and then recombining stromal and epithelial components which may be deficient in a particular signaling molecule. Such recombination experiments have allowed insight into the nature of interactions between the stroma and epithelium in the regulation of tissue fate determination by the androgen receptor as well as in mechanisms of epithelial transformation (4–15).

Direct evidence for the role of the PR in mammary gland development had been restricted to *in vivo* hormone binding studies and *in vitro* culture experiments

[1] National Institutes of Health, Developmental Biology Section, Laboratory of Biochemistry and Metabolism, Bethesda, Maryland 208922.

[2] Department of Cell Biology, Baylor College of Medicine, One Baylor Plaza, Houston, Texas 77030.

[3] To whom correspondence should be addressed. e-mail: jrosen@bcm.tmc.edu

[4] **Abbreviations:** progesterone receptor knockout (PRKO); progesterone receptor (PR); embryonic stem cells (ES cells); estrogen receptor knockout (ERKO); estrogen receptor (ER).

1083-3021/97/1000-0343$12.50/0

(16–19). Recently, a PR knockout mouse ($PR^{-/-}$) was generated (20). In this chapter we will describe the generation of this mouse and the recombination experiments performed to explore the role of this critical steroid receptor in mammary gland development.

Receptor Ontology and Biochemistry

Alterations in systemic blood levels of steroid hormones synthesized by the pituitary and the ovaries regulate the global development of the mammary gland (3). These systemic changes in hormone levels are manifested at the cellular level by changes in receptor activation, the induction of second messenger signaling pathways and the expression of a number of different locally-acting growth factors, including members of the EGF, IGF and FGF families (21–23). The localized effects of most of these growth factors are variously due to protein stability, adhesion and residence in the extracellular matrix, transport and secretion, and availability of receptor molecules. For this reason they are believed to act as local mediators of the differentiative and proliferative signals of the systemic hormones. This systemic regulation of locally-acting growth factor activity allows for fine regulation of large scale developmentally-associated proliferative and differentiative functions, as well as coordination of the development of the stromal and epithelial compartments.

The steroid hormones, estrogen and progesterone, have pronounced effects on the development of the mammary gland. In cooperation with pituitary hormones, these steroids are the primary systemic regulatory molecules for the induction of proliferation and differentiation of epithelial and stromal cells leading first to the formation of ductal and alveolar structures, and finally, to a functional, secretory mammary gland. The interactions of estrogen and progesterone with growth hormone, prolactin and insulin in regulating this differentiative process have been well documented (24).

The physiological effects of progesterone are mediated, at the cellular level, by a specific intracellular receptor, termed the PR (25,26), a member of an expanding superfamily of nuclear transcription factors (27,28). Upon progesterone binding, the receptor undergoes a series of complex conformational changes, including phosphorylation, before interacting with regulatory sequences in target genes. Activation and/or repression of these genes leads to the physiological response of the progestin-target tissue to progesterone.

Expression and transcriptional activity of the PR gene is regulated in most tissues by estrogen and pituitary hormones (17,29). In addition, there are two isoforms of the receptor both of which are capable of binding ligand (26,30). Activation of receptor and the developmental consequences of this activation can be modulated by transcriptional activation of its gene, changes in receptor stability, multiple receptor isoforms, the presence of binding proteins, and intracellular localization of the receptor binding complex. The majority of the receptor, when complexed with ligand, localizes to the nucleus (31). The PR appears to be directly involved in gene regulation as evidenced by the localization of potential progesterone response elements (PRE) in the promoters of certain genes. However, relatively few specific progesterone-regulated target genes have been identified to date.

Biochemical analysis of isolated mammary stroma and epithelium demonstrated the presence of two separable progesterone binding activities. Early experiments by Haslam *et al.* suggested that there were two populations of PR; one in the stroma and the other in the epithelium (17,18,29,32). These two populations of receptor have been distinguished by their ontology and biochemistry. The stromal receptor appears earlier in development at five weeks postnatal life; the epithelial receptor appears later at eight weeks. The two receptor populations are also distinguished by their ability to respond to induction of transcription by the steroid hormone estrogen. Hormone treatment of ovariectomized mice revealed that the level of stromal receptor is refractory to estrogen, whereas epithelial receptor expression decreases after ovariectomy and can be restored by addition of estrogen.

Recently Silberstein *et al.* (33) reported the presence of PR in the epithelial cells of the terminal endbud and duct. In the virgin animal, PR positive cells exhibited both cytoplasmic and nuclear localization of the receptor. In contrast, during pregnancy the proportion of cells with nuclear localization of the receptor increased, suggesting a different mechanism for PR action in the pregnant gland. Interestingly, no immunoreactive material was detected in the stroma of these murine mammary glands. In fact, no direct evidence has been presented, to date, to localize the stromal PR *in situ*. These differing biochemical, molecular and ontological observations imply some functional distinctions between the two populations of receptors.

Generation of a PR-Deficient Mouse Model

In most target tissues examined, PR gene transcription is stimulated by estrogen via the estrogen receptor (ER), implying that many of the observed physiological responses attributed to PR could conceivably be due to the combined effects of progesterone and estrogen. Therefore, to understand better the distinct physiological roles of the PR and ER, as well as to study PR function directly in an *in vivo* context, a novel mutant mouse strain, PRKO mouse, was generated using the techniques of gene targeting in mouse embryonic stem (ES) cells. This mouse carries a germline loss of function mutation at the PR locus (20). The experimental approach that was used to mutate the PR gene in mouse ES cells was a positive/negative selection strategy described previously (34). The mutation consisted of insertion of a bacterially-derived, neomycin resistance cassette into the first exon of the PR gene, downstream from the initiating codons ATG_A and ATG_B that encode the A and B forms of the receptor, respectively (25,26,30). This type of insertion effectively disrupts the transcription of both forms of the PR.

ES cells carrying the PR-targeted mutation were used to generate mice heterozygous and then homozygous for this mutation. Interestingly, previous studies had revealed the existence of transcripts for both PR and ER in the early stages of mouse blastocyst development (35), suggesting an essential role for these nuclear receptors in early embryogenesis. However, intercrossing mice heterozygous for the PR mutation resulted in the generation of viable homozygous PR mutant pups at the normal Mendelian frequency and sex ratio. These results demonstrate that embryonically-derived PR, like embryonically-derived ER (36,37) is not required for embryonic survival or for prenatal development of the female reproductive system.

To date, adult homozygous mice for both sexes appear healthy and have developed normal external genitalia. Gross anatomical examination has not revealed obvious differences in organ morphology between the homozygous and their wild type or heterozygous littermates. However, as might be expected, female homozygotes proved to be infertile in crosses with wild type males. Conversely, male homozygotes were found to be as fertile as their wild type and heterozygous male siblings. This phenotypic result not only differs strikingly from that observed for the ER knockout (ERKO) mutant male mouse (36) but also provides the necessary *in vivo* support for the purported involvement of a nonclassical receptor (membrane receptor) in the mediation of the progesterone-initiated acrosome reaction in sperm development (38).

Although both male and female mice deficient in PR underwent apparently normal embryogenesis and developed to adulthood, female mice homozygous for this mutation exhibited extensive functional abnormalities in a number of reproductive tissues including the uterus, ovary and mammary gland, as well as an inability to display a normal sexual behavioral response (20,39). Based on the established role of PR in uterine development, an infertility phenotype was expected in the female mouse; however, the variety of reproductive systems that were affected was surprising. Collectively, these results underscore the essential role that this nuclear receptor occupies in coordinating the diverse events that ensure the reproductive success of the species.

The original description of this animal model has been published (20). This review specifically details the mammary gland phenotypic results obtained to date as a consequence of removing PR function in the mouse.

Complete Mammary Gland Development Requires PR

Until recently, it was generally assumed that the normal proliferation of the mammary gland epithelium, as well as the initiation and progression of mammary tumorigenesis, were dependent primarily on the ovarian steroid estrogen (40). This assumption was based largely on established estrogen-induced proliferative effects on the endometrial luminal epithelial cell. Progesterone, based on its anti-estrogenic effects in the endometrium, was also assumed to have anti-proliferative effects in the mammary gland. However, a number of recent observations challenge this assumption and support a proliferative role for progesterone in both the normal growth of the mammary gland and in mammary tumorigenesis.

In the case of normal development, a number of experiments provided evidence that, although estradiol can induce DNA synthesis in the mammary glands of ovariectomized mice (32,41,42), the proliferative response is enhanced when progesterone is included (41,42). Further, during normal development, progesterone was implicated both in growth of the mammary ductal system during puberty (16) as well as in the development of the lobuloalveolar system during pregnancy (16,43).

Although controversial, the proposed involvement of progesterone in mammary tumorigenesis is currently under intense scrutiny (44). A number of studies have linked progesterone to the progression of certain carcinogen-induced (45) and transplantable rat mammary tumors (46). Others suggest that progesterone may play a role in spontaneous tumorigenesis in the murine mammary gland (47).

Insight into progesterone action during mammary development *in vivo* has come from the comparative whole mount analysis of mammary glands isolated from the PRKO and wild type female mouse (20). Unlike the ERKO virgin mammary gland phenotype (36,37), initial morphological analysis did not reveal discernible structural differences between the intact virgin homozygous and wild type mammary glands (data not shown). This result is not surprising, since unlike the human four week ovarian cycle, the murine four to five day ovarian cycle contains a very short luteal phase, and, therefore, proliferative effects due to rising serum levels of progesterone are diminished. However, following exogenous estrogen and progesterone treatment, a dramatic phenotype in lobuloalveolar development was observed in the PRKO mouse (Fig. 1). In the case of the ovariectomized wild type animal, hormone treatment with estrogen plus progesterone produced a fully differentiated mammary gland, characterized by an extensively branched ductal epithelium with a highly developed interductal lobuloalveolar system (Fig. 1A, C, and E). In contrast, the PR-deficient female exhibited striking impairment in development of the typical pregnancy-associated mammary phenotype. Specifically, whole mount analysis revealed a ductal structure with less extensive dichotomous branching (i.e., tertiary side branching) and a complete absence of interductal lobuloalveolar bodies (Fig. 1B and D). Further examination using confocal laser scanning microscopy confirmed the absence of lobuloalveolar structures in the PR mutant (compare Fig. 1E and F).

Currently, the progesterone-regulated gene products responsible for its proliferative effects in the mammary gland epithelium are unknown. Recent *in vitro* studies have revealed that progesterone can induce expression of the cell cycle regulatory protein, cyclin D1, in cultured T47D breast cancer cells (48,49). Although preliminary, these results provide suggestive evidence that the proliferative effects of progesterone in the mammary epithelia may be mediated by influencing cell cycle progression through modulation of cyclin D1 expression. In further support of this proposal, the mammary gland phenotype of the cyclin D1 null mutant mouse, recently reported (50–52), displays a striking similarity to that of the PRKO mouse. In addition, recent *in situ* hybridization studies (53) have shown that the highest levels of cyclin D1 expression occur during mid-pregnancy in the normal mouse, a time period which corresponds to the highest levels of progesterone secretion. Together these observations suggest that cyclin D1 may mediate, in part, the progesterone-induced proliferative signal in the mammary gland during pregnancy.

Transplantation as a Tool for Investigating Stromal-Epithelial Interactions

The use of tissue recombination experiments with mammary gland epithelium and stroma was pioneered by Klaus Kratochwil, Ken DeOme, and Teruyo Sakakura (7,8,54–56). These early studies demonstrated that interactions between the stromal and the epithelial compartments could be analyzed by examining growth and morphological changes induced by recombination of heterogeneous epithelium and stroma. These techniques have been utilized more recently to explore the steroid receptor signaling pathways [(4,5) for a review see (57)]. Studies in TfM mice (58), which lack androgen receptor expression, revealed that there is a reciprocal interaction between these two compartments which regulates the induction of androgen receptor expression and the regression of epithelium in the male mouse. Similar tissue recombination techniques were applied to the $PR^{-/-}$ mouse to investigate the role of each compartment in the development of the gland and the potential interactions between these two receptor populations (59).

Knockout Epithelium into Wildtype Stroma

When fragments of $PR^{-/-}$ mammary epithelium are removed from a 10 week old mature virgin $PR^{-/-}$ donor and transplanted into the cleared fat pads of several 3 week old wildtype $PR^{+/+}$, the $PR^{-/-}$ epithelium formed normal appearing ductal structures after 8 weeks (Fig. 2A). The rate of ductal penetration appeared relatively normal when compared to the wildtype control transplant gland. Interestingly, some transplanted mammary $PR^{-/-}$ epithelium displayed unusual ductal structures which deviated from the predicted growth patterns. Several mice were subsequently treated with estrogen and progesterone for 8 days, which stimulates alveolar production in mature murine

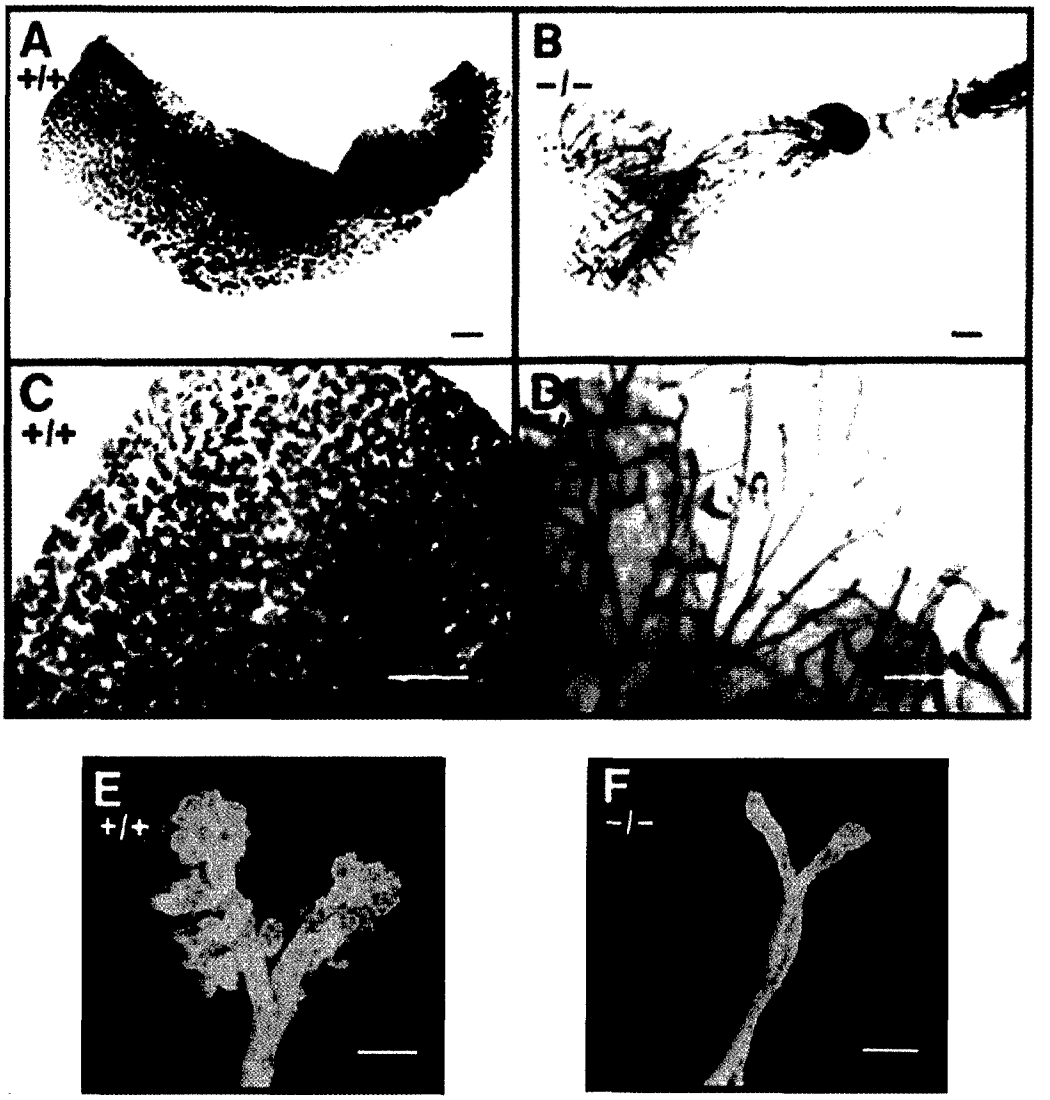

Fig. 1. Morphologic appearance of wild type and PRKO mutant (8-weeks-old) mammary glands with or without progesterone and estrogen treatment. Whole mount preparations of the inguinal mammary glands of ovariectomized, progesterone- and estrogen-treated [see (20)] wild type (A) and the PRKO mutant (B) female. Scale bar 1mm. At higher magnification, note the absence of lobuloalveolar structures and the lack of extensive tertiary side branching in the PRKO mammary gland (D) as compared to wild type (C). Scale bars, 50μm. Confocal microscopy of the terminal end of a typical wild type (E) and PR mutant (F) epithelial duct confirms the lack of development of alveolar bodies in the PRKO mouse. Scale bars, 20μm. This representative result was typical of six mice per genetic group examined. Reproduced with the permission of Lydon *et al.* (20).

$PR^{+/+}$ mammary glands (Fig. 2D). As seen in Fig. 2B the $PR^{-/-}$ epithelium failed to generate alveoli in response to the steroid hormone treatment. The control, $PR^{+/+}$ contralateral glands which contain transplanted $PR^{+/+}$ epithelium, respond as expected to the steroid hormones and produce alveoli (Panel 2D). These data demonstrate that the epithelial PR signaling pathway is necessary for the production of alveoli in the ductal epithelium supporting the observations made in the $PR^{-/-}$ mouse. In addition, the presence of stromal PR cannot compensate for the absence of the PR in the epithelium.

Wildtype Epithelium into Knockout Stroma

A surprising result was obtained in the reciprocal experiment, where wildtype $PR^{+/+}$ epithelium was removed from a 10 day pregnant donor, and trans-

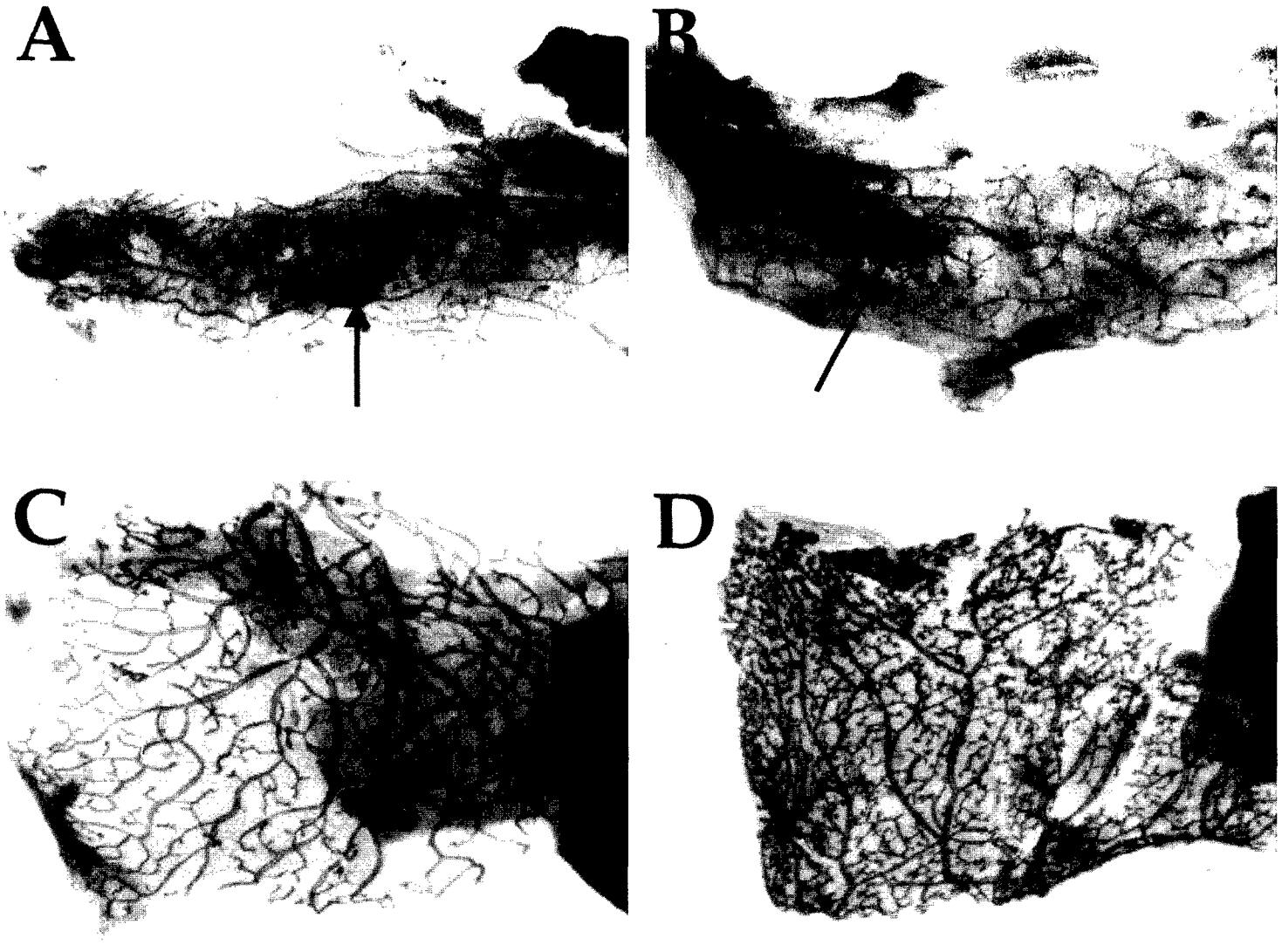

Fig. 2. Absence of lobuloalveolar development in transplanted $PR^{-/-}$ epithelium.PR−/− (A and B) epithelium was transplanted into cleared fat pads of PR+/+ 129SvEv mice. After 10 weeks of growth, the mice were injected daily with estrogen and progesterone, s.c., and the mammary glands collected prior to the injection (A and C) and after eight days of injection (B and D). The arrows in 2A and 2B denote the site of transplantation. Note in A that the fat pad has been penetrated with ductal epithelium after ten weeks of growth *in vivo*. Note the increase in alveolar development in the ipsilateral control PR+/+ glands (C and D) after hormonal stimulation (compare 2C and 2D). Reproduced with the permission of Humphreys *et al.* (59).

planted into the cleared fat pad of a $PR^{-/-}$ mouse. Restricted ductal growth of the $PR^{+/+}$ transplants was observed in the presence of $PR^{-/-}$ stroma (Fig. 3C). The $PR^{+/+}$ epithelium failed to fill the fat pad and in those transplants where some ductal growth did occur outgrowth was minimal. In addition, the shape and growth pattern of the terminal endbuds was abnormal (Fig. 3E). Even after treatment with estrogen and progesterone the impaired ductal phenotype persisted. The epithelium did respond to the exogenous hormonal stimulus by producing alveoli as would be expected, but ductal growth was still inhibited (Fig. 3D and F).

In some glands there was contaminating epithelial ingrowth from the number five mammary gland. The growth of this $PR^{-/-}$ epithelium was not restricted by the absence of the PR in the stroma (Fig. 3G and H). This demonstrated that even in the presence of $PR^{-/-}$ epithelium, the $PR^{+/+}$ epithelium would still not develop a ductal pattern. Thus, in comparison to the $PR^{-/-}$ epithelial and $PR^{+/+}$ epithelial transplants into $PR^{+/+}$ stroma there is a significant disruption of the ductal growth and TEB pattern of the $PR^{+/+}$ epithelium. This restricted ductal growth may be due to disruption of reciprocal interactions between the stromal and epithelial compartments required for this stage of development. Less dramatic effects on ductal morphogenesis have been observed in the $PR^{-/-}$ mouse (20). These data suggest that there is a defect in the signaling mechanism which prevents ductal epithelial growth in the presence of $PR^{-/-}$ stroma, but this only occurs when $PR^{+/+}$ epithelium interacts with $PR^{-/-}$ stroma. We theorize that the $PR^{+/+}$ epithelium requires a progesterone-dependent signal from the stroma in order to stimulate ductal growth. In the $PR^{-/-}$ mouse, the epithelium, having never been exposed to this stromal PR-dependent signal has adapted to the absence of this signal, and, therefore, does not require it for ductal development. One important caveat to these conclusions is the need to perform transplants of $PR^{-/-}$ epithelium into $PR^{-/-}$ stroma. This control was not performed because of the limited number of $PR^{-/-}$ recipients available due to the difficulty of breeding the PRKO 129Sv mice. It may be possible to perform these transplants using mice with a 129SvEvxC57B1/6 background (Dr. S. Krnacik, personal communication), or alternatively using the epithelial/stroma reconstitution method described by Cunha *et al.* (58).

Wildtype Epithelium into Heterozygote Stroma

Epithelial $PR^{+/+}$ transplants were also performed with $PR^{+/-}$ heterozygote hosts. These $PR^{+/+}$ epithelial transplant outgrowths generated two distinct phenotypes. One group had transplants whose epithelium failed to generate ducts and whose endogenous $PR^{+/-}$ epithelium failed to respond to the addition of estrogen and progesterone, as if the host mouse was genotypically a $PR^{-/-}$ homozygote (Fig. 4A and B). The other group displayed complete ductal outgrowth of the transplanted $PR^{+/+}$ epithelium and the endogenous epithelium produced a normal alveolar growth response to estrogen and progesterone treatment (Fig. 4C and D). The phenotypes of these two groups of heterozygote transplants replicated the results obtained in the $PR^{+/+}$ epithelial transplants into $PR^{+/+}$ stroma and $PR^{-/-}$ stroma (see Fig. 3). The penetrance of the wildtype allele of the host PR is most probably effecting a change in the level of stromal receptor expression which influences the observed phenotype of the transplants. Therefore the $PR^{+/+}$ epithelium is again apparently dependent on the presence of an intact stromal PR to mediate ductal development.

Epithelial and Stromal PRs Have Separate Roles in Mammary Gland Development

This animal model unequivocally demonstrates a proliferative role for progesterone in mammary gland as well as providing a powerful research tool to explore the relative contributions of estradiol and progesterone to normal and neoplastic mammary gland proliferation. The results from analysis of the PRKO mouse support the theory that the PR is intimately and directly involved in the development of the mammary gland. In addition, these results suggest distinct functional roles for the stromal and epithelial PRs (Fig. 5). Whole mount analysis of transplanted and hormonally-treated epithelium has exposed a new pathway of interaction between the two compartments of the mammary gland which influences development of the gland. Specifically, the epithelial receptor is required for alveolar development, and the mechanism which mediates lobuloalveolar development is contained within the epithelium as the stromal receptor could not compensate for its absence. The stromal receptor possibly mediates a progesterone-dependent signal for ductal development and probably interacts with the epithelium through a secondary signaling mechanism.

Locally-secreted growth factors are the most likely candidates for mediators of the stromal PR-dependent signal. This mechanism of secondary growth factor signals may also be employed by estrogen and EGF. Although there is evidence that estrogen

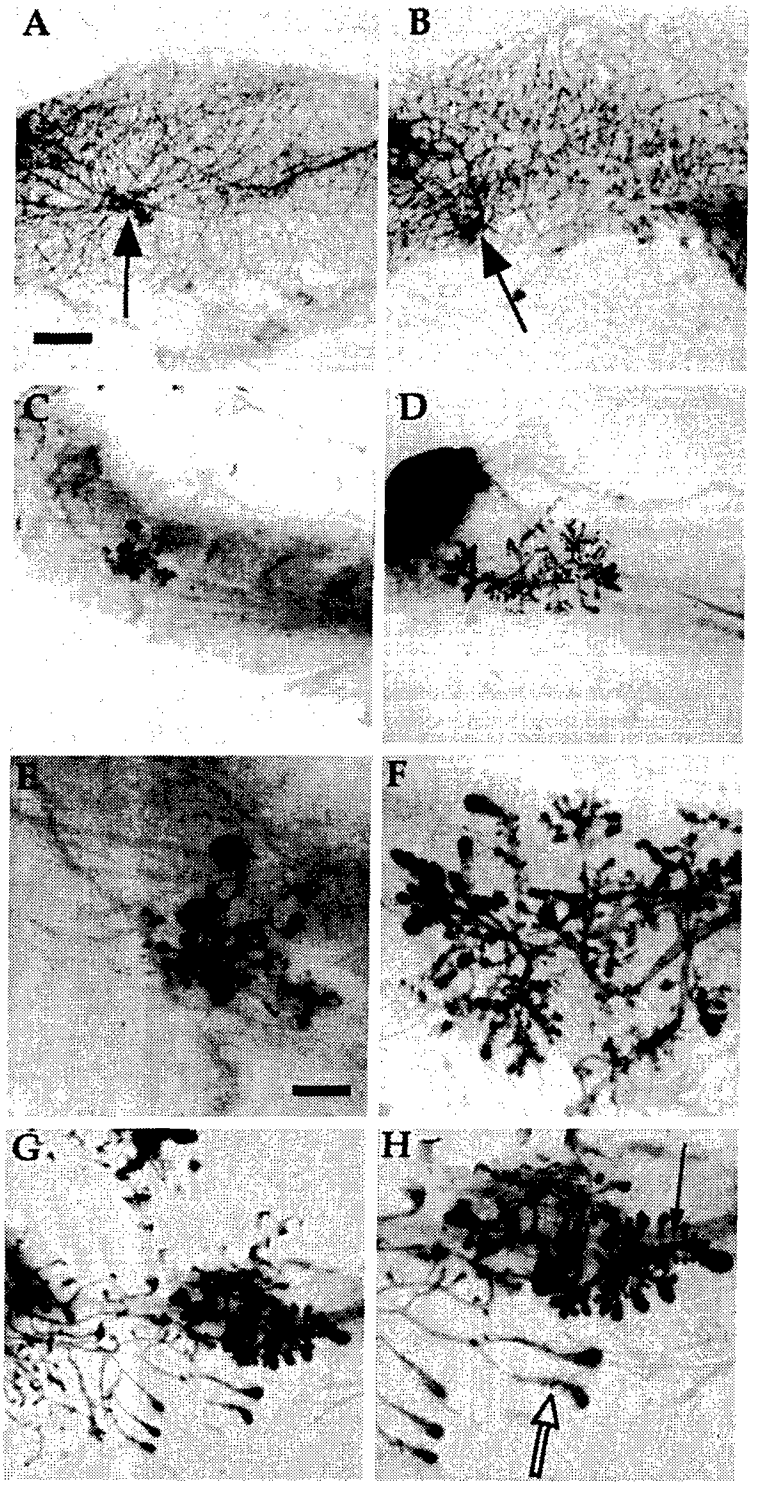

Fig. 3. The effect of steroid hormone treatment on the morphology of $PR^{+/+}$ epithelium transplanted into $PR^{-/-}$ and $PR^{+/+}$ stroma.$^{PR+/+}$ epithelium was transplanted into $PR^{+/+}$ (A and B) and $PR^{-/-}$ (C, D, E, F, G and H) stroma. After 10 weeks of growth, the mice were injected daily with estrogen and progesterone, s.c. and the mammary glands collected at days 0 (A, C and E) and 8 (B, D, F, G, and H) after injection. Alveolar formation is evident in $PR^{+/+}$ (epithelium) transplanted into $PR^{-/-}$ (stroma) after 8 days of estrogen and progesterone treatment (e.g., see panel F). Note the reduction in ductal outgrowth in these same transplants, $PR^{+/+}/PR^{-/-}$ (C and D) compared to the PR+/+ (B) epithelium transplanted into $PR^{+/+}$ stroma (Fig. 2A and B). $PR^{+/+}$ epithelium in $PR^{+/+}$ stroma responded to steroid hormone treatment with extensive alveolar growth and an increase in secondary branching (B). The arrows in A and B define the site of transplantation. Open arrow in H is $PR^{-/-}$ endogenous epithelium, the closed arrow is transplanted PR+/+. Magnification in A, B, C, D and G is defined by bar in A = 0.8 mm. Magnification in E, F, and H is defined by bar in E = 0.30mm. ($PR^{-/-}/PR^{+/+}$, $n = 4$ and $PR^{+/+}/PR^{+/+}$, $n = 4$). Adapted from Humphreys *et al.* (59).

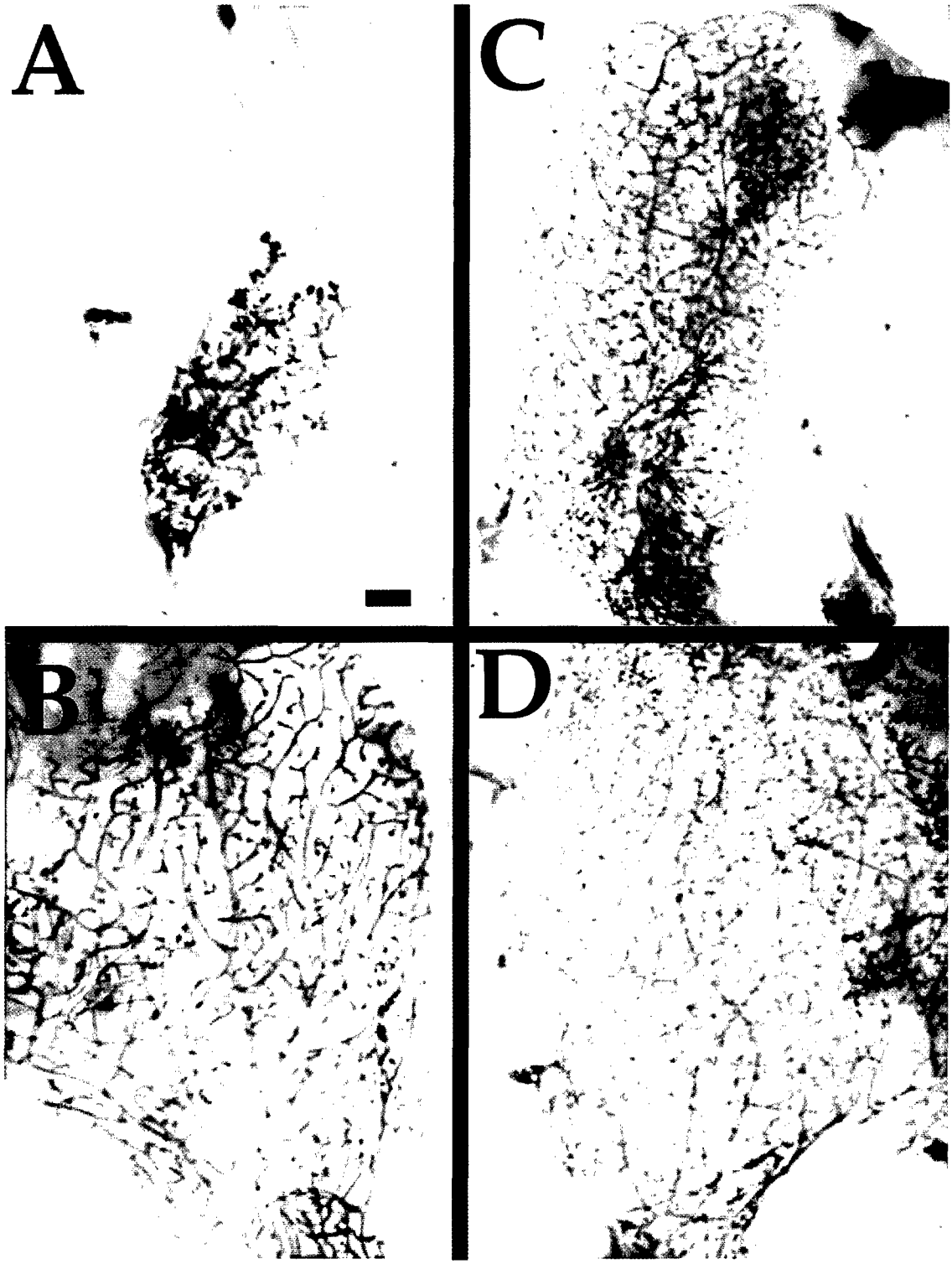

Fig. 4. Heterozygote stroma generates two distinct phenotypes when recombined with $PR^{+/+}$ epithelium. $PR^{+/+}$ epithelium was transplanted into $PR^{+/-}$ stroma. After 10 weeks of growth, the mice were injected daily with estrogen and progesterone, s.c., and the mammary glands collected at day 8. One set of heterozygous hosts permitted normal ductal development of the transplanted $PR^{+/+}$ epithelium (C) and responded to estrogen and progesterone treatment with the production of at least some alveoli (D). The other group failed to generate the complete ductal pattern (A) and responded very poorly to estrogen and progesterone (B). Magnification in A, B, C. and D is defined by bar in A = 0.8 mm. (A: $PR^{+/+}/PR^{+/-}$, $n = 6$ and B: $PR^{+/+}/PR^{+/-}$, $n = 4$).

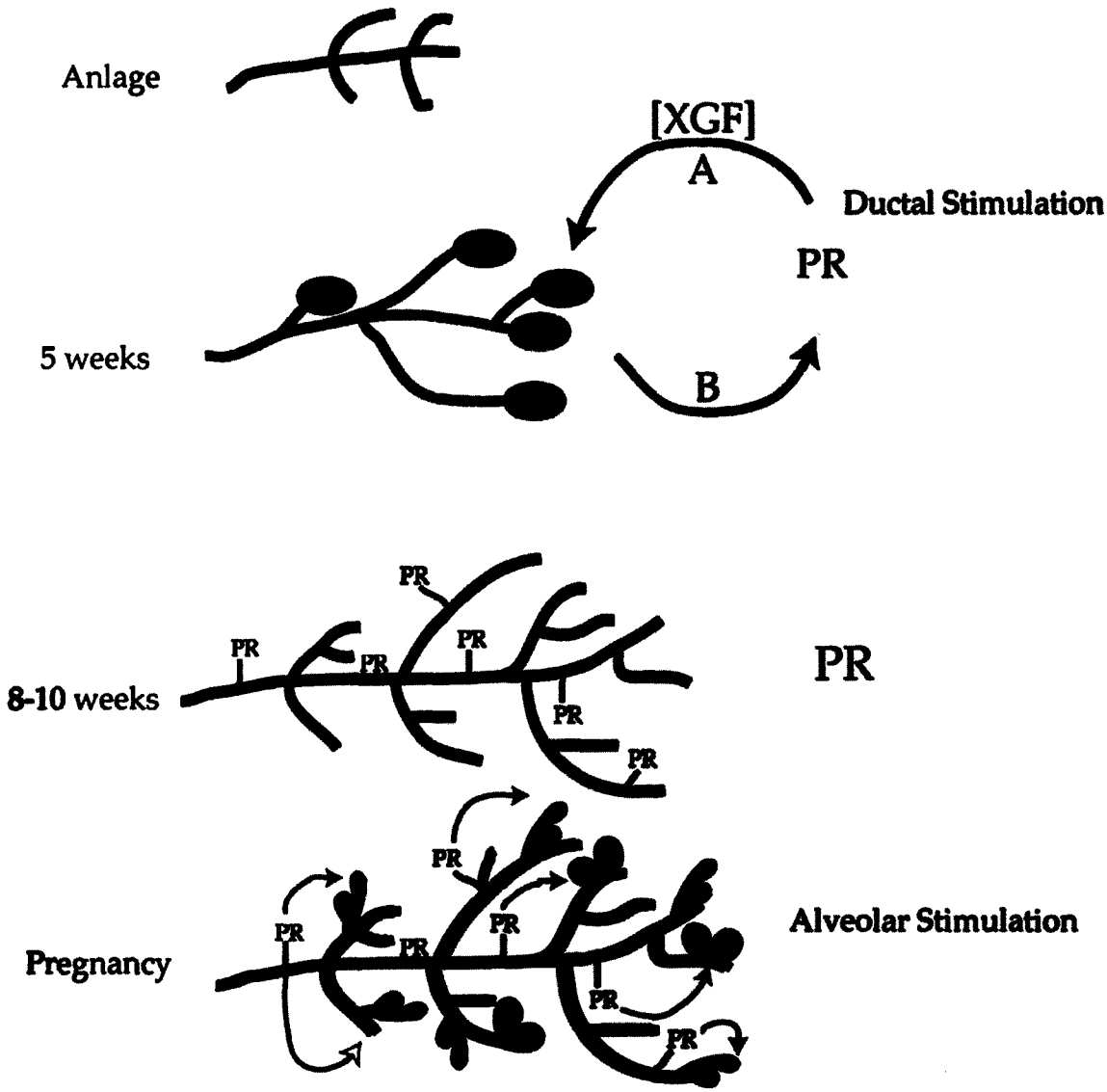

Fig. 5. A model for progesterone action in the development of the mammary gland. Initial postnatal growth of mammary anlagen is independent of stromal PR. The first appearance of the stromal PR coincides with initial ductal development at about 5 weeks of age. Stimulation of ductal development (A) by the PR is mediated by a unknown secondary signaling molecule, possibly a growth factor (XGF). The continued stimulation of the stromal PR is dependent on reciprocal signal(s) from the epithelium (B). In the PRKO mouse this feedback loop is interrupted and the epithelium adapts to the absence of the stimulus provided by the stromal receptor. The appearance of the epithelial PR occurs at 8–10 weeks just prior to the maturation of the gland. Estrogen stimulates the appearance of these receptors and their activation stimulates the production of alveoli.

can act directly on the endbud, EGF can supplant the requirement for estrogen-dependent stimulation of proliferation in virgin animals (21,60). Hepatocyte growth factor has been demonstrated to affect ductal branching (61,62). It remains to be seen if this molecule can rescue the observed ductal phenotype when $PR^{+/+}$ epithelial elements are transplanted into $PR^{+/-}$ and $PR^{-/-}$ stroma.

Finally, the observed growth stimulatory effects of progesterone in this tissue may prompt a reevaluation of the current use of progestins in contraception and post-menopausal hormonal replacement therapies,

as well as underscoring the potential importance of antiprogestins in the treatment of certain hormone-dependent breast cancers.

ACKNOWLEDGMENTS

The authors thank Dr. Susanne Krnacik for critical comments. This work was supported by grant CA64255 from the National Institutes of Health and DAMD17-94-J-4253 from the USAMRMC to J.M.R.

REFERENCES

1. Y. J. Topper and C. S. Freeman (1980). Multiple hormone interactions in the developmental biology of the mammary gland. *Physiol. Rev.* **60**:1049–1106.
2. C. H. Knight and M. Peaker (1982). Development of the mammary gland. *J. Reprod. Fertil.* **65**:521–536.
3. S. Nandi (1959). Hormonal control of mammogenesis and lactogenesis in the C3H/He Crgl mouse. In C. Stern, S. Benson, and W. Quay (eds.), *University of California Berkeley Publications in Zoology,* University of California Press, Berkeley, pp. 1–128.
4. B. Heuberger, I. Fitzka, G. Wasner, and K. Kratochwil (1982). Induction of androgen receptor formation by epithelium-mesenchyme interaction in embryonic mouse mammary gland. *Proc. Natl. Acad. Sci. U.S.A.* **79**:2957–2961.
5. H. Durnberger, B. Heuberger, P. Schwartz, G. Wasner, and K. Kratochwil (1978). Mesenchyme-mediated effect of testosterone on embryonic mammary epithelium. *Cancer Res.* **38**:4066–4070.
6. T. Sakakura, I. Kusano, M. Kusakabe, Y. Inaguma, and Y. Nishizuka (1987). Biology of mammary fat pad in fetal mouse: capacity to support development of various fetal epithelia *in vivo. Development* **100**:421–430.
7. T. Sakakura, Y. Nishizuka, and C. J. Dawe (1979). Capacity of mammary fat pads of adult C3H/HeMs mice to interact morphogenetically with fetal mammary epithelium. *J. Natl. Cancer Inst.* **63**:733–736.
8. T. Sakakura, Y. Nishizuka, and C. J. Dawe (1976). Mesenchyme-dependent morphogenesis and epithelium-specific cytodifferentiation in mouse mammary gland. *Science* **194**:1439–1441.
9. K. B. DeOme, L. J. Faulkin, H. A. Bern, and P. B. Blair (1958). Development of mammary tumors from hyperplastic alveolar nodules transplanted into gland-free mammary pads of female C3H mice. *Cancer Res.* **19**:515–519.
10. K. Kratochwil (1977). Development and loss of androgen responsiveness in the embryonic rudiment of the mouse mammary gland. *Devel. Biol.* **61**:358–365.
11. K. Kratochwil and P. Schwartz (1976). Tissue interaction in androgen response of embryonic mammary rudiment of mouse: identification of target tissue for testosterone. *Proc. Natl. Acad. Sci. U.S.A.* **73**:4041–4044.
12. T. Sakakura (1987). Mammary embryogenesis. In M. C. Neville and C. W. Daniel (eds.), *The Mammary Gland,* Plenum Press, New York, pp. 37–66.
13. S. Z. Haslam and L. J. Counterman (1991). Mammary stroma modulates hormonal responsiveness of mammary epithelium *in vivo* in the mouse. *Endocrinology* **129**:2017–2023.
14. G. R. Cunha (1994). Role of mesenchymal-epithelial interactions in normal and abnormal development of the mammary gland and prostate. *Cancer* **74**:1030–1044.
15. G. R. Cunha, P. Young, S. Hamamoto, R. Guzman, and S. Nandi (1992). Developmental response of adult mammary epithelial cells to various fetal and neonatal mesenchymes. *Epithelial Cell Biol.* **1**:105–118.
16. S. J. Haslam (1988). Progesterone effects on deoxyribonucleic acid synthesis in normal mouse mammary glands. *Endocrinology* **122**:464–470.
17. S. Z. Haslam (1988). Acquisition of estrogen-dependent progesterone receptors by normal mouse mammary gland. Ontogeny of mammary progesterone receptors. *J. Steroid Biochem.* **31**:9–13.
18. S. Z. Haslam and G. Shyamala (1981). Relative distribution of estrogen and progesterone receptors among the epithelial, adipose, and connective tissue components of the normal mammary gland. *Endocrinology* **108**:825–830.
19. S. Wang, L. J. Counterman, and S. Z. Haslam (1990). Progesterone action in normal mouse mammary gland. *Endocrinology* **127**:2183–2189.
20. J. P. Lydon, F. J. DeMayo, C. R. Funk, S. K. Mani, A. R. Hughes, C. A. Montgomery Jr., G. Shyamala, O. M. Conneely, and B. W. O'Malley (1995). Mice lacking progesterone receptor exhibit pleiotropic reproductive abnormalities. *Genes Devel.* **9**:2266–2278.
21. C. W. Daniel and G. B. Silberstein (1987). Postnatal development of the rodent mammary gland. In M. C. Neville and C. W. Daniel (eds.), *The Mammary Gland,* Plenum Press, New York, pp. 3–36.
22. B. K. Vonderhaar (1984). Hormone and growth factors in mammary gland development. In C. M. Veneziale (eds.), *Control of Cell Growth and Proliferation,* Van Nostrand-Reinhold, Princeton, pp. 11–33.
23. K. Plaut, M. Ikeda, and B. K. Vonderhaar (1993). Role of growth hormone and insulin-like growth factor-I in mammary development. *Endocrinology* **133**:1843–1848.
24. W. Imagawa, J. Yang, R. Guzman, and S. Nandi (1994). Control of Mammary Gland Development. In E. Knobrl and J. D. Neill (eds.), *The Physiology of Reproduction,* Raven Press, New York, pp. 1033–1063.
25. W. T. Schrader and B. W. O'Malley (1972). Progesterone-binding components of chick oviduct. IV. Characterization of purified subunits. *J. Biol. Chem.* **247**:51–59.
26. L. Tung, M. K. Mohamed, J. P. Hoeffler, G. S. Takimoto, and K. B. Horwitz (1993). Antagonist-occupied human progesterone B-receptors activate transcription without binding to progesterone response elements and are dominantly inhibited by A-receptors. *Mol. Endocrinol.* **7**:1256–1265.
27. M. Beato, P. Herrlich, and G. Schutz (1995). Steroid hormone receptors: many actors in search of a plot. *Cell* **83**:851–857.
28. M. J. Tsai and B. W. O'Malley (1994). Molecular mechanisms of action of steroid/thyroid receptor superfamily members. *Ann. Rev. Biochem.* **63**:451–486.
29. S. Z. Haslam (1989). The ontogeny of mouse mammary gland responsiveness to ovarian steroid hormones. *Endocrinology* **125**:2766–2772.
30. P. Kastner, A. Krust, B. Turcotte, U. Strupp, L. Tora, H. Gronemyer, and P. Chambon (1990). Two distinct estrogen-regulated promoters generate transcripts encoding the two functionally different human progesterone receptor forms A and B. *EMBO J.* **9**:1603–1614.
31. A. Guiochon-Mantel, H. Loosfelt, P. Lescop, S. Christin-Maitre, M. Perrot-Applanat, and E. Milgrom (1992). Mechanisms of nuclear localization of the progesterone receptor. *J. Steroid Biochem.* **41**:209–215.

32. G. Shyamala and A. Ferenczy (1984). Mammary fat pad may be a potential site for initiation of estrogen action in normal mouse mammary glands. *Endocrinology* **115**:1078–1081.
33. G. B. Silberstein, K. Van Horn, G. Shyamala, and C. W. Daniel (1996). Progesterone receptors in the mouse mammary duct: distribution and developmental regulation. *Cell Growth Diff.* **7**:945–952.
34. S. L. Mansour, K. R. Thomas, and M. R. Capecchi (1988). Disruption of the proto-oncogene int-2 in mouse embryo-derived stem cells: a general strategy for targeting mutations to non-selectable genes. *Nature* **336**:348–352.
35. Q. Hou and J. Gorski (1993). Estrogen receptor and progesterone receptor genes are expressed differentially in mouse embryos during preimplantation development. *Proc. Natl. Acad. Sci. U.S.A.* **90**:9460–9464.
36. D. B. Lubahn, J. S. Moyer, T. S. Golding, J. F. Couse, K. S. Korach, and O. Smithies (1993). Alteration of reproductive function but not prenatal sexual development after insertional disruption of the mouse estrogen receptor gene. *Proc. Natl. Acad. Sci. U.S.A.* **90**:162–166.
37. W. P. Boccinfuso and K. S. Korach (1997). Mammary gland development and tumorigenesis in estrogen receptor knockout mice. *J. Mam. Gland Biol. Neoplasia* **2**:323–334.
38. E. Baldi, C. Krauz, M. Luconi, L. Bonaccorsi, M. Maggi, and G. Forti (1995). Actions of progesterone on human sperm: a model of non-genomic effects of steroids. *J. Steroid Biochem. Mol. Biol.* **53**:199–203.
39. S. K. Mani, J. M. Allen, J. P. Lydon, B. Mulac-Jericevic, J. D. Blaustein, F. J. DeMayo, O. Conneely, and B. W. O'Malley (1996). Dopamine requires the unoccupied progesterone receptor to induce sexual behavior in mice. *Mol. Endocrinol.* **10**:1728–1737.
40. C. L. Clarke and R. L. Sutherland (1990). Progestin regulation of cellular proliferation. *Endocrine Rev.* **11**:266–300.
41. F. Bresciani (1968). Topography of DNA synthesis in the mammary gland of the C3H mouse and its control by ovarian hormones: an autoradiographic study. *Cell Tissue Kinet.* **1**:51–63.
42. G. Shyamala (1987). Endocrine and other influences in the normal development of the breast. In A. H. G. Paterson and A. W. Lees (eds.), *Fundamental Problems in Breast Cancer,* Martinus Nijhof, Boston, pp. 127–137.
43. W. Imagawa, Y. Tomooka, S. Hamamoto, and S. Nandi (1985). Stimulation of mammary epithelial cell growth *in vitro* and interaction of epidermal growth factor and mammogenic hormones. *Endocrinology* **116**:1514–1524.
44. K. B. Horwitz (1992). The molecular biology of RU486. Is there a role for antiprogestins in the treatment of breast cancer? *Endocrine Rev.* **13**:146–163.
45. C. W. Welsch (1985). Host factors affecting the growth of carcinogen-induced rat mammary carcinomas: a review and tribute to Charles Brenton Huggins. *Cancer Res.* **45**:3415–3443.
46. S. P. Robinson and V. C. Jordan (1987). Reversal of the antitumor effects of tamoxifen by progesterone in the 7, 12-dimethylbenzanthracene-induced rat mammary carcinoma model. *Cancer Res.* **47**:5386–5390.
47. N. Nagasawa, M. Aoki, N. Sakagami, and M. Ishida (1988). Medroxyprogesterone acetate enhances spontaneous mammary tumorigenesis and uterine adenomyosis in mice. *Breast Cancer Res. Treatment* **12**:59–66.
48. E. A. Musgrave, J. A. Hamilton, C. S. Lee, K. J. E. Sweeney, C. K. W. Watts, and R. L. Sutherland (1993). Growth factor, steroid, and steroid antagonist regulation of cyclin gene expression associated with changes in T-47D human breast cancer cell cycle progression. *Mol. Cell. Biol.* **13**:3577–3587.
49. E. A. Musgrave, C. S. L. Lee, A. L. Cornish, A. Swarbrick, and R. L. Sutherland (1997). Antiprogestin inhibition of cell cycle progression in T-47D breast cancer cells is accompanied by induction of cyclin-dependent kinase inhibitor p21. *Mol. Endocrinol.* **11**:54–66.
50. P. Sicinski, J. L. Donaher, S. B. Parker, T. Li, A. Fazeli, H. Gardner, S. Z. Haslam, R. T. Bronson, S. J. Elledge, and R. A. Weinberg (1995). Cyclin D1 provides a link between development and oncogenesis in the retina and breast. *Cell* **82**:621–630.
51. V. Fantl, G. Stamp, A. Andrews, I. Rosewell, and C. Dickson (1995). Mice lacking cyclin D1 are small and show defects in eye and mammary gland development. *Genes Devel.* **9**:2364–2372.
52. P. Sicinski and R. A. Weinberg (1997). A specific role for cyclin D1 in mammary gland development. *J. Mam. Gland Biol. Neoplasia* **2**:335–342.
53. L. Stepanova, X. Leng, S. B. Parker, and J. W. Harper (1996). Mammalian p50Cdc37 is a protein kinase-targeting subunit of Hsp 90 that binds and stabilized Cdk4. *Genes Devel.* **10**:1491–1502.
54. K. Kratochwil (1986). Tissue combination and organ culture studies in the development of the embryonic mammary gland. *Devel. Biol.* **4**:315–333.
55. C. W. Daniel, L. J. Young, D. Medina, and K. B. DeOme (1971). The influence of mammogenic hormones on serially transplanted mouse mammary gland. *Exp. Gerontol.* **6**:95–101.
56. K. K. Sekhri, D. R. Pitelka, and K. B. DeOme (1967). Studies of mouse mammary glands. II. Cytomorphology of mammary transplants in inguinal fat pads, nipple-excised host glands, and whole mammary-gland transplants. *J. Natl. Cancer Inst.* **39**:491–527.
57. G. R. Cuhna and Y. K. Hom (1996). Role of mesenchymal-epithelial interactions in mammary gland development. *J. Mam. Gland Biol. Neoplasia* **1**:21–36.
58. G. R. Cunha, P. Young, Y.-K. Hom, P. S. Cooke, J. A. Taylor, and D. B. Lubahn (1997). Mechanism of estrogen action in mesenchymal-epithelial interaction in the mammary gland. *J. Mam. Gland Biol. Neoplasia* **2**:393–402.
59. R. C. Humphreys, J. Lydon, B. W. O'Malley, and J. M. Rosen (1997). Mammary gland development is mediated by both stromal and epithelial progesterone receptors. *Mol. Endocrinol.* **11**:801–811.
60. S. Coleman, G. B. Silberstein, and C. W. Daniel (1988). Ductal morphogenesis in the mouse mammary gland: evidence supporting a role for epidermal growth factor. *Devel. Biol.* **127**:304–315.
61. Y. Yang, E. Spitzer, D. Meyer, M. Sachs, C. Niemann, G. Hartmann, K. M. Weidner, C. Birchmeier, and W. Birchmeier (1995). Sequential requirement of hepatocyte growth factor and neuregulin in the morphogenesis and differentiation of the mammary gland. *J. Cell Biol.* **131**:215–226.
62. B. Niranjan, L. Buluwela, J. Yant, N. Perusinghe, A. Atherton, D. Phippard, T. Dale, B. Gusterson, and T. Kamalati (1995). HGF/SF: a potent cytokine for mammary growth, morphogenesis and development. *Development* **121**:2897–2908.

CHAPTER 4

Methods for *in Situ* Localization of Proteins and DNA in the Centromere–Kinetochore Complex

A. Van Hooser and B. R. Brinkley

Department of Cell Biology
Baylor College of Medicine
Houston, Texas 77030

I. Introduction

Centromeres are heterochromatin-rich loci located at the primary constriction of most eukaryotic chromosomes. These complex arrays of DNA and protein

METHODS IN CELL BIOLOGY, VOL. 61

0091-679X/99 $25.00

are essential for sister chromatid attachment, kinetochore organization, and chromosome movement on spindles during mitosis and meiosis (Brinkley *et al.,* 1992). Recent molecular studies indicate that the greater centromere or centromere–kinetochore complex (Zinkowski *et al.,* 1991) may be involved in a variety of more subtle mitotic functions, including the signaling and integration of complex chromosome behavior on the mitotic spindle (Sullivan, 1998). Recently, we demonstrated that the centromere is a principal site for the initiation of chromosome condensation at the onset of mitosis (He and Brinkley, 1996; Hendzel *et al.,* 1997).

Gorbsky 199 AA

Centromeres were long known as impenetrable "black boxes" on chromosomes that defied structural and molecular analysis due to the lack of reagents available to detect specific DNA sequences or proteins within the region. Although the centromere stains intensely with some chromatin dyes, a Giemsa staining technique called C-banding, described by Pardue and Gall (1970), provided the first specific information on DNA composition. C-banding takes advantage of the highly compact, repetitive nature of DNA contained within most eukaryotic centromeres. Its specificity is thought to depend on the differential denaturation and renaturation properties of DNA in methanol–acetic acid-fixed chromosome preparations. The highly repetitive base sequences composing centromeric DNA will anneal more rapidly after denaturation and subsequently stain more intensely with Giemsa than the nonrepetitive DNA of other chromosomal regions (Waring and Britten, 1966; Britten and Kohne, 1968; Mace *et al.,* 1972).

Electron microscopy first opened the door for structural analysis of the centromere, revealing a trilaminar plate-like structure at the kinetochore of most eukaryotic chromosomes. Thin sections of cells fixed in glutaraldehyde and osmium revealed a dense outer plate, a lightly stained middle layer, and a dense inner layer juxtaposed to the centromeric chromatin (Brinkley and Stubblefield, 1966; Jokelainen, 1967). A prominent "fuzzy coat" or corona exists along the surface of the outer plate, to which microtubules become attached at prometaphase. Although very little was known of the molecular composition of the centromere–kinetochore complex, early studies suggested that the structure was largely proteinaceous. Tubulin was found to be associated with the kinetochore (Pepper and Brinkley, 1977), and ribonucleoprotein was detected using Bernard's uranyl acetate–EDTA staining procedure (Rieder, 1979a,b).

The technique of indirect immunofluorescence ushered in the era of immunocytochemistry and opened the way for *in situ* localization of both rare and common proteins in eukaryotic cells. Still in widespread use, this procedure was of historical significance in the characterization of the cytoskeleton and mitotic apparatus (Lazarides and Weber, 1974; Fuller *et al.,* 1975; Brinkley *et al.,* 1975). Indirect immunofluorescence was first used effectively to detect centromeres of eukaryotic chromosomes by Tan and coworkers (Moroi *et al.,* 1980) following their important discovery of human autoantibodies in the serum of patients with the CREST (calcinosis, Raynaud's phenomenon, esophageal dysmotility, sclerodactyly, and telangiectasia) variant of scleroderma. Their studies clearly showed discrete CREST staining in the centromeres of human metaphase chromosomes

and identified centromeric domains in interphase nuclei (Fig. 1). Subsequently, Brenner *et al.* (1980) demonstrated specific staining along the surface of the centromere and concluded that CREST antiserum recognized a zone that corresponded to the kinetochore in PtK1 rat kangaroo cells. These investigators further demonstrated a direct correlation between the number of fluorescent spots in the interphase nuclei and the diploid chromosome number. Using CREST staining in combination with BrdU labeling, they showed that the fluorescent spots doubled during the late stages of S phase, concomitant with the replication of centromeric DNA. The centromere, once accentuated only by primitive, nonspecific staining reagents, was opened to structural and molecular analysis by the discovery of scleroderma CREST antiserum. In the following sections, we describe the most commonly used methods for centromere/kinetochore analysis using this antiserum.

II. *In Situ* Localization of Proteins: Indirect Immunofluorescence

The techniques of indirect immunofluorescence are established, reliable, and relatively easy to accomplish. The only specialized equipment needed is an epifluorescence microscope, equipped with an appropriate set of quartz objectives, exciter and barrier filters, and a standard or digital camera for photomicroscopy. Of course, the more advanced digital equipment one can access, such as cooled charge couple device color cameras, confocal or deconvolution microscopes, and image analysis software, dye sublimation printers, the greater the latitude of image acquisition. The procedures described in the following section have been used by our laboratory for many years and give consistently reliable results.

A. Collection, Titering, and Storage of CREST Antisera

The most available source of human autoantisera can be found in patients treated in rheumatism and arthritis clinics. We were successful in collecting CREST autoantiserum from blood samples of patients admitted to the Comprehensive Arthritis Center at University Hospital, University of Alabama at Birmingham, as well as from arthritis patients of physicians at Baylor College of Medicine. Although anti-centromere autoantibodies are most frequently found in the serum of patients with the CREST variant of scleroderma (Moroi *et al.*, 1980), autoantibodies are also found in some patients with Raynaud's phenomenon. Before collecting blood samples, it is necessary to solicit the participation of the physician in charge and to complete all patient consent forms and other legal documents required by the hospital and/or granting agency. The physicians or their appointees collect blood samples from arm veinipuncture, and the sam-

ples are allowed to sit at room temperature (RT) overnight to facilitate clotting. Subsequently, the plasma is removed with a small syringe or carefully decanted into conical tubes for storage at −80°C until use. The antiserum should be titered by dilution in TBS-T (see buffered solutions in Section II,E). We have obtained best results with CREST antiserum diluted 1:500 to 1:1000, but even greater dilutions may be possible with some antisera. Testing is done by indirect immunofluorescence using tissue culture cells, as described in Section II,E. The titer that gives crisp centromere staining with minimal background is selected.

B. Cell Culture Conditions

We use a variety of mammalian tissue culture cells in our studies. For *in situ* staining, cells are maintained in a humidified 37°C incubator with a 5% CO_2 atmosphere. Cell cultures are grown in any number of suitable culture media. We have used the following with excellent results: McCoy's 5A (Gibco Laboratories, Grand Island, NY) medium supplemented with 10% CPSR-4 (Sigma Chemical Co., St. Louis, MO), Ham's F-10 medium supplemented with 15% FBS (Gibco Laboratories), DMEM supplemented with 10% FBS (Gibco Laboratories), and OptiMEM supplemented with 4% FBS (Gibco Laboratories). All growth media are supplemented with 1% penicillin and 1% streptomycin (Gibco Laboratories). Almost every laboratory has slightly modified conditions for cell culture. The main requirement for centromere/kinetochore staining is that the cell monolayers are contiguous, not overgrown or overlapping, and remain reasonably flat. If you wish to observe mitotic cells, it is, of course, essential to select growth conditions that favor cells entering mitosis. Cultures should be given fresh medium the day prior to harvest. For some experiments, it may be necessary to add a mitotic inhibitor, such as 0.1 μg/ml Colcemid (Gibco Laboratories) or 0.1 μg/ml nocodazole (Sigma Chemical Co.), to arrest cells in mitosis.

C. Mitotic Shake-Off

Tissue culture cells tend to round during mitosis. Cells arrested with mitotic inhibitors can be selectively detached from cell monolayers by lightly tapping the sides of tissue culture flasks. Detached cells are then pelleted in a centrifuge at 1000*g* for 5 min, resuspended in PBS (0.14 *M* NaCl, 2.5 m*M* KCl, 8 m*M* Na_2HPO_4, 1.6 m*M* KH_2PO_4, pH 7.4), and pelleted a second time. When experiments call for the collection of cells that have not been exposed to arresting agents, mitotic cells can be selectively detached by lightly tapping the tissue culture flask during brief, sequential rinses in PBS and 0.03% EDTA in Puck's saline. Both rinses are added to the aspirated medium in a conical tube and pelleted in a centrifuge at 1000*g* for 5 min. At this point, cells may be swollen briefly (<15 min) in hypotonic solution (75 m*M* KCl containing multiple protease inhibitors) at 37°C to improve the visualization of metaphase chromosomes (Fig. 2).

D. Cytocentrifugation

It is often necessary to carry out immunofluorescence on cells that have been detached from monolayers or grown in suspensions, rounded cells such as blood samples, or lysed cell extracts. Cytocentrifugation flattens cells onto coverslips and enables one to obtain improved images of objects such as chromosomes and mitotic spindles. We have obtained excellent results with a Cytospin 3 cytocentrifuge (Shandon Instruments, Inc., Pittsburgh, PA). Cell pellets are resuspended in 1 or 2 ml of PBS (see Section II,E) providing a final concentration of about 1×10^6 cells per milliliter. It may be necessary to adjust the concentration of cells or cell extract so as to obtain a thin monolayer without overcrowding or piling up objects on the slide. Approximately 100 μl of the cell suspension is pipetted into a cytocentrifuge cup and spun through an aperture in a porous card onto acid-etched and/or poly-amino acid-coated coverslips at speeds from 800 to 2000 rpm for 2 min. The coverslips are then removed and immediately processed, as described later. If cytocentrifuged material tends to wash off during the immunostaining process, the preparation may be coated with a thin layer of parlodian or colloidin before processing. However, this is usually not necessary when using etched, poly-amino acid-coated slides or coverslips.

E. Staining of Cell Monolayers

Reagents

1. Buffered solutions: The amount of each reagent needed will vary, depending on whether you use 13-mm round coverslips in 24-well trays (250 μl per well), 11 × 22-mm coverslips in small Coplin jars (5 ml per jar), 75 × 25-mm glass slides in large Coplin jars (50 ml per jar), etc.

   PBS (0.14 *M* NaCl, 2.5 m*M* KCl, 8 m*M* Na_2HPO_4, 1.6 m*M* KH_2PO_4, pH 7.4).

   PEM [80 m*M* K-Pipes (pH 6.8), 5 m*M* EGTA (pH 7.0), 2 m*M* $MgCl_2$].

   TBS-T [20 m*M* Tris–Hcl, (pH 7.6), 137 m*M* NaCl, 0.1% Tween-20].

2. Permeabilization solution

   0.5% Triton X-100 in PEM: To preserve the cytoskeleton and nuclear matrix while extracting soluble proteins, we recommend the use of 0.5% Triton X-100 in CSK [10 m*M* Pipes (pH 6.8), 100 m*M* NaCl, 300 m*M* sucrose, 3 m*M* $MgCl_2$, 1 m*M* EGTA] containing 4 m*M* vanadryl riboside complex (VRC) and multiple protease inhibitors [1.2 m*M* phenylmethylsulfonyl fluoride (PMSF), and 1 μg/ml each of aprotinin, leupeptin, antipain, and pepstatin]. Prepare immediately before use and keep on ice. Make a 1:20 dilution of 10% stock Triton X-100.

3. Fixative

   3.7% formaldehyde, diluted in PEM from 16% ultrapure electron microscope (EM)-grade formaldehyde (Polysciences, Inc., Warrington, PA) or freshly prepared from paraformaldehyde.

4. Blocking agent

5 g dry milk per 100 ml of ~~1:500 to 1:1000 in~~ delete TBS-T. PE

5. Antibodies

CREST antisera is diluted 1:500 to 1:1000 in TBS-T.

Fluorophore-conjugated anti-human IgG(H+L) secondary antibodies (Pierce Chemicals) are diluted 1:500 in TBS-T.

6. Counterstains

DNA is counterstained with 0.1 μg/ml 4′,6-diamidino-2-phenylin-dole (DAPI), 0.5 μg/ml propidium iodide, 1 μg/ml Hoechst 33258, or 10 μg/ml ethidium bromide, diluted in 1 × TBS-T.

Protocol

1. Cells are grown on or cytospun (800 rpm, 2 min) onto acid-etched and/or poly-amino acid-coated glass coverslips.

2. Transfer coverslips to a multiwell tissue culture tray or to Coplin jars containing cold PBS. Keep on ice.

3. ~~Aspirate PBS (gently so as to not draw off mitotic cells) and~~ delete rinse coverslips with cold PEM. R AA

4. To better visualize chromosomes and centromeres, soluble proteins may be extracted prior to fixation with 0.5% Triton X-100 in PEM or CSK (see above) for 2 min at 4°C. This step is omitted for whole cell preparations. Rinse cells briefly in fresh, cold PEM.

5. Preparations are fixed in 3.7% formaldehyde ~~and~~ in PEM for 40 min at 4°C. in EA

6. Rinse coverslips three times in PEM, 5 min each while on rotator.

7. Whole cell preparations are permeabilized postfixation with 0.5% Triton X-100 in PEM for 30 min at RT. This step is optional if cells were extracted prior to fixation. Some cells require more permeabilization than do others. Rinse cells three times in PEM for 2 min.

8. Incubate samples in 5% milk in TBS-T for at least 30 min at RT or overnight at 4°C to block nonspecific staining.

9. Without rinsing, incubate primary antibodies, diluted in TBS-T, on preparations for 30–60 min at 37°C in a humid chamber.

10. The samples are then rinsed three times in TBS-T for 5 min each.

11. Block in 5% milk and TBS-T for 10 min at RT. Do not rinse.

12. Protect samples from light during all remaining steps. Fluorophore-conjugated secondary antibodies (see Section II,F), diluted in TBS-T, are incubated with samples for 30–60 min at 37°C in a humid chamber.

13. The samples are then rinsed three times in TBS-T for 5 min at RT.

14. DNA is counterstained with DAPI, propidium iodide, Hoechst 33258, or ethidium bromide for 15–45 sec at RT.

15. Rinse samples three times in TBS-T, 2 min each.

16. Coverslips are mounted onto glass slides using Vectashield antifade medium (Vector Laboratories, Inc., Burlingame, CA) or 1 mg/ml *p*-phenylenediamine in a 1:10 (v/v) mixture of PBS:glycerol, pH 8.0 (Johnson and Nogueira Araujo, 1981).

17. Seal coverslips with nail polish. Stained preparations should be examined and images captured immediately for best results. Slides may be stored at 4°C for a few weeks in a light-tight box.

F. Double- and Triple-Staining Techniques

When examining the centromere or kinetochore, it is often necessary to use double- and triple-staining techniques to examine multiple antigens, such as motors, microtubules, and chromatin in the same preparation. This can be readily accomplished by carefully selecting combinations of primary and secondary antibodies conjugated to a variety of fluorescent tags, such as fluorescein isothiocyanate (FITC) (excitation/emission = 494/518 nm), tetramethylrhodamine isothiocyanate (TRITC) (552/570 nm), and Texas Red (TXRD) (595/615 nm) (Molecular Probes, Inc.). In applying combinatory immunofluorescence, it is critical to avoid antibody cross-reaction. For example, if you wish to stain both the centromere and mitotic spindle in the same preparation, you would use CREST antisera primary antibody, followed by FITC-labeled goat anti-human secondary antibody, and then apply anti-tubulin primary antibody from a different organism, such as mouse, followed by TXRD-labeled sheep anti-mouse secondary antibody. In actual practice, we stain first with a mixture of the two primary antibodies, followed by a mixture of the two secondary antibodies. Chromatin can be enhanced with an appropriate counterstain, such as DAPI (ex/em = 358/461 nm), propidium iodide (535/617 nm), bis-benzimide (Hoechst 33258) (352/461 nm), or ethidium bromide (518/605 nm). With the proper selection of activating filters, you may view multiple antigens in the same sample. If you wish to produce a single image with multiple fluorescent probes, you must use image processing software to merge the collected data (as shown in Fig. 2).

III. *In Situ* Localization of Proteins: Immunogold EM

AUTHOR SEE QUERY ON MS P 93

OK as set

Reagents (Fig. 3)

1. Buffered solutions

PBS (0.14 *M* NaCl, 2.5 m*M* KCl, 8 m*M* Na_2HPO_4, 1.6 m*M* KH_2PO_4, pH 7.4).

PEM [80 m*M* K-Pipes (pH 6.8), 5 m*M* EGTA (pH 7.0), 2 m*M* $MgCl_2$]. PIPES EA

TBS-1 [10 m*M* Tris (pH 7.7), 150 m*M* NaCl, 3 m*M* KCl, 1.5 m*M* $MgCl_2$, 0.05% Tween-20, 0.1% BSA, 0.2% glycine] (Nickerson *et al.*, 1990).

TBS-2 [20 m*M* Tris (pH 8.2), 140 m*M* NaCl, 0.1% BSA] (Nickerson *et al.*, 1990).

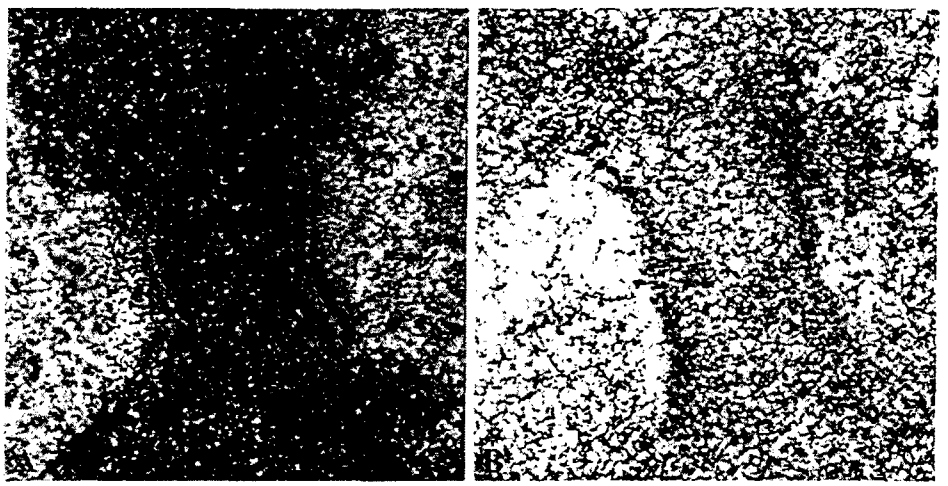

Fig. 3 (A and B) Indian muntjac chromosomes observed by EM. Prior to fixation, the chromosome in B was swollen in hypotonic solution and does not display the trilaminar kinetochore plate morphology seen along each chromatid in A. Centromere–kinetochore antigens were detected in preparation B using SH-CREST autoantiserum and immunogold labeling according to the protocol given in Section III. Thin sections were made using an RMC 6000 ultramicrotome, collected on copper mesh grids, and stained with uranyl acetate and Reynold's lead citrate. Electron micrographs were captured on a Hitachi H-7000 electron microscope operated at 75 kV.

0.1 *M* cacodylate, diluted in ddH_2O from a 0.2 *M* stock (Electron Microscopy Sciences, Ft. Washington, PA).

2. Permeabilization solution

   0.5% Triton X-100 in PEM. Make a 1 : 20 dilution of 10% stock Triton X-100.

3. Fixatives

   3.7% formaldehyde (diluted from 16% ultrapure EM-grade formaldehyde; Polysciences, Inc.) in PEM containing 0.1% glutaraldehyde (diluted from 25% ultrapure EM grade; Polysciences, Inc.).

   1% glutaraldehyde diluted from 25% ultrapure EM grade (Polysciences, Inc.) in 0.1 *M* sodium cacodylate (pH 7.4).

   1% osmium tetroxide (OsO_4) (Electron Microscopy Sciences) in 0.1 *M* sodium cacodylate (pH 7.4).

4. Reducing agent

   PEM + 1 mg/ml sodium borohydrate ($NaBH_4$), freshly prepared. To a tube containing preweighed sodium borohydrate, slowly add the appropriate amount of PEM buffer to bring the final concentration to 1 mg/ml. This reducing agent eliminates reactive aldehydes after fixation.

5. Blocking agent

   5% heat-inactivated normal goat serum (NGS) in TBS-1.

6. Antibodies

CREST antisera is diluted 1:500 to 1:1000 in TBS-1.

Colloidal gold-conjugated (5, 10, or 12 nm diameter) anti-human IgG(H+L) secondary antibody (Amersham Life Science, Inc.) is diluted 1:5 in TBS-2.

Protocol

1. Cells are harvested by mitotic shake-off (see Section II) and cytospun (800 rpm, 2 min) onto poly-amino acid-coated Thermanox coverslips (Nunc, Inc., Naperville, IL). This provides a highly concentrated monolayer of mitotic cells within a small area for ease of sectioning. Alternatively, cells can be grown and processed in Contur Permanox tissue culture dishes (Miles Scientific, Naperville, IL).

2. Transfer coverslips to a multiwell tissue culture tray or to Coplin jars containing cold PBS. Keep on ice.

3. ~~Aspirate PBS (gently so as to not draw off mitotic cells) and~~ rinse coverslips with cold PEM.

4. Cells should be permeabilized prior to fixation to allow greater accessibility of the colloidal gold immunoprobes to intracellular antigens. Permeabilization and extraction is achieved by treating preparations with 0.5% Triton X-100 in PEM or CSK for 2 min at 4°C. Some cell types require longer exposures. To preserve the cytoskeleton and nuclear matrix while extracting soluble proteins, we recommend the use of 0.5% Triton X-100 in CSK [10 m*M* Pipes, (pH 6.8), 100 m*M* NaCl, 300 m*M* sucrose, 3 m*M* $MgCl_2$, 1 m*M* EGTA] containing 4 m*M* VRC and multiple protease inhibitors (1.2 m*M* PMSF and 1 μg/ml each of aprotinin, leupeptin, antipain, and pepstatin). Prepare immediately before use and keep on ice.

5. Rinse briefly in fresh, cold PEM.

6. Preparations are fixed in 3.7% paraformaldehyde and PEM containing 0.1% glutaraldehyde for 40 min at 4°C.

7. Remove fixative and wash coverslips three times with PEM, 5 min each on a rotator. Do not remove the last PEM wash until your are ready to perform the next step.

8. Quench in $NaBH_4$ and PEM as follows: Gently mix the freshly prepared $NaBH_4$ and PEM by pipetting in and out. It may be difficult to pipette accurately because of the air bubbles formed. Immerse the coverslips and place on a rotator for 5 min.

9. Repeat the above step with fresh $NaBH_4$.

10. Rinse coverslips three times in PEM, 5 min each while on rotator.

11. Nonspecific binding of antibodies is blocked with 5% NGS in TBS-1 for at least 30 min at RT or overnight at 4°C.

12. Without rinsing, the cells are incubated for 2 hr at 37°C in CREST antiserum diluted in TBS-1.

13. The samples are then washed three times in TBS-1, 5 min each.

14. Block in 5% NGS for 10 min.

15. Without rinsing, incubate preparations for 1 hr at 37°C with gold-conjugated anti-human secondary antibody, diluted in TBS-2.

16. The preparations are then washed three times for 5 min in TBS-2.

17. Postfix cells with 1% glutaraldehyde in 0.1 *M* sodium cacodylate for 5 min. This and the remaining steps are done at RT.

18. Follow with three 5-min washes in 0.1 *M* sodium cacodylate.

19. The samples are then fixed for 10–15 min in 1% OsO_4 ~~and~~ in 0.1 *M* sodium cacodylate.

20. Wash coverslips extensively in ddH_2O.

21. The samples are then dehydrated in a graded series of ethanols: 5 min in 30, 50, 70, 90, and 100%.

22. Infiltrate overnight with Spurr's resin (Spurr, 1969).

23. Cell monolayers are flat embedded according to the procedure of Brinkley and Chang (1973).

24. Thin sections are made using an ultramicrotome and collected on copper mesh grids.

25. Contrast briefly (5 min each) with uranyl acetate and Reynolds' lead citrate (Reynolds, 1963).

IV. Fluorescent *in Situ* Hybridization Using DNA Satellite Probes

Perhaps one of the most powerful tools in cell and molecular biology to be developed in this century is the technique of fluorescent *in situ* hybridization (FISH), used for detecting specific nucleic acid sequences in cells (John *et al.*, 1969; Lawrence *et al.*, 1988). Used widely for mapping DNA on metaphase chromosomes, this method is especially useful for the analysis of centromeric DNA. The centromeres of higher eukaryotes are composed of highly repetitive, noncoding DNA sequences. In humans and other primates, the centromere consists of a tandem series of 171-bp monomeric repeats, arranged in higher-order families known as α-satellite or alphoid DNA (Wevrick *et al.*, 1992; Haaf and Willard, 1992). By synthesizing probes from cloned fragments of alphoid DNA, it is possible to localize these sequences in the centromeres of specific human chromosomes using FISH. It is also possible to use a combination of FISH and indirect immunofluorescence to localize both DNA and protein in the same centromere (Fig. 4; the method for combination staining is given in Section V). The technique for FISH that we use routinely is described below. Before you begin, it is helpful to prepare the following stock and working solutions:

Reagents

PBS (0.14 *M* NaCl, 2.5 m*M* KCl, 8 m*M* Na_2HPO_4, 1.6 m*M* KH_2PO_4, pH 7.4).

PBD (PBS + 0.1% Tween-20).

0.5% Triton X-100 in PBS.

20× SSC (1× SSC = 0.15 *M* NaCl, 15 m*M* sodium citrate, pH 7.0). Dilutions of 4×, 2×, and 0.5–0.75× will be needed.

4× and 2× SSC containing 0.1% Tween-20.

2.5–3% formaldehyde in PBS. Dilute 16% ultrapure EM-grade formaldehyde (Polysciences, Inc.) or freshly prepare from paraformaldehyde.

Carnoy's fixative (3:1 methanol:glacial acetic acid).

70% formamide + 2× SSC [dilute 100% formamide (Gibco Laboratories) and 20× SSC, pH 7.0].

70, 85, and 100% ethanol series.

Satellite DNA probes prepared by nick translating centromeric DNA with biotin-labeled dNTPs (Langer *et al.*, 1981). Digoxigenin-labeled deoxynucleotide oligomers also give excellent results.

Fluorophore-conjugated avidin (Vector Laboratories, Inc.) is diluted 1:200 in 4× SSC containing 1% BSA,

Fluorophore-conjugated anti-avidin antibody (Vector Laboratories, Inc.) is diluted 1:500 in 1× PBD.

Or, fluorophore-conjugated sheep anti-digoxigenin antibody (Oncor, Inc., Gaithersburg, MD), diluted 1:100 in 1× PBD,

And, fluorophore-conjugated rabbit anti-sheep antibody (Oncor, Inc.), diluted 1:500 in 1× PBD.

DNA is counterstained with 0.1 μg/ml DAPI, 0.5 μg/ml propidium iodide, 1 μg/ml Hoechst 33258, or 10 μg/ml ethidium bromide, diluted in 1× PBD.

Protocol

Denaturation

Pub: spacing above + below ok as set?

1. Cells are grown on or cytospun (800 rpm, 2 min) onto acid-etched and/or poly-amino acid-coated glass coverslips (as described in Section II).

2. Transfer coverslips to Coplin jars containing cold PBS. Keep on ice.

3. Cells are permeabilized prior to fixation with 0.5% Triton X-100 in PBS for 1 min.

4. Rinse briefly in fresh, cold PBS.

5. Preparations are fixed in 2.5–3% formaldehyde and PBS for 15 min on ice.

6. Remove fixative and wash coverslips three times with ddH_2O, 5 min each.

7. The cells are then fixed in freshly prepared Carnoy's fixative for 20 min at RT.

8. Dehydrate samples in a graded series of ethanols: 70, 85, and 100%, 2 min each at RT.

9. The coverslips are allowed to air-dry and should be stored at −20°C with desiccant for a few days.

10. Preparations are denatured in 70% formamide, 2× SSC (pH 7.0) for 9 min at ~~78 or~~ delete 79°C (place Coplin jar in a water bath). AA

11. The coverslips are immediately placed in 70% ethanol at −20°C for 2 min, moved to 85% ethanol at −20°C for 2 min, and finally to 100% ethanol at −20°C for 2 min.

12. Air dry the preparations and immediately begin hybridization.

Probe Preparation

13. 50 ng of probe is suspended in 13 μl of deionized formamide with 10 μg of sheared salmon sperm DNA (Sigma Chemical Co.) and 15 μg of *Escherichia coli* tRNA (Boehringer–Mannheim Biochemicals, Indianapolis, IN).

14. The probe is then denatured at 70°C for 5 min and immediately put on ice.

15. 7 μl of hybridization buffer is added to the probe so that the final hybridization solution consists of 65% formamide, 2× SSC, 10% dextran sulfate, and 1% BSA.

Hybridization

16. Each coverslip is inverted onto 20 μl of hybridization solution on parafilm and incubated at 37°C overnight in a humidified chamber.

17. Samples are then rinsed in 0.75× (or 0.5×) SSC for 5 min at 72°C.

Detection

18. Protect samples from light during all remaining steps. Hybridization of biotinylated probes is detected by incubating fluorophore-conjugated avidin on samples for 30–60 min at RT. See step 20 for digoxigenin-labeled probes.

19. The preparations are rinsed in 2× and 4× SSC containing 0.1% Tween-20 at RT, 10 min each. Skip to step 21.

20. When using digoxigenin-labeled probes, hybridization is detected by incubating samples with fluorophore-conjugated anti-digoxigenin antibody for 15 min at 37°C.

21. The preparations are rinsed three times in PBD, 5 min each.

22. DNA is counterstained with DAPI, propidium iodide, Hoechst 33258, or ethidium bromide for 15–45 sec at RT.

23. Rinse samples three times in PBD, 2 min each.

24. Coverslips are mounted onto glass slides using Vectashield antifade medium (Vector Laboratories, Inc.) or 1 mg/ml *p*-phenylenediamine in a 1:10 (v/v) mixture of PBS:glycerol (pH 8.0).

25. Seal coverslips with nail polish. Stained preparations should be examined and images captured immediately for best results. Slides may be stored at 4°C for a few weeks in a light-tight box.

Signal amplification

26. Peel the nail polish off and soak the slides in PBD until the coverslip moves freely.

27. Remove coverslips and rinse them thoroughly in PBD at RT.

28. Incubate avidin-labeled samples for 15 min at 37°C with fluorophore-conjugated anti-avidin antibody. Complete steps 21–25.

29. Amplification of digoxigenin-conjugated probes is achieved by incubating samples with rabbit anti-sheep antibody at 37°C for 15 min.

30. Rinse three times 5 min in PBD at RT.

31. Incubate with fluorophore-labeled anti-rabbit antibody for 15 min at 37°C.

32. Complete steps 21–25.

V. Combination Staining: DNA/Protein

Reagents

PBS (0.14 *M* NaCl, 2.5 m*M* KCl, 8 m*M* Na_2HPO_4, 1.6 m*M* KH_2PO_4, pH 7.4).

PBD (PBS + 0.1% Tween-20).

PEM [80 m*M* K-Pipes (pH 6.8), 5 m*M* EGTA (pH 7.0), 2 m*M* $MgCl_2$]. PIPES EA

0.5% Triton X-100 in PEM.

20× SSC (1× SSC = 0.15 *M* NaCl, 15 m*M* sodium citrate, pH 7.0). Dilutions of 4×, 2×, and 0.5–0.75× will be needed.

4× and 2× SSC containing 0.1% Tween-20.

0.5–1.5% and 2.5–3% formaldehyde in PEM. Dilute 16% ultrapure EM-grade formaldehyde (Polysciences, Inc.) or freshly prepare from paraformaldehyde.

Carnoy's fixative (3:1 methanol:glacial acetic acid).

70% formamide + 2× SSC [dilute 100% formamide (Gibco Laboratories) and 20× SSC, pH 7.0].

70, 85, and 100% ethanol series.

Satellite DNA probes prepared by nick translating centromeric DNA with biotin-labeled dNTPs (Langer *et al.*, 1981). Digoxigenin-labeled deoxynucleotide oligomers also give excellent results.

Fluorophore-conjugated avidin (Vector Laboratories, Inc.) is diluted 1:200 in 4× SSC containing 1% BSA,

And fluorophore-conjugated anti-avidin antibody (Vector Laboratories, Inc.) is diluted 1:500 in 1× PBD.

Or, fluorophore-conjugated sheep anti-digoxigenin antibody (Oncor, Inc.), diluted 1:100 in 1× PBD.

And fluorophore-conjugated rabbit anti-sheep antibody (Oncor, Inc.), diluted 1:500 in 1× PBD.

CREST antisera is diluted 1:500 to 1:1000 in PEM.

Fluorophore-conjugated anti-human IgG(H+L) secondary antibodies (Pierce Chemicals) are diluted 1:500 in PEM.

DNA is counterstained with 0.1 μg/ml DAPI, 0.5 μg/ml propidium iodide, 1 μg/ml Hoechst 33258, or 10 μg/ml ethidium bromide, diluted in 1× PBD.

Protocol

Immunostaining

1. Cells are grown on or cytospun (800 rpm, 2 min) onto acid-etched and/or poly-amino acid-coated glass coverslips (as described in Section II).
2. Transfer coverslips to Coplin jars containing cold PBS. Keep on ice.
3. Rinse slides with cold PEM.
4. Cells are permeabilized prior to fixation with 0.5% Triton X-100 in PEM or CSK for 1 min on ice. Rinse briefly in fresh, cold PEM. To preserve the cytoskeleton and nuclear matrix while extracting soluble proteins, we recommend the use of 0.5% Triton X-100 in CSK [10 m*M* Pipes (pH 6.8), 100 m*M* NaCl, 300 m*M* sucrose, 3 m*M* $MgCl_2$, 1 m*M* EGTA] containing 4 m*M* VRC and multiple protease inhibitors (1.2 m*M* PMSF and 1 μg/ml each of aprotinin, leupeptin, antipain, and pepstatin). Prepare immediately before use and keep on ice.
5. Preparations are fixed in 0.5–1.5% formaldehyde, PEM for 15 min on ice.
6. Wash coverslips three times in PEM, 5 min each on a rotator.
7. Primary antibodies in PEM are incubated on preparations for 30–60 min at 37°C in a humid chamber.
8. The samples are then rinsed three times in PEM, 5 min each.
9. *Protect samples from light during all remaining steps.* Labeled secondary antibodies in PEM are incubated with samples for 30–60 min at 37°C in a humid chamber.
10. The coverslips are rinsed ~~three times in~~ PEM for 5 min at RT.
11. Fix samples in 2.5–3% formaldehyde, PEM for 15 min at RT.
12. Wash coverslips three times with ddH_2O, 5 min each.

Denaturation

13. The cells are fixed in freshly prepared Carnoy's fixative for 20 min at RT.
14. Dehydrate samples in a graded series of ethanols: 70, 85, and 100%, 2 min each at RT.
15. The coverslips are then allowed to air-dry and should be stored at −20°C with desiccant for a few days.

16. Preparations are denatured in 70% formamide, 2× SSC (pH 7.0) for 9 min at 78 or 79°C (place Coplin jar in a water bath).

17. The coverslips are immediately placed in 70% ethanol at −20°C for 2 min and moved to 85% ethanol at −20°C for 2 min, and finally to 100% ethanol at −20°C for 2 min.

18. After air-drying the coverslips, immediately begin hybridization.

Probe preparation

19. Suspend 50 ng of probe in 13 μl of deionized formamide with 10 μg of sheared salmon sperm DNA (Sigma Chemical Co.) and 15 μg of *E. coli* tRNA (Boehringer–Mannheim Biochemicals).

20. The probe is then denatured at 70°C for 5 min and immediately put on ice.

21. Prior to hybridization, 7 μl of hybridization buffer is added to the probe so that the final hybridization solution consists of 65% formamide, 2× SSC, 10% dextran sulfate, and 1% BSA.

Hybridization

22. Each coverslip is inverted onto 20 μl of hybridization solution on parafilm and incubated at 37°C overnight in a humidified chamber.

23. Samples are then rinsed in 0.5–0.75× SSC for 5 min at 72°C.

Detection

24. Hybridization of biotinylated probes is detected by incubating fluorophore-conjugated avidin on samples for 30–60 min at RT. See step 26 for digoxigenin-labeled probes.

25. The preparations are rinsed in 2× and 4× SSC containing 0.1% Tween-20 at RT, 10 min each. Skip to step 27.

26. When using digoxigenin-labeled probes, hybridization is detected by incubating samples with fluorophore-conjugated anti-digoxigenin antibody for 15 min at 37°C.

27. The preparations are rinsed three times in PBD, 5 min each.

28. DNA is counterstained with DAPI, propidium iodide, Hoechst 33258, or ethidium bromide for 15–45 sec at RT.

29. Rinse samples three times in PBD, 2 min each.

30. Coverslips are mounted onto glass slides using Vectashield antifade medium (Vector Laboratories, Inc.) or 1 mg/ml *p*-phenylenediamine in a 1:10 (v/v) mixture of PBS:glycerol, pH 8.0.

31. Seal coverslips with nail polish. Stained preparations should be examined and images captured immediately for best results. Slides may be stored at 4°C for a few weeks in a light-tight box.

Signal amplification

32. Peel the nail polish off and soak the slides in 1× PBD until the coverslip moves freely.

33. Rinse the coverslips thoroughly in 1× PBD at RT.

34. Incubate avidin-labeled samples for 15 min at 37°C with fluorophore-conjugated anti-avidin antibody. Complete steps 27–31.

35. Amplification of digoxigenin-conjugated probes is achieved by incubating samples with rabbit anti-sheep antibody at 37°C for 15 min.

36. Rinse three times for 5 min in 1× PBD at RT.

37. Incubate with fluorophore-labeled anti-rabbit antibody for 15 min at 37°C.

38. Complete steps 27–31.

VI. Specialized Techniques

The intact centromere is arranged as a series of repetitive subunits, folded tightly into a dense array of heterochromatin, often making it a difficult region of the chromosome to analyze by standard fluorescent staining techniques. A number of specialized techniques have been developed by our laboratory and others to make the centromere–kinetochore complex more accessible to structural and molecular analysis.

A. Centromere Fragmentation in Mitotic Cells with Unreplicated Genomes

In the late 1980s, we discovered that the centromere could be fragmented into small functional subunits that retain their capacity to capture microtubules and become aligned on the metaphase plate (Fig. 5). This phenomenon is produced *in situ* by exposing cells to caffeine that have been arrested at the G_1/S phase boundary with hydroxyurea (Brinkley *et al.,* 1988). By an unknown mechanism, cells treated under these conditions circumvent the DNA replication checkpoint and enter mitosis prematurely without progressing through S phase (Schlegel and Pardee, 1986; Hartwell and Weinert, 1989). Such cells display a highly fragmented genome, consisting of small chromosome fragments scattered throughout the cytoplasm (Ishida *et al.,* 1985).

Recently, we identified two types of centromere fragments in these mitotic cells with unreplicated genomes (MUGs): those that display kinetochore plates [centromere–kinetochore fragments (CFKs); Wise and Brinkley, 1997] and those that lack kinetochores. The CFKs are CREST-positive and undergo attachment to the spindle (Fig. 5), whereas those that lack kinetochores are CREST-negative and lack the capacity to attach and undergo movements. The latter can only be detected by FISH, using selected α-satellite DNA probes (D. He and B. R. Brinkley, manuscript in preparation). For details on the structure and movement of CKFs in MUGs, as well as interpretations of their relationship to centromere structure and function, readers are referred to earlier publications (Zinkowski *et al.,* 1991; Christy *et al.,* 1995; Wise and Brinkley, 1997). Although MUGs represent highly

perturbed cells that have been subjected to catastrophic conditions, much can still be learned about the structure and behavior of the eukaryotic centromere–kinetochore complex from this unique model.

In our hands, the MUG technique works only on certain mammalian cell types (rodents and muntjac deer) and is only useful for human chromosomes in rodent × human somatic cell hybrids. Although conditions may vary with different cell cultures, we have obtained excellent results with Chinese hamster ovary (CHO) cells. In this procedure, cell cultures are first arrested at G_0 by growing them until confluent and allowing them to undergo contact inhibition in nutrient-depleted medium. The cultures are then rinsed and replated to a density of 1×10^6 cells/28 mm^2 flask and incubated in serum-free medium for 66 hr at 37°C (Ashihara and Baserga, 1979; O'Keefe *et al.,* 1992). Cultures synchronized in G_0 should lack rounded mitotic cells when examined under the phase contrast microscope. The cells are then incubated in fresh, serum-containing medium for 4 hr, allowing progression into the G_1 phase of the cell cycle. Subsequent incubation in 2 m*M* hydroxyurea (HU) for 16–20 hr results in the arrest of cells at the G_1/S boundary of the cell cycle. Fresh medium is added containing 2 m*M* HU plus 5 m*M* caffeine, and the cells are cultured for an additional 2–6 hr. In order to increase the mitotic index, MUGs may be arrested in mitosis with 0.1 μg/ml Colcemid (Gibco Laboratories) concurrent to caffeine treatment. MUGs are selectively harvested by mitotic shake-off (described in Section II), cytocentrifuged onto coverslips, and processed according to given protocols.

B. Cloning Centromere DNA from MUGs

In many ways the MUG procedure utilizes the living cell to achieve the first step in isolating centromere fragments for *in vitro* analysis. We have adapted this procedure to facilitate the isolation and cloning of DNA from the centromere fragments of CHO cells (Ouspenski and Brinkley, 1993). The schematic shown in Fig. 6a illustrates the basic procedure that utilizes several previously described probes and techniques in a novel way to isolate a chromosome-specific centromere DNA sequence. The isolation of functional centromeric fragments involves three steps: (i) *in vivo* chromosome fragmentation, (ii) isolation of total chromosome fragments, and (iii) immunoprecipitation of the centromere fragments using antibodies from scleroderma CREST antiserum. After following the MUG procedure described in Section VI, A, we (as ~~quoted~~ stated in Ouspenski and Brinkley, 1993).

EA CaC

Stated EA

Adapted the polyamine chromosome isolation procedure of Gasser and Laemmli (1987) for the isolation of dispersed mitotic chromatin. The strategy of the method is to homogenize hypotonically swollen cells in a buffer that stabilizes the compact structure of mitotic chromatin, and then to fractionate the lysate by rate-zonal and isopycnic centrifugations. Centrifugation through a glycerol gradient as the first step allowed the separation of fine chromatin particles from unlysed cells, nuclei, whole chromosomes and chromatin aggregates (which sedimented into the lower part of the gradient) and soluble proteins (which remained in the supernatant).

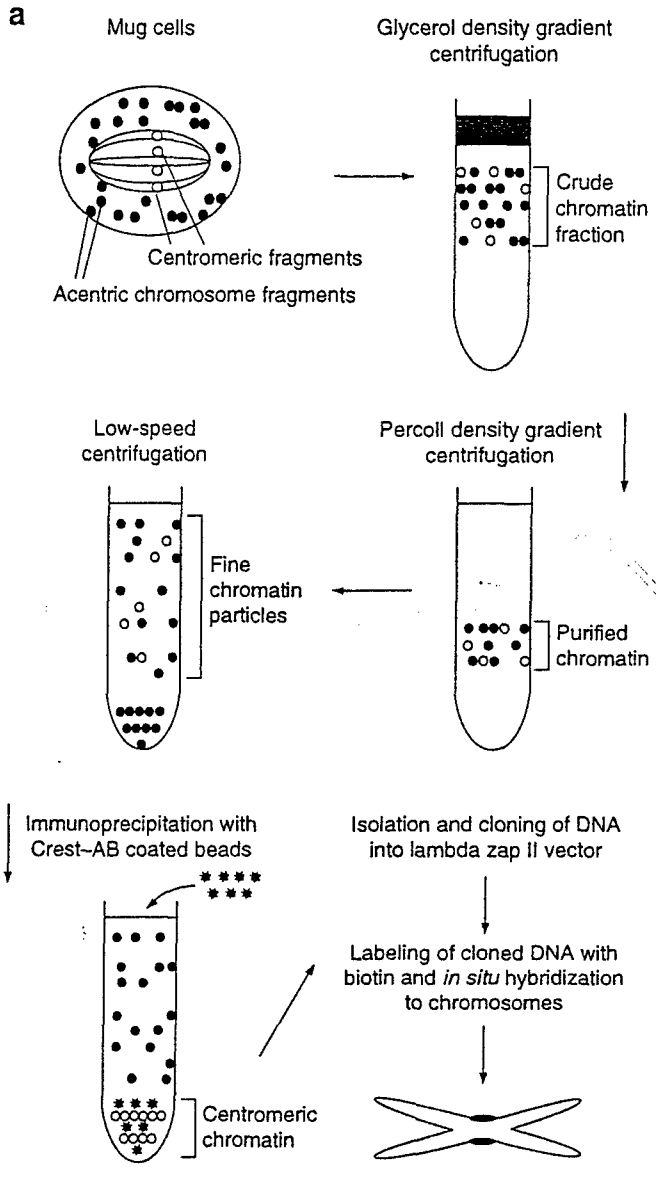

Fig. 6 (a) Isolation of functional centromeric fragments involving three steps: (i) *in vivo* chromosome fragmentation, (ii) isolation of total chromosome fragments, and (iii) immunoprecipitation of the centromere fragments using antibodies from scleroderma CREST antiserum (see Section VI,B) ~~(b) *In situ* hybridization of a unique centromere sequence to chromosome 1 of a metaphase CHO cell. Hybridization of the biotinylated probe was detected using avidin FITC (green), followed by amplification with anti-avidin FITC antibody (see Section IV). Chromosomes were stained with Hoechst 33258 (red). Images were collected and processed as described in the legend to Fig. 1~~ (reproduced from Ouspenski and Brinkley, 1993).

delete FA

AUTHOR SEE QUERY ON MS P 111 EA

P. 362

The chromatin was purified further by "banding" in an isopycnic gradient of Percoll, resulting in a preparation that was essentially free of cytoskeletal debris, as determined by microscopic observation. P. 362

The technical details of chromatin isolation, immunoaffinity purification of centromere fragments, and DNA cloning analysis are beyond the scope of this chapter and may be found in the original paper. To validate the specificity of the procedure, a randomly selected clone was labeled by nick translation with biotin-11-dUTP and hybridized to CHO chromosomes using the FISH procedure described in Section IV. Localization was observed exclusively at the centromere of chromosome 1 (Fig. 6b). Further analysis of this and other clones is under way.

C. Centromere Stretching

The tightly compacted centromere–kinetochore complex can be relaxed considerably, allowing the application of immunofluorescence, immunogold EM, or FISH to evaluate the organization of this complicated structure. This technique was inspired by earlier work, which showed that metaphase chromosomes can be microscopically identified and examined in much greater detail after mild hypotonic treatment (Fig. 2), a procedure that revolutionized the field of cytogenetics (Hsu, 1952; Tjio and Levan, 1956). Using a modified procedure developed in our laboratory, one can stretch or extend the centromere in such a way as to uncoil its structure and better resolve the repetitive pattern of DNA and proteins (Zinkowski *et al.*, 1991; Haaf and Ward, 1994a).

In one procedure, cells are harvested by mitotic shake-off (described in Section II) and suspended in 1 or 2 ml of PBS, containing a protease inhibitor cocktail [0.1 m*M* PMSF and 1 μg/ml each of chymostatin, leupeptin, antipain, and pepstatin (P-CLAP)], for a final concentration of about 1×10^6 cells per milliliter. The cells are then lysed by forcing the suspension through a 26-gauge syringe three times. Approximately 100 μl of the lysed cell preparation is added to a cytocentrifuge cup, and the chromosomes and cell debris are spun onto acid-etched and/or poly-amino acid-coated slides or coverslips using a Cytospin cytocentrifuge (Shandon Instruments, Inc.) at 800–1200 rpm for 2 min. The preparations are promptly removed and processed according to the given protocols.

In a second procedure, hypotonic stretching of chromosomes is achieved by incubating mitotic cells (harvested by shake-off) or cell lysates (from the previous procedure) in 75 m*M* KCl containing P-CLAP for 5–15 min. The preparations are then spun onto coverslips using a cytocentrifuge at 2000 rpm for 2 min with high acceleration. Generally, short exposures to hypotonic solution produce swollen chromosomes, whereas longer exposures improve the centromere stretching process. Chromosomes generally stretch poorly in the center of the cell spot (usually the most crowded area), whereas chromosomes along the outer perimeter are maximally stretched. This produces a gradient in centromere distension that is often useful in structural interpretations (Fig. 7).

Centromere stretching may be facilitated by growing cells in the presence of nonintercalating DNA-binding agents, such as Hoechst 33258 or DAPI, which induce the undercondensation of chromatin, especially heterochromatin, by unknown mechanisms (Hilwig and Gropp, 1973; Rocchi *et al.,* 1979). For example, human cells are grown in the presence of 100 μg/ml DAPI for 16–18 hr prior to metaphase arrest in order to facilitate centromere stretching. The cytidine analog 5-azacytidine and 5-azadeoxycytidine also induce undercondensation, most likely by inhibiting DNA methylation (Jones and Taylor, 1980; Schmid *et al.,* 1983). In a comparative study using a variety of treatments, the overall length of human chromosomes was greatest after treatment with 5-azacytidine following a fluorodeoxyuridine (FUdR)/uridine metabolic block (Jeppesen *et al.,* 1992). Cell cultures are synchronized in 0.1 μM FUdR and 1 μM uridine for 13 hr. The block is then removed by adding thymidine to a final concentration of 10 μM, at which time 5-azacytidine is added to 0.37 μM. Cells are harvested 5 hr after treatment and processed according to the previously discussed hypotonic procedure.

The degree of centromere stretching produced by these procedures can range from zero in some chromosomes to maximum centromere stretching of 20 times their normal metaphase length in the same preparation. In a study of muntjac chromosomes, we found that centromeres were stretched about 11- or 12-fold on average (Zinkowski *et al.,* 1991). Interphase chromatin, including chromatin in prekinetochores, may be stretched to a much greater degree. It should be pointed out, however, that this procedure has certain limitations and, by its nature, produces considerable artifact and perturbation of structure. Careful controls must be followed, and interpretations must be made with caution. Hypotonic swelling of mammalian cells leads to the loss of kinetochore plate morphology as well as the disruption of microtubules, centrioles, and centrosomes (Brinkley *et al.,* 1980; Ris and Witt, 1981). However, if the period of hypotonic swelling is brief (under 15 min), the damage can be reversed by returning the cells to an isotonic tissue culture environment (Brinkley *et al.,* 1980). Under these conditions, cell viability will not be adversely affected.

With these caveats in mind, much can be learned about chromatin organization from centromere stretching experiments. Using a combination of immunofluorescence and FISH (see Section V) on the same stretched preparations, we discovered several new features of the centromere–kinetochore complex. Prior to stretching, CREST staining reveals a single plate or band along the outer surface of the centromere. Immunogold EM images show that most of the CREST antigens are subjacent to the inner kinetochore plate and totally excluded from the outer plate. After stretching, a series of punctate, CREST-positive segments become increasingly separated by unstained regions, producing the beads-on-a-string appearance (Zinkowski *et al.,* 1991) seen in Fig. 7. When stretched human chromosomes are stained with a combination of CREST immunofluorescence and FISH using a consensus α-satellite probe, one can see that the repetitive subunits are connected by a continuous fiber of α-satellite DNA (Haaf and Ward, 1994a; D. He and B. R. Brinkley, manuscript in preparation). Haaf and Ward

(1994a,b) noted DNA resolution of around 10 kb/μm and concluded that such preparations were extremely useful for long-range mapping research of both interphase and metaphase chromatin.

D. Frozen Sections

The study of centromere–kinetochores in whole tissues is difficult because one must resort to sectioning. Standard paraffin sections can be used if the cells are properly fixed and deparaffinized prior to staining, but they are still of limited value due to section thickness. We have obtained excellent results using a cryomicrotome to cut thick (up to 50 μm) frozen (−80°C) sections of tissues dissected from experimental animals. The frozen sections are mounted on precoated slides (Fisher Scientific, Pittsburgh, PA), permeabilized with 0.5% Triton X-100 for 3 min, and fixed in 3.7% formaldehyde in PBS for 15 min at room temperature. The sections are stained by standard procedures (refer to Section II) using a combination of CREST immunofluorescence for 3 hr at 37°C, detected by fluorophore-conjugated secondary antibody, and nucleic acid counterstaining. Sections are examined by confocal microscopy [in our case, using a Molecular Dynamics (Sunnyvale, CA) Multiprobe 2001 laser scanning confocal microscope] and images are collected at 0.2–5.0 μm steps. Three-dimensional projections are then rendered using an appropriate software package (ImageSpace by Molecular Dynamics). Examples of centromere staining in rat mammary gland tissues are shown in Fig. 8.

E. Centromere–Kinetochores of Plant Chromosomes

The centromere and kinetochore of many plant chromosomes, like those of animal chromosomes, are confined to a single focus. Those of other plant species may be diffuse or polycentric in their distribution along the chromosomes. Relatively little is known about the molecular composition of plant centromeres, largely due to the fact that human anticentromere autoantibodies have had limited application. A clear exception is found in an antiserum designated EK, collected from a patient with the CREST variant of scleroderma. EK-CREST stains both prekinetochores in interphase nuclei and centromeres on metaphase chromosomes of the higher plant *Haemanthus katherinae* Bak and the spiderwort plant *Tradescantia virginiana* (Mole-Bajer *et al.*, 1990; Wolniak and Larsen, 1992). In western blots using *Haemanthus* cell extracts, EK-CREST predominantly recognizes two bands of 65 and 135 kDa. In human (HeLa) cell extracts, EK-CREST recognizes bands of 52, 80, and 110 kDa as well as two or three minor bands between 140 and 200 kDa. Other CREST antisera in our collection fail to stain the centromere of plant chromosomes.

1. Protocol for CREST Immunofluorescence

Endosperm cells are spun onto clean glass microscope slides at 1500 rpm for 3 min using a cytocentrifuge (see Section II). The preparations are permeabilized

and fixed in 100% methanol at −20°C for 7 min and then rinsed and rehydrated twice in PBS, 5 min each. The slide preparations are incubated in CREST antiserum ~~and~~ diluted 1:20 in PBS for 30 min in a humidified 37°C incubator. After three 5-min rinses in PBS, the preparations are incubated in 1:20 FITC-conjugated goat anti-human IgG (Boehringer–Mannheim Biochemicals) for 30 min at 37°C. The preparations are rinsed for 5 min in PBS, counterstained for DNA in PBS containing 10 μg/ml Hoechst 33258 (Sigma Chemical Co.), and rinsed again for 5 min in PBS. The slides are overlaid with 50 μl of mounting medium [1 mg/ml *p*-phenylenediamine in a 1:10 (v/v) mixture of PBS:glycerol], and a coverslip is applied. Preparations may be examined using a standard fluorescence microscope.

2. Protocol for Silver Enhancement

Excellent contrast and resolution of the centromere can be obtained by bright-field microscopy using the silver enhancement procedure. Cells are fixed as described previously and incubated with CREST antiserum at a 1:5 to 1:10 dilution overnight at room temperature. The preparations are incubated with 5 nm immunogold for 6 hr. Immunogold silver-enhanced staining is then accomplished by the method of Hoefsmit *et al.* (1986), as modified for *Haemanthus* by Mole-Bajer *et al.* (1990). Preparations are embedded in Permount (Fisher Scientific), a mounting medium that matches the refractive index of chromosomes and nuclei fixed with methanol. A glass coverslip is placed over the cellular material prior to examination with brightfield optics.

Acknowledgments

We thank L. Zhong for contributing technical expertise throughout the writing of the manuscript. Appreciation is also extended to M. G. Mancini for technical ~~advice~~ assistance and to M. A. Mancini and I. Ouspenski ~~for reading the manuscript and~~ for helpful suggestions. These studies were supported in part by Grants CA41424 and CA64235 from the National Institutes of Health to BRB and Grant DAMD17-94-J-4253 from the Department of the Army to J. Rosen.

References

Ashihara, T., and Baserga, R. (1979). Cell synchronization. *Methods Enzymol.* **58**, 248–262.

Brenner, S., Pepper, D., Berns, M. W., Tan, E., and Brinkley, B. R. (1981). Kinetochore structure, duplication, and distribution in mammalian cells: Analysis by human autoantibodies from scleroderma patients. *J. Cell Biol.* **91**, 95–102.

Brinkley, B. R., and Chang, J. P. (1973). Embedding *in situ*. *In* "Tissue Culture: Methods and Applications," pp. 438–443. Academic Press, New York.

Brinkley, B. R., and Stubblefield, E. (1966). The fine structure of the kinetochore of a mammalian cell *in vitro*. *Chromosoma* **19**, 28–43.

Brinkley, B. R., Fuller, G. M., and Highfield, D. P. (1975). Cytoplasmic microtubules in normal and transformed cells in culture: Analysis by tubulin antibody immunofluorescence. *Proc. Natl. Acad. Sci. USA* **72**, 4981–4985.

Brinkley, B. R., Cox, S. M., and Pepper, D. A. (1980). Structure of the mitotic apparatus and chromosomes after hypotonic treatment of mammalian cells *in vitro*. *Cytogenet. Cell Genet.* **26**, 165–174.

Brinkley, B. R., Zinkowski, R. P., Mollon, W. L., Davis, F. M., Pisegna, M. A., Pershouse, M., and Rao, P. N. (1988). Movement and segregation of kinetochores experimentally detached from mammalian chromosomes. *Nature* **336**, 251–254.

Brinkley, B. R., Ouspenski, I., and Zinkowski, R. P. (1992). Structure and molecular organization of the centromere–kinetochore complex. *Trends Cell Biol.* **2**, 15–21.

Britten, R. J., and Kohne, D. E. (1968). Repeated sequences in DNA. Hundreds of thousands of copies of DNA sequences have been incorporated into the genomes of higher organisms. *Science* **161**, 529–540.

Christy, C. S., Deden, M., and Snyder, J. A. (1995). Localization of kinetochore fragments isolated from single chromatids in mitotic CHO cells. *Protoplasma* **186**, 193–200.

Fuller, G. M., Brinkley, B. R., and Boughter, J. M. (1975). Immunofluorescence of mitotic spindles by using monospecific antibody against bovine brain tubulin. *Science* **187**, 948–950.

insert ref. see below

Gasser, S. M., and Laemmli, U. K. (1987). Improved methods for the isolation of individual and clustered mitotic chromosomes. *Exp. Cell Res.* **173**, 85–98.

Haaf, T., and Ward, D. C. (1994a). Structural analysis of alpha-satellite DNA and centromere proteins using extended chromatin and chromosomes. *Hum. Mol. Genet.* **3**, 697–709.

Haaf, T., and Ward, D. C. (1994b). High resolution ordering of YAC contigs using extended chromatin and chromosomes. *Hum. Mol. Genet.* **3**, 629–633.

Haaf, T., and Willard, H. F. (1992). Organization, polymorphism, and molecular cytogenetics of chromosome-specific alpha-satellite DNA from the centromere of chromosome 2. *Genomics* **13**, 122–128.

Hartwell, L. H., and Weinert, T. A. (1989). Checkpoints: Controls that ensure the order of cell cycle events. *Science* **246**, 629–634.

He, D., and Brinkley, B. R. (1996). Structure and dynamic organization of centromeres/prekinetochores in the nucleus of mammalian cells. *J. Cell Sci.* **109**, 2693–2704.

Hendzel, M. J., Yi, W., Mancini, M. A., Van Hooser, A., Ranalli, T., Brinkley, B. R., Bazett-Jones, D. P., and Allis, C. D. (1997). Mitosis-specific phosphorylation of histone H3 initiates primarily within pericentromeric heterochromatin during G_2 and spreads in an ordered fashion coincident with mitotic chromosome condensation. *Chromosoma* **106**, 348–360.

Hilwig, I., and Gropp, A. (1973). Decondensation of constitutive heterochromatin in L. cell chromosomes by a benzimidazole compound ("33258 Hoechst"). *Exp. Cell Res.* **81**, 474–477.

Hoefsmit, E. C., Korn, C., Blijleven, N., and Ploem, J. S. (1986). Light microscopical detection of single 5 and 20 nm gold particles used for immunolabelling of plasma membrane antigens with silver enhancement and reflection contrast. *J. Microsc.* **143**, 161–169.

Hsu, T. C. (1952). Mammalian chromosomes *in vitro*. I. The karyotype of man. *J. Heredity* **43**, 167–172.

Ishida, R., Kozaki, M., and Takahashi, T. (1985). Caffeine alone causes DNA damage in Chinese hamster ovary cells. *Cell Struct. Funct.* **10**, 405–409.

Jeppesen, P., Mitchell, A., Turner, B., and Perry, P. (1992). Antibodies to defined histone epitopes reveal variations in chromatin conformation and underacetylation of centric heterochromatin in human metaphase chromosomes. *Chromosoma* **101**, 322–332.

John, H. A., Birnstiel, M. L., and Jones, K. W. (1969). "RNA–DNA hybrids at the cytological level. *Nature* **223**, 582–587.

Johnson, G. D., and Nogueira Araujo, G. M. D. C. (1981). A simple method of reducing the fading of immunofluorescence during microscopy. *J. Immunol. Methods* **43**, 349–350.

Jokelainen, P. T. (1967). The ultrastructure and spatial organization of the metaphase kinetochore in mitotic rat cells. *J. Ultrastruct. Res.* **19**, 19–44.

Jones, P. A., and Taylor, S. M. (1980). Cellular differentiation, cytidine analogs and DNA methylation. *Cell* **20**, 85–93.

Langer, P. R., Waldrop, A. A., and Ward, D. C. (1981). Enzymatic synthesis of biotin labeled polynucleotides: Novel nucleic acid affinity probes. *Proc. Natl. Acad. Sci. USA* **78**, 6633–6637.

Gorbsky, G.J. (1997). Cell cycle checkpoints: Arresting progress in mitosis. Bioessays 19, 193-197.

(ital) (bf)

Lawrence, J. B., Villnave, C. A., and Singer, R. H. (1988). Sensitive, high-resolution chromatin and chromosome mapping *in situ:* Presence and orientation of two closely integrated copies of EBV in a lymphoma line. *Cell* **52**, 51–61.

Lazarides, E., and Weber, K. (1974). Actin antibody: The specific visualization of actin filaments in non-muscle cells. *Proc. Natl. Acad. Sci. USA* **71**, 2268–2272.

Mace, M. L., Jr., Tevethia, S. S., and Brinkley, B. R. (1972). Differential immunofluorescence labeling of chromosomes with antisera for single stand DNA. *Exp. Cell Res.* **75**, 521–523.

Mole-Bajer, J., Bajer, A. S., Zinkowski, R. P., Balczon, R. D., and Brinkley, B. R. (1990). Autoantibodies from a patient with scleroderma CREST recognized kinetochores of the higher plant *Haemanthus. Proc. Natl. Acad. Sci. USA* **87**, 3599–3603.

Moroi, Y., Peebles, C., Fritzler, M. J., Steigerwald, J., and Tan, E. M. (1980). Autoantibody to centromere (kinetochore) in scleroderma sera. *Proc. Natl. Acad. Sci. USA* **77**, 1627–1631.

Nickerson, J. A., Krockmalnic, G., He, D., and Penman, S. (1990). Immunolocalization in three dimensions: Immunogold staining of cytoskeletal and nuclear matrix proteins in resinless electron microscopy sections. *Proc. Natl. Acad. Sci. USA* **87**, 2259–2263.

O'Keefe, R. T., Henderson, S. C., and Spector, D. L. (1992). Dynamic organization of DNA replication in mammalian cell nuclei: Spatially and temporally defined replication of chromosome-specific α-satellite DNA sequences. *J. Cell Biol.* **116**, 1095–1110.

Ouspenski, I. I., and Brinkley, B. R. (1993). Centromeric DNA cloned from functional kinetochore fragments in mitotic cells with unreplicated genomes. *J. Cell Sci.* **105**, 359–367.

Pardue, M. L., and Gall, J. G. (1970). Chromosomal localization of mouse satellite DNA. *Science* **168**, 1356–1358.

Pepper, D. A., and Brinkley, B. R. (1977). Localization of tubulin in the mitotic apparatus of mammalian cells by immunofluorescence and immunoelectron microscopy. *Chromosoma* **60**, 223–235.

Reynolds, E. S. (1963). The use of lead citrate of high pH as an electron-opaque stain in electron microscopy. *J. Cell Biol.* **17**, 208–212.

Rieder, C. L. (1979a). Ribonucleoprotein staining of centrioles and kinetochores in newt lung cell spindles. *J. Cell Biol.* **80**, 1–9.

Rieder, C. L. (1979b). Localization of ribonucleoprotein in the trilaminar kinetochore of Ptk1. *J. Ultrastruct. Res.* **66**, 109–119.

Ris, H., and Witt, P. L. (1981). Structure of the mammalian kinetochore. *Chromosoma* **82**, 153–170.

Rocchi, A., Di Castro, M., and Prantera, G. (1979). Effects of DAPI on human leukocytes *in vitro. Cytogenet. Cell Genet.* **23**, 250–254.

Schlegel, R., and Pardee, A. B. (1986). Caffeine-induced uncoupling of mitosis from the completion of DNA replication in mammalian cells. *Science* **232**, 1264–1266.

Schmid, M., Grunert, D., Haaf, T., and Engel, W. (1983). A direct demonstration of somatically paired heterochromatin of human chromosomes. *Cytogenet. Cell Genet.* **36**, 554–561.

Spurr, A. R. (1969). A low-viscosity epoxy resin embedding medium for electron microscopy. *J. Ultrastruct. Res.* **26**, 31–43.

Sullivan, K. F. (1998). A moveable feast: The centromere/kinetochore complex in cell division. *In* "Mechanisms of Cell Division: Frontiers in Molecular Biology" (S. Endow ~~and~~ D. Glover, Eds.). A Oxford Univers: Press Oxfor England

Tjio, J. H., and Levan, A. (1956). The chromosome number of man (*Hereditas* **42**) 1–6.

Waring, M., and Britten, R. J. (1966). Nucleotide sequence repetition: ~~A rapidly re~~associating fraction of mouse DNA. *Science* **154**, 791–794.

Wevrick, R., Willard, V. P., and Willard, H. F. (1992). Structure of DNA near long tandem arrays of alpha satellite DNA at the centromere of human chromosome 7. *Genomics* **14**, 912–923.

Wise, D. A., and Brinkley, B. R. (1997). Mitosis in cells with unreplicated genomes (MUGs): Spindle assembly and behavior of centromere fragments. *Cell Motil. Cytoskel.* **36**, 291–302.

Wolniak, S. M., and Larsen, P. M. (1992). Changes in the metaphase transit times and the pattern of sister chromatid separation in stamen hair cells of *Tradescantia* after treatment with protein phosphatase inhibitors. *J. Cell Sci.* **102**, 691–715.

Zinkowski, R. P., Meyne, J., and Brinkley, B. R. (1991). The centromere–kinetochore complex: A repeat subunit model. *J. Cell Biol.* **113**, 1091–1110.

AUTHOR SEE QUERY ON MS P 125

Yes, see insert to left

VIEWS AND REVIEWS

CELL MOTILITY AND THE CYTOSKELETON (IN PRESS, 1998)

SUPERNUMERARY CENTROSOMES AND CANCER: BOVERI'S HYPOTHESIS RESURRECTED

B. R. Brinkley and T. M. Goepfert, Department of Cell Biology,
Baylor College of Medicine, Houston, TX 77030

Introduction

The centrosome, a paternal gift to the cytoplasm of fertilized eggs (Simerly et al., 1995), plays a vital role in cell division at all stages of human development. Identified in the cytoplasm of many eukaryotic cells as a discrete microscopic domain containing one or more pairs of centrioles surrounded by amorphous pericentriolar material (PCM), the centrosome functions as a microtubule organizing center (MTOC) that controls the number, polarity and orientation of microtubules in cells (see **Views and Reviews** by Sluder and Rieder, 1996). Faithfully inherited by each daughter cell following mitosis, the centrosome divides once, and only once, and undergoes a maturation phase in each cell cycle (Balczon et al., 1995). Through their well-established role in the assembly of microtubule arrays (Karsenti et al., 1984), and impact on other structures such as the actin cytoskeleton (Raff and Glover, 1989), centrosomes are essential in cell proliferation and can influence many other aspects of development, cell motility and differentiation. Therefore, it is not surprising that this unique cytoplasmic domain, discovered over a

In a 1914 treaties *Zur Frage der Enstehung Maligner Tumoren,* Th. Boveri made a remarkable proposal that cancer cells arise by the aberrant replication and activity of centrosomes producing extra spindle poles that effect the gain or loss of chromosomes from a diploid set (aneuploidy) during mitosis. Boveri also proposed a link between shapes and forms of cancer cells and the role centrosomes play in maintaining cell polarity. In spite of the knowledge that nearly all of the 20,000 solid tumors in humans are aneuploid, few have taken Boveri's proposal seriously, until very recently.

Following the discovery of genes and later, oncogenes and tumor suppressors, somatic mutations became the favored hypothesis for the origin of malignancy, with aneuploidy relegated to an epiphenomenon of cancer. With the discovery of genes controlling the cell cycle and more recently, the localization of their products in and around the poles of mitotic spindles, a renewed interest in the biology of the centrosome has evolved. In addition, the availability of new tools such as anticentrosome antibodies and confocal microscopy has facilitated the imaging of these organelles within cells of intact tissues. Thus, it is becoming well established that many tumor cells display multiple (supernumerary) centrosomes instead of the expected one or two normally found in diploid cells. This surprising observation raises the question of how an extra load of centrosomes affects cell division and polarity. It also resurrects Boveri's early hypothesis and raises a similar question: Which comes first, cancer, aneuploidy or aberrant centrosomes and what role, if any, does centrosome hypertrophy play in the cascade of events leading to cell transformation and malignancy? An answer may be found in emerging studies of the molecular biology of centrosomes, and elucidation of genes and gene products controlling cycles of their replication, maturation and mitosis.

Molecular Biology of Centrosomes. Although the anatomical history of the centrosome extends back for over a century, its molecular biology is only just now emerging. Genetic and biochemical studies of yeast, *Drosophila, Xenopus, Spisula* and humans have identified a growing list of centrosome-associated proteins involved in spindle assembly and chromosome segregation as summarized in Table 1. The regulation of protein function through phosphorylation is fundamental in controlling cell cycle progression and much attention has focused on the cyclin-dependent protein kinases (cdks). However, a number of other proteins also influence the overall organization of cells and control the dynamics of cellular architecture via the centrosomes.

Disruption of most of these proteins can lead to chromosome missegregation, multipolar or monopolar spindles or otherwise aberrant spindle assembly and organization. Several proteins represent distinct families identified as serine/threonine kinases. Cdc2 (p34cdc2), a cyclin-dependent kinase, highly conserved from yeast to mammals, is required for centrosome separation and formation of bipolar spindles. MPS1, a *Saccharomyces cerevisiae* dual specificity kinase is required for spindle pole body duplication, and polo-like kinases, also highly conserved, orchestrate several mitotic events including the formation of bipolar spindles. The expression of PLK1, the human homolog to polo, is elevated in a majority of non-small cell lung carcinomas and high levels correlate with poor prognosis (Wolfe et al., 1997), implying a role in cancer for a protein involved in centrosome regulation. New members of the aurora subfamily including aurora1, and STK15/BTAK (Zhou et al., 1998) also identified as aurora2 (Bischoff et al., 1998) have recently been identified and characterized and will be discussed later. STK15/BTAK, henceforth called BTAK or aurora2, is amplified and

over-expressed in many human breast cancer cell types and in breast, ovarian, colon, prostate, neuroblastoma and cervical cancer cell lines. This kinase-encoding gene is mapped to chromosome 20q13p, a region frequently amplified in human tumors (Sen et al., 1997). Conceivably, these proteins, together with PLK1, form a centrosome-associated kinase cascade whose disruption leads to centrosome amplification, genomic instability and chromosome segregation defects.

Kinases and phosphatases interact with centrosomes during both interphase and mitosis. A good example is seen in Ipl1-kinase and protein phosphatase 1 (PP1). Type 1 PP acts in opposition to Ipl1 in regulating yeast chromosome segregation. Another centrosome-associated protein kinase co-localized in the centrosome is Nek2, a closely related protein of the mitotic regulator NIMA of *Aspergillus nidulans*. Nek2 phosphorylates C-Nap 1, implicating both in regulation of centriole-centriole cohesion during the cell cycle. In addition to the serine/threonine kinases, a src-type tyrosine kinase, Fyn, also co-localizes with centrosomes during M-phase.

It is well documented that $Ca2^{+}$ is required for cell cycle progression and mediates its action via calmodulin. The $Ca2^{+}$/CaM kinase II found in centrosomes phosphorylates several centrosomal proteins. One substrate, centrin, a 20 kDa calcium-binding phosphoprotein, is associated with centrioles/basal bodies in cells from diverse evolutionary lineages. In normal breast epithelial cells, centrin appears phosphorylated at various times in the cell cycle and phosphocentrin has been reported to accumulate in the unusually large centrosomes of tumor cells (Lingle et al., 1998).

Dynamic aspects of mitosis such as centrosome separation, formation of a bipolar spindle and anaphase movement of chromosomes, involve a number of microtubule-based

motor proteins. Kinesin-like proteins (KLPs) are responsible for many such motile events. At the onset of mitosis, the association of motors with the spindle apparatus is promoted by phosphorylation. Prominent among the KLPs is the BimC family, members of which are found in eukaryotic cells ranging from yeast to human. The regulation of human HsEg5 activated through phosphorylation by p34cdc2 provides an example for regulated targeting of a temporal activation of motors and centrosome separation at the beginning of mitosis.

Mammalian mitotic kinesin-like protein1 (MKLP-1) has been implicated in the process of anapahse B and cytokinesis. A similar gene ZEN-4 in *C. elegans* has also been identified and associated with spindle elongation and cytokinesis. The precise localization of MKLP-1 and its counterpart in *Drosophila,* pavarotti (PAV-KLP), at the centrosomes and near the central region of the spindle, raises the possibility that these factors may function in transporting signaling molecules needed in coordinating centrosomes with cleavage furrow formation and cytokinesis (for references, see Table I). Also, the spatial positioning of the serine/threonine kinase polo with PAV-KLP implicates polo as a candidate for a similar function.

Where exactly these many intermediates in centrosome regulation are localized within the ultrastructure of the centrosome remains an important question. Obviously, some proteins such as centrin, the centrosome autoantigen PCM-1 (Balczon et al, 1995), α-, β- and γ-tubulin are likely to be constitutive proteins that play important roles in maintaining structure-function relationships in the centrosome, while many catalytic proteins may be more transient cell cycle regulators. The ability of centrosomes to nucleate microtubules correlates with the presence of γ-tubulin and a 25 nm diameter ring

complex (Moritz et al., 1995) present in the PCM. Although little is known about the composition of PCM, Palazzo and coworkers recently described this component as a three-dimensional "centromatrix" associated with centrosomes of *Spisula* (Schnackenberg et al., 1998). Built of 12-15 nm fibers that form an insoluble meshwork around the centrioles, this component appears to serve as a fibrous lattice into which various intermediates such as the 25 nm γ-tubulin rings, centrioles and other constitutive elements are embedded. The PCM may also serve to spatially arrange various molecules such as those identified in Table 1. Collectively, the centrosome is a dynamic and structurally complex domain that embraces a growing number of intermediates needed for cell division. Therefore, further knowledge of centrosome-associated molecular components that control maturation, duplication and partitioning of this cytoplasmic domain will likely be of considerable importance in understanding mitosis and the maintenance of cell polarity.

Centrosome Anomalies in Tumor Cells *in vitro* and *in vivo*. Recently, several studies reporting centrosome anomalies in cancer have appeared, including observations of striking abnormalities such as hypertrophy and amplification in various rodent and human cells and tissues. All studies intimate centrosomes as a factor in aneuploidy, genomic instability and adverse effects on cell polarity in tumor cells. A paper by George Vande Woude's group reported on centrosome replication in cultured fibroblasts deficient for p53, a tumor suppressor gene found to be mutated in a majority of human and rodent tumors (Fukasawa et al., 1996). In knockout mice where the p53 gene has been deleted, multiple tumors occur in adult animals. The mice develop normally and fail to show appreciable neoplasia until they reach maturity (Donehower et al., 1992). The Vande

Woude group examined mouse embryonic fibroblasts (MEFs) *in vitro* with p53 -/-, +/- and -/- phenotypes and found that null MEFs displayed multiple centrosomes, whereas +/- and +/+ cells contained the expected one or two centrosomes per cell shown by staining with anti-gamma tubulin antibodies and examination by immunofluorescence. Control MEFs prepared from normal mice, as well as mice null for the retinoblastoma tumor suppressor gene product (Rb), displayed a normal number of centrosomes. Serum-starved and serum-stimulated +/+ cells continued to display the normal complement of centrosomes (one in serum-starved G_0 cells and one or two in stimulated cycling cells), whereas cells with the -/- phenotype displayed multiple centrosomes in both populations. They found that centrosome amplification could affect mitotic fidelity, causing unequal segregation of chromosomes that could lead to genomic stability. It was noted, however, that a majority of cells with elevated centrosome numbers displayed metaphase spindles with bipolar axes. This is an important observation that we will revisit later in this report. It is also significant that the p53 protein has been localized at centrosomes in interphase cells but not in mitotic cells (Blair-Zajdel and Blair, 1988; Brown et al., 1994).

Although the report by Fukasawa, (1996) suggested that p53 might participate in maintaining centrosome stability in normal cells and cause loss of stability in transformed cells, the study involved cells *in vitro*. In support of the *in vitro* studies, several other groups provided corroborating evidence for centrosome amplification in full-blown tumors *in vivo*.

Experiments performed by Dennis Roop's group at Baylor College of Medicine (Wang et al., 1998), done in collaboration with our own group, provided confirmation *in vivo* that centrosome amplification occurred in papillomas and metastatic skin carcinomas

in transgenic mice expressing the mutant p53 gene, HK1.p53^{m} . In this study, thick (30 μm) cryosections, stained with a human autoimmune serum containing anticentrosome antibodies (Balczon and West, 1991) and examined by confocal microscopy, revealed aberrant amplification of centrosomes in cells throughout the tumors. *In situ* examination revealed striking abnormalities, with 75% of the tumor cells containing three or more centrosomes, whereas normal skin cells and benign papillomas from control animals displayed the expected one or two centrosomes. Moreover, BrdU uptake and staining provided a positive correlation between centrosome amplification and increased genomic instability in the mouse tumor cells.

Documentation of centrosome hypertrophy in human breast tumor cells was provided in a study from Jeffrey Salisbury's laboratory (Lingle et al., 1998). These investigators obtained human breast tissues immediately after surgery and prepared 12 μm-thick cryosections that were processed for anti-centrin immunofluorescent staining. Observations by confocal microscopy of a set of 35 high-grade human breast tumors revealed that human adenocarcinoma cells generally displayed a number of abnormalities including an increase in centrosome number and volume, accumulation of excess pericentriolar material, supernumerary centrioles and aberrant protein phosphorylation. Using a novel *in vitro* assembly assay involving tissue sections, these investigators showed increased MTOC activity in the supernumerary centrosomes.

An almost identical observation was made by Pihan et al., (1998) from Stephen Doxsey's laboratory, who examined a variety of tumors and tumor derived cell lines. These investigators also concluded that aberrant centrosome could contribute to genetic instability in cancer.

What is Centrosome Amplification? The term amplification implies that cells replicate more centrosomes than the two copies needed for normal cell division. Most recent reports document amplification using centrosome-specific antibodies and immunofluorescence to detect extra fluorescent spots in the cytoplasm. The technique is limited in that it does not provide information on what exactly the supernumerary spots represent; are they exact duplications of centrosomes or only partial centrosomes produced either by ectopic assembly of PCM or fragmentation of a parent centrosome? Answers to these questions await more detailed electron microscopic analysis of supernumerary centrosomes. Under normal conditions a centrosome duplicates once in late S- or early G_2-phase of the cycle (Brinkley, 1985; Vandre and Borisy, 1989). Abnormalities, such as those reported in cancer cells could be accounted for by any number of factors involved in pathways controlling cell cycle progression, the centrosome cycle or a combination of both. In one scenario cell transformation could cause delay in cell cycle progression, enabling the continuation of centrosome replication as seen in cells chemically arrested at the G_1/S boundary (Balczon et al., 1995). Thus, when cells eventually reach mitosis, they would contain extra copies of the centrosomes. A second way that cells can gain extra centrosomes is through a failure of daughter cells to complete division and separate at telophase due to a defect in cytokinesis, leading to the restitution of a single cytoplasm with a double set of centrosomes. Alternatively, the aberration could involve the centrosome machinery itself and genes directly involved in the centrosome replication pathway. The latter scenario is supported by recent reports mentioned earlier of a link between a family of serine/threonine kinases localized at centrosomes and their over-expression in human breast cancer cells. In 1997, Subrata Sen

and his co-workers at the M.D. Anderson Cancer Center identified a partial cDNA sequence cloned from a DNA amplicon on chromosome 20q13p of breast cancer patients called STK15 and later, breast tumor amplified kinase (BTAK). More recently, in collaborations with our laboratory at Baylor College of Medicine, Sen's group learned that an antibody raised against BTAK localized the gene product at the centrosomes of mitotic and interphase cells (Zhou et al., 1998). The full-length BTAK cDNA indicated an open reading frame encoding a 403 amino acid protein with MW of 46 kDa. Moreover, the amino acid sequence revealed the conservation of twelve kinase-specific subdomains with a 40% and 48% sequence identity to *S. cerevisae* Ipl1 and *Drosophila* serine/threonine kinase aurora, respectively (Table 1). In an independent study, Bischoff et al., (1998) identified an identical kinase called aurora2, and reported its amplification in colon tumor cells.

Could the BTAK (aurora2) gene, amplified in 12% of primary human breast tumors and a variety of other cancers, be directly responsible for centrosome duplication-distribution abnormalities and aneuploidy? To test this notion, we elevated BTAK expression by transiently transfecting NIH 3T3 and human breast carcinoma MCF7 cells and looked for centrosome amplification, aneuploidy and transformation. In both cell lines, centrosome amplification was noted along with growth of colonies in soft agar of cells exposed to low (0.5%) serum, but not those grown in regular (5%) serum containing media. It was suggested that growth in low serum might have activated some factor(s) that favored promiscuous activity of BTAK protein (Zhou et al., 1989). Moreover, the MCF7 cells grown under the same conditions expressed multiple centrosomes and exhibited aberrations in chromosome segregation and aneuploidy.

Centrosomes and Cancer. There is little doubt that chromosome imbalance (genomic instability) is a hallmark of nearly all solid cancers. Where centrosome imbalance and aneuploidy occur concomitantly, in the same tumors, a history of mitotic error and faulty chromosome segregation caused by multipolar spindles can be surmised; but what about cell division in the growing tumor itself? Since supernumerary centrosomes persist in tumor cells, one wonders how cell division continues to occur efficiently, as it apparently does in most tumors. In our studies, mitotic spindle aberrations and multipolar spindles are rarely seen in established breast tumors in rats (unpublished observations).

To account for this finding, we predict a two-stage process where centrosome amplification initiates before, or at a very early, perhaps premalignant, stage of cell transformation followed by clonal selection of viable tumor progenitor cells. Spindle aberrations and resulting mitotic chaos caused by supernumerary centrosomes is likely confined to early stages of carcinogenesis, leading to catastrophic loss or gain of chromosomes. Therefore, most of the early progeny of cells with dysfunctional spindles fail to survive and are removed by apoptosis, leaving an occasional progenitor, with just the right combination of chromosomes and oncogenes to transform into a tumor via natural selection. Surprisingly, in the selection process, fully transformed cells continue to proliferate supernumerary centrosomes with enhanced MTOC capacity (Lingle et al., 1998). This raises the question of how mature tumor cells with multiple centrosomes assemble a functional, bipolar spindle. Apparently, a process occurring early in transformation selects for cells that form functional bipolar spindles even with a burden of a centrosome overload. How this is accomplished is not known. Either the

supernumerary centrosomes are physically clustered together as one to form spindle poles, or all but one pair of dominant centrosomes is inactivated in each mitotic cell. Evidence for clustering is reported in electron microscopic studies of mouse neuroblastoma cells that possess large numbers of centrioles and MTOCs (Brinkley et al., 1981; Sharp et al., 1982; Ring et al., 1982) but manages to cluster them into two functional spindle poles during mitosis (Ring et al., 1982). Still, very little is known about how cells divide correctly with an enhanced complement of centrosomes or how such burden impacts cell shape and polarity. Obviously, additional knowledge about this and other aspects of centrosome biology will likely prove useful in understanding the intricacies of cell transformation to malignancy. It is humbling to note that Boveri came to the same conclusion a century ago without the benefits of antibodies, confocal microscopy or molecular biology. Hopefully, the new findings will lead to the discovery of additional genetic targets and improvements in therapeutic and diagnostic strategies for cancer in the next century.

TABLE 1
CENTROSOME RELATED CATALYTICAL PROTEINS

protein	organism	function	reference
1. serine-threonine-kinases			
- Cdc2 kinase	human	phosphorylates HsEg5, which regulates association of HsEg5 with mitotic spindle	(Lane and Nigg, 1996), (Pockwinse et al., 1997)
- p34cdc2 protein kinase	mammals, S.cerevisiae	phosphorylation of HsEg5	(Blangy et al., 1997) (Sherr, 1994)
- MPS1	S.cerevisiae	spindle pole body duplication and cell cycle control	(Lauze et al., 1995) (Weiss and Winey, 1996)
- LK6	Drosophila embryo	regulation of microtubule function	(Kidd and Raff, 1997)
polo-like kinases			
- polo, Plk1, Cdc5p, plo1+, Plx1	Drosophila / mammals/ S..cerevisiae/ S. pombe/ Xenopus	maturation of centrosomes, establishment of bipolar spindle	(Lane and Nigg, 1996) (Lee et al., 1998) (Wolf et al., 1997)
aurora subfamily:			
- aurora	Drosophila	centrosome separation and formation of bipolar spindle	(Glover et al., 1995)
- aurora 1 and aurora2	human	aurora2:centrosome-associated protein, potential oncogene	(Bischoff et al., 1998)
- Ayk1	mammals	mitotic cell: chromosome segregation	(Yanai et al., 1997)
- Aik	human	possibly involved in chromosome segregation or spindle formation	(Kimura et al., 1997)
- STK15 (BTAK)	human	centrosome amplification, aneuploidy, cell transformation	(Zhou et al., 1998)
- IAK1	S. cerevisiae, mammals,	regulator of chromosome segregation	(Gopalan et al., 1997)
- Ipl1	S. cerevisiae	chromosome segregation	(Francisco and Chan, 1994)
- pEG2	Xenopus	assembly of bipolar mitotic spindles	(Roghi et al., 1998)
NIMA family			
- Nek2	mammals	relates to centrosome cycle	(Fry et al., 1998)
		plays together with C-Nap1a role in centriole-centriole cohesion during cell-cycle	(Fry et al., 1998)
other kinases			
- casein kinase I (CSKI), HRR25	eukaryotic cells, S.cerevisiae	stability of specific microtubule arrays role in segregation of chromosomes	(Brockman et al., 1992)

- cAMP-dependent kinase II	human	phosphorylates centrosomal proteins, use same substrates as p34cdc2	(Keryer et al., 1993) (Keryer et al., 1995)
src family kinases - Fyn	T-lymphocytes	co-localize with mitotic spindle and poles, possibly functions at the M-phase in mitotic cells	(Ley et al., 1994)
2. Calcium-binding proteins			
- Ca2+/calmodulin-dependent kinase	hemopoietic cells	phophorylates several centrosomal proteins e.g., centrin	(Pietromonaco et al., 1995) (Espreafico et al., 1998)
- centrin, Cdc 31	vertebrate/ yeast/ algae	duplication of centrosomes	(Salisbury, 1995)
3. phosphoprotein			
- Spc110 (Nuf1), Spc110 related	S.cerevisiae, vertebrates	structural component of SPB that is phosphorylated during spindle formation and dephosphorylated as cells enter anaphase	(Friedman et al., 1996) (Tassin et al., 1997)
- γ-tubulin	A. nidulans, Drosophila, Xenopus, invertebrates and vertebrates	centrosomal form: MT nucleation, required for structural integrity of the centrosome	(Oakley and Oakley, 1989) (Vogel et al., 1997) (Stearns et al., 1991) (Moudjou et al., 1996)
4. phosphatases			
- PP-1 proteinphosphatase-1	mammals	PP-1 alpha is localized to centrosome, possible role in regulating anaphase	(Andreassen et al., 1998) (Francisco et al., 1994)
5. kinesin-like protein			
- pavarotti (PAV-KLP), MKLP	Drosophila / mammals	establishes the structure of the telophase spindle and mobilizes mitotic regulator proteins	(Adams et al., 1998) (Nislow et al., 1992)
-ZEN-4	C. elegans	essential for cytokinesis	(Raich et al., 1998)
- Xklp2	Xenopus	centrosome separation during mitosis and maintenance of spindle bipolarity	(Boleti et al., 1996)
- BimC, HsEg5	Aspergillus nidulans/ human	spindle dynamics, centrosome separation	(Enos and Morris, 1990) (Karsenti, 1991) (Whitehead and Rattner, 1998)
6. tumor suppressor p53	mouse, human	regulator of centrosome function	(Blair Zajdel and Blair, 1988) (Fukasawa et al., 1996) (Winey, 1996)
7. 14-3-3 protein	human	play a role in signaling pathways regulating centrosome function and/or duplication	(Pietromonaco et al., 1996)

Acknowledgement

The authors would like to thank I. Ouspenski and M. Mancini for discussions and critical reading of the manuscript in draft form and Betty Ledlie for proof reading and secretari al assistance. We are also grateful for helpful discussions with L. Zhong, R.Palazzo, C. Rieder, A. Khodjakov, J. Rosen, D. Medina and S. Sen. The authors were supported by grants from NCI CA-64255 and CA-41424 to D. Medina andBRB, and from the Department of the Army, DAMD17-94-J-4253 to Jeffrey Rosen and BRB.

References

Adams, R. R., Tavares, A. A., Salzberg, A., Bellen, H. J., and Glover, D. M. (1998): pavarotti encodes a kinesin-like protein required to organize the central spindle and contractile ring for cytokinesis. Genes Dev. 12 (10):1483-94.

Andreassen, P. R., Lacroix, F. B., Villa-Moruzzi, E., and Margolis, R. L. (1998): Differential subcellular localization of protein phosphatase-1 alpha, gamma1, and delta isoforms during both interphase and mitosis in mammalian cells. J. Cell Biol. 141 (5):1207-15.

Balczon, R., Bao, L., Zimmer, W. E., Brown, K., Zinkowski, R. P., and Brinkley, B. R. (1995): Dissociation of centrosome replication events from cycles of DNA synthesis and mitotic division in hydroxyurea-arrested Chinese hamster ovary cells. J. Cell Biol. 130 (1):105-15.

Balczon, R., and West, K. (1991): The identification of mammalian centrosomal antigens using human autoimmune anticentrosome antisera. Cell Motil. Cytoskeleton. 20 (2):121-35.

Bischoff, J. R., Anderson, L., Zhu, Y., Mossie, K., Ng, L., Souza, B., Schryver, B., Flanagan, P., Clairvoyant, F., Ginther, C., Chan, C. S., Novotny, M., Slamon, D. J., and Plowman, G. D. (1998): A homologue of Drosophila aurora kinase is oncogenic and amplified in human colorectal cancers. Embo J. 17 (11):3052-65.

Blair Zajdel, M. E., and Blair, G. E. (1988): The intracellular distribution of the transformation-associated protein p53 in adenovirus-transformed rodent cells. Oncogene. 2 (6):579-84.

Blangy, A., Arnaud, L., and Nigg, E. A. (1997): Phosphorylation by p34cdc2 protein kinase regulates binding of the kinesin-related motor HsEg5 to the dynactin subunit p150. J. Biol. Chem. 272 (31):19418-24.

Boleti, H., Karsenti, E., and Vernos , I. (1996): Xklp2, a novel Xenopus centrosomal kinesin-like protein required for centrosome separation during mitosis. Cell. Jan12 (84 (1)):49-59.

Boveri, T. (1888): Zellen-Studien II. Die Befruchtung und Teilung des Eies von *Ascaris megalocephala*. Fischer, Jena.

Boveri, T. (1901): Zellenstudien IV. Ueber die Natur der Centrosomen. Fischer, Jena.

Boveri, T. (1914): Zur Frage der Entstehung maligner Tumoren. Fischer Verlag, Jena, Germany.

Brinkley, B. R. (1985): Microtubule organizing centers. Ann. Rev. Cell Biol. 1:145-72.

Brinkley, B. R., Cox, S. M., Pepper, D. A., Wible, L., Brenner, S. L., and Pardue, R. L. (1981): Tubulin assembly sites and the organization of cytoplasmic microtubules in cultured mammalian cells. J. Cell Biol. 90 (3):554-62.

Brockman, J. L., Gross, S. D., Sussman, M. R., and Anderson, R. A. (1992): Cell cycle-dependent localization of casein kinase I to mitotic spindles. Proc. Natl. Acad. Sci. U S A. 89 (20):9454-8.

Brown, C. R., Doxsey, S. J., White, E., and Welch, W. J. (1994): Both viral (adenovirus E1B) and cellular (hsp 70, p53) components interact with centrosomes. J. Cell Physiol. 160 (1):47-60.

Donehower, L.A., Harvey, M., Slagle, B.L., McArthur, M.J., Montgomery, C.A., Jr., Butel, J.S., and Bradley, A. (1992): Mice deficient for p53 are developmentally normal but susceptible to spontaneous tumors. Nature. 356(6366):215-221.

Enos, A. P., and Morris, N. R. (1990): Mutation of a gene that encodes a kinesin-like protein blocks nuclear division in A. nidulans. Cell. 60 (6):1019-27.

Espreafico, E. M., Coling, D. E., Tsakraklides, V., Krogh, K., Wolenski, J. S., Kalinec, G., and Kachar, B. (1998): Localization of myosin-V in the centrosome. Proc. Natl. Acad. Sci. U S A. 95 (15):8636-41.

Francisco, L., and Chan, C. S. (1994): Regulation of yeast chromosome segregation by Ipl1 protein kinase and type 1 protein phosphatase. Cell Mol. Biol. Res. 40 (3):207-13.

Francisco, L., Wang, W., and Chan, C. S. (1994): Type 1 protein phosphatase acts in opposition to IpL1 protein kinase in regulating yeast chromosome segregation. Mol. Cell Biol. 14 (7):4731-40.

Friedman, D. B., Sundberg, H. A., Huang, E. Y., and Davis, T. N. (1996): The 110-kD spindle pole body component of Saccharomyces cerevisiae is a phosphoprotein that is modified in a cell cycle-dependent manner. J. Cell Biol. 132 (5):903-14.

Fry, A. M., Mayor, T., Meraldi, P., Stierhof, Y. D., Tanaka, K., and Nigg, E. A. (1998): C-Nap1, a novel centrosomal coiled-coil protein and candidate substrate of the cell cycle-regulated protein kinase Nek2. J. Cell Biol. 141 (7):1563-74.

Fry, A. M., Meraldi, P., and Nigg, E. A. (1998): A centrosomal function for the human Nek2 protein kinase, a member of the NIMA family of cell cycle regulators. Embo J. 17 (2):470-81.

Fukasawa, K., Choi, T., Kuriyama, R., Rulong, S., and Vande Woude, G. F. (1996): Abnormal centrosome amplification in the absence of p53. Science. 271 (5256):1744-7.

Fukasawa, K., Wiener, F., Vande Woude, G. F., and Mai, S. (1997): Genomic instability and apoptosis are frequent in p53 deficient young mice. Oncogene. 15 (11):1295-302.

Glover, D. M., Leibowitz, M. H., McLean, D. A., and Parry, H. (1995): Mutations in aurora prevent centrosome separation leading to the formation of monopolar spindles. Cell. 81 (1):95-105.

Gopalan, G., Chan, C. S., and Donovan, P. J. (1997): A novel mammalian, mitotic spindle-associated kinase is related to yeast and fly chromosome segregation regulators. J. Cell Biol. 138 (3):643-56.

Karsenti, E. (1991): Mitotic spindle morphogenesis in animal cells. Semin Cell Biol. 2 (4):251-60.

Karsenti, E., Kobayashi, S., Mitchison, T., and Kirschner, M. (1984): Role of the centrosome in organizing the interphase microtubule array: properties of cytoplasts containing or lacking centrosomes. J. Cell Biol. 98 (5):1763-76.

Keryer, G., Celati, C., and Klotz, C. (1995): In isolated human centrosomes, the associated kinases phosphorylate a specific subset of centrosomal proteins. Biol. Cell. 84 (3):155-65.

Keryer, G., Rios, R. M., Landmark, B. F., Skalhegg, B., Lohmann, S. M., and Bornens, M. (1993): A high-affinity binding protein for the regulatory subunit of cAMP-dependent protein kinase II in the centrosome of human cells. Exp. Cell Res. 204 (2):230-40.

Kidd, D., and Raff, J. W. (1997): LK6, a short lived protein kinase in Drosophila that can associate with microtubules and centrosomes. J. Cell Sci. 110 (Pt 2):209-19.

Kimura, M., Kotani, S., Hattori, T., Sumi, N., Yoshioka, T., Todokoro, K., and Okano, Y. (1997): Cell cycle-dependent expression and spindle pole localization of a novel human protein kinase, Aik, related to Aurora of Drosophila and yeast Ipl1. J. Biol. Chem. 272 (21):13766-71.

Lane, H. A., and Nigg, E. A. (1996): Antibody microinjection reveals an essential role for human polo-like kinase 1 (Plk1) in the functional maturation of mitotic centrosomes. J. Cell Biol. 135 (6 Pt 2):1701-13.

Lauze, E., Stoelcker, B., Luca, F. C., Weiss, E., Schutz, A. R., and Winey, M. (1995): Yeast spindle pole body duplication gene MPS1 encodes an essential dual specificity protein kinase. Embo J. 14 (8):1655-63.

Lee, K. S., Grenfell, T. Z., Yarm, F. R., and Erikson, R. L. (1998): Mutation of the polo-box disrupts localization and mitotic functions of the mammalian polo kinase Plk [In Process Citation]. Proc. Natl. Acad. Sci. U S A. 95 (16):9301-6.

Ley, S. C., Marsh, M., Bebbington, C. R., Proudfoot, K., and Jordan, P. (1994): Distinct intracellular localization of Lck and Fyn protein tyrosine kinases in human T lymphocytes. J. Cell Biol. 125 (3):639-49.

Lingle, W. L., Lutz, W. H., Ingle, J. N., Maihle, N. J., and Salisbury, J. L. (1998): Centrosome hypertrophy in human breast tumors: implications for genomic stability and cell polarity. Proc. Natl. Acad. Sci. U S A. 95 (6):2950-5.

Moritz, M., Braunfeld, J., Sedat, J.W., Alberts, B.M., and Agard, D.A. (1995). Nature. 378:638-640.

Moudjou, M., Bordes, N., Paintrand, M., and Bornens, M. (1996): Gamma-Tubulin in mammalian cells: the centrosomal and the cytosolic forms. J. Cell Sci. 109 (Pt 4):875-87.

Nislow, C., Lombillo, V. A., Kuriyama, R., and McIntosh, J. R. (1992): A plus-end-directed motor enzyme that moves antiparallel microtubules in vitro localizes to the interzone of mitotic spindles [see comments]. Nature. 359 (6395):543-7.

Oakley, C. E., and Oakley, B. R. (1989): Identification of gamma-tubulin, a new member of the tubulin superfamily encoded by mipA gene of Aspergillus nidulans. Nature. 338 (6217):662-4.

Pietromonaco, S. F., Seluja, G. A., Aitken, A., and Elias, L. (1996): Association of 14-3-3 proteins with centrosomes. Blood Cells Mol. Dis. 22 (3):225-37.

Pietromonaco, S. F., Seluja, G. A., and Elias, L. (1995): Identification of enzymatically active Ca2+/calmodulin-dependent protein kinase in centrosomes of hemopoietic cells. Blood Cells Mol. Dis. 21 (1):34-41.

Pihan, G. A., Purohit, A , Wallace, J., Knecht, H., Woda, B., Quesenberry, P.and Doxsey, S. J. (1998). Centrosome defects and genetic instability in malignant tumors. Cancer Res. 58:3974-3985.

Pockwinse, S. M., Krockmalnic, G., Doxsey, S. J., Nickerson, J., Lian, J. B., van Wijnen, A. J., Stein, J. L., Stein, G. S., and Penman, S. (1997): Cell cycle independent interaction of CDC2 with the centrosome, which is associated with the nuclear matrix-intermediate filament scaffold. Proc. Natl. Acad. Sci. U S A. 94 (7):3022-7.

Raff, J. W., and Glover, D. M. (1989): Centrosomes, and not nuclei, initiate pole cell formation in Drosophila embryos. Cell. 57 (4):611-9.

Raich, W. B. , Moran, A. N., Rothman, J. H. , and Hardin, J. (1998). Cytokinesis and midzone microtubule organization in caenorhabditis elegans require the kinesin-like protein ZEN-4. Mol Biol Cell 9(8):2037-2049.

Ring, D., Hubble, R., and Kirschner, M. (1982): Mitosis in a cell with multiple centrioles. J. Cell Biol. 94 (3):549-56.

Roghi, C., Giet, R., Uzbekov, R., Morin, N., Chartrain, I., Le Guellec, R., Couturier, A., Doree, M., Philippe, M., and Prigent, C. (1998): The Xenopus protein kinase pEg2 associates with the centrosome in a cell cycle-dependent manner, binds to the spindle microtubules and is involved in bipolar mitotic spindle assembly. J. Cell Sci. 111 (Pt 5):557-72.

Salisbury, J. L. (1995): Centrin, centrosomes, and mitotic spindle poles. Curr. Opin. Cell Biol. 7 (1):39-45.

Schnackenberg, B. J., Khodjakov, A., Rieder, C. L., and Palazzo, R. E. (1998): The disassembly and reassembly of functional centrosomes in vitro. Proc. Natl. Acad. Sci. U S A. 95 (16):9295-9300.

Sen, Subrata, Zhou, H., and White, R.A.. (1997): A putative serine/threonine kinase encoding gene BTAK on chromosome 20q13 is amplified and overexpressed in human breast cancer cell lines. Oncogene. 14:2195-2200.

Sharp, G. A., Weber, K., and Osborn, M. (1982): Centriole number and process formation in established neuroblastoma cells and primary dorsal root ganglion neurones. Eur. J. Cell Biol. 29 (1):97-103.

Sherr, C. J. (1994): G1 phase progression: cycling on cue [see comments]. Cell. 79 (4):551-5.

Simerly, C., Wu, G. J., Zoran, S., Ord, T., Rawlins, R., Jones, J., Navara, C., Gerrity, M., Rinehart, J., and Binor, Z. (1995): The paternal inheritance of the centrosome, the cell's microtubule- organizing center, in humans, and the implications for infertility [see comments] [published erratum appears in Nat Med 1995 Jun;1(6):599]. Nat Med. 1 (1):47-52.

Sluder, G., and Rieder, C. L. (1996): Controls for centrosome reproduction in animal cells: issues and recent observations. Cell Motil. Cytoskeleton. 33 (1):1-5.

Stearns, T., Evans, L., and Kirschner, M. (1991): Gamma-tubulin is a highly conserved component of the centrosome. Cell. 65 (5):825-36.

Tassin, A. M., Celati, C., Paintrand, M., and Bornens, M. (1997): Identification of an Spc110p-related protein in vertebrates. J. Cell Sci. 110 (Pt 20):2533-45.

Vandre, D. D., and Borisy, G. G. (1989): The centrosome cycle in animal cells: In Hyams, J.S. and Brinkley, B.R. (eds.):"Mitosis: Molecules and Mechanisms." San Diego, CA: Academic Press, pp. 39-75.

Vogel, J. M., Stearns, T., Rieder, C. L., and Palazzo, R. E. (1997): Centrosomes isolated from Spisula solidissima oocytes contain rings and an unusual stoichiometric ratio of alpha/beta tubulin. J. Cell Biol. 137 (1):193-202.

Wang, X.-J., Greenhalgh, D. A., Jiang, A., He, D., Zhong, L., Medina, D., Brinkley, B. R., and Roop, D. R. (1998): Expression of a p53 mutant in the epidermis of transgenic mice accelerates chemical carcinogenesis. Oncogene. 17 (1):35-45.

Weiss, E., and Winey, M. (1996): The Saccharomyces cerevisiae spindle pole body duplication gene MPS1 is part of a mitotic checkpoint. J. Cell Biol. 132 (1-2):111-23.

Whitehead, C. M., and Rattner, J. B. (1998): Expanding the role of HsEg5 within the mitotic and post-mitotic phases of the cell cycle. J Cell Sci. 111 (Pt 17):2551-61.

Winey, M. (1996): Keeping the centrosome cycle on track. Genome stability. Curr. Biol. 6 (8):962-4.

Wolf, G., Elez, R., Doermer, A., Holtrich, U., Ackermann, H., Stutte, H. J., Altmannsberger, H. M., Rubsamen-Waigmann, H., and Strebhardt, K. (1997): Prognostic significance of polo-like kinase (PLK) expression in non-small lung cancer. Oncogene. 14 543-549.

Yanai, A., Arama, E., Kilfin, G., and Motro, B. (1997): ayk1, a novel mammalian gene related to Drosophila aurora centrosome separation kinase, is specifically expressed during meiosis. Oncogene. 14 (24):2943-50.

Zhou, H., Kuang, J., Zhong, L., Kuo, W.-L., Gray, J. W., Sahin, A., Brinkley, B. R., and Sen, S. (1998): Tumour amplified mitotic kinase STK15/BTAK induces centrosome amplification, aneuploidy and transformation. Nature Genetics, in press.

MOLECULAR MARKERS FOR BREAST CANCER SUSCEPTIBILITY

Dr. Jeffrey M. Rosen, Deana Roy, Alejandro Contreras, Dr. Dacheng He, Ling Zhong and Dr. William (B.R.) Brinkley

Baylor College of Medicine, Department of Cell Biology
One Baylor Plaza, Houston, TX 77030

A woman's reproductive history is one of the principal determinants of her susceptibility to breast cancer. An early full-term pregnancy is protective and the length of time between menarche and the first full term-pregnancy appears to be critical for the initiation of breast cancer. This research is based upon the hypothesis that the protective effects of an early pregnancy and lactation result from estrogen (E) and progesterone (P)-induced differentiation and the resultant loss of cells susceptible to carcinogenesis. These effects of E and P are mediated by the induction of growth factors that act via autocrine and paracrine mechanisms to influence terminal end bud (TEB) growth and differentiation. The rapidly proliferating cells of the TEB are the most susceptible to neoplastic transformation. When these studies were initiated no molecular markers were available to identify and follow the fate of these susceptible cells, yet this information is required to develop effective diagnostic tools and preventive therapies for breast cancer. Thus, the initial objective of this grant was to identify molecular markers for TEBs in order to follow their fate during mammary development and carcinogenesis. In addition, we proposed to define the topology and compare the cell cycles of susceptible and refractory cells, to identify local mediators of E- and P-treatment in the TEB and surrounding stroma, and to characterize the changes in their expression patterns.

Differential Display PCR (DD-PCR) was used to identify candidate molecular markers of TEB, as well as, factors which may be important for virgin mammary gland development. Thus far, 14 clones isolated from the TEB DD-PCR fraction have been sequenced. RNA expression levels of EDD-C3, C6, C11, C14, C15, C18, G5, G6 and G7 were analyzed by RT-PCR in an attempt to identify clones which are expressed predominantly in the TEB RNA. Four clones; EDD-G5, G6, G7 and C18 were more highly expressed in the TEB RNA. One of these DD-PCR cDNAs, EDD-G5, which was originally identified as an

Keywords: Terminal End Bud, Differential Display PCR, Confocal Microscopy, Cell Cycle, Nuclear Matrix Proteins

This work was supported by the U. S. Army Medical Research and Materiel Command under DAMD17-94-J-4253.

Expressed Sequence Tag (EST), has recently been found to be related to a novel mammalian LDL family member termed LR11. EDD-C2 is the rat homologue of human p190-B which is a Rho GTPase Activating Protein (GAP). p190-B and Rho are induced to cluster after integrin cross-linking. Thus, p190-B may be involved in an integrin-mediated signal transduction pathway important for ductal morphogenesis. EDD-C12 is rat adrenomedullin, a secreted peptide factor that is expressed in a variety of tissues (lung, heart, kidney, brain and mammary gland) and is a potent vasodilator. A polyclonal antiserum has been used to determine the temporal and spatial expression of adrenomedullin in the mammary gland by immunohistochemistry. Adrenomedullin was localized to the cytoplasm of epithelial and stromal cells of the virgin gland. Staining was most prominent in TEB and ductal epithelium. However, staining was also detected in the alveolar buds (AB), stroma, blood vessels and lymph node. The physiological significance of this localized expression of adrenomedullin is currently under study in our laboratory.

An alternative approach to isolating TEB-specific markers has been to analyze the nuclear matrix protein components of terminal end buds (TEB) and AB in control rat mammary glands and in tumors induced with the chemical carcinogen, MNU. TEB and mid-gland regions were dissected and each fraction was digested to separate the stromal cells from the AB and TEB. The analysis of nuclear matrix proteins by 2-D gel electrophoresis has revealed several proteins detected only in the TEB and not in the AB or stromal fractions. One of these was also expressed in the tumors suggesting that the tumors may have arisen from the TEB. These studies have validated the approach of using microdissection, DD-PCR and 2D-gel analysis of nuclear matrix proteins to identify genes expressed preferentially in the mammary TEB and TD.

An analysis of cell cycle kinetics was carried out on frozen sections of 50 μm thickness triply stained with anti-BrdU, anti-cytokeratin 14 and the DNA dye propidium iodide visualized by confocal microscopy. The growth fraction of the cells in TEB of 45 day old rat mammary tissue was three times higher than in alveolar buds (AB). The labeling index and duration of S phase were comparable to that reported previously on paraffin sections. Studies in our laboratory have also demonstrated that the TEB is a dynamic structure regulated by a balance of proliferation and apoptosis, and that apoptosis in the TEB plays a major role in ductal morphogenesis during murine mammary gland development (Humphreys, et al., Development 122:4013-4022, 1996). Apoptosis was very low in the highly proliferative cap cell layer and in regions of active proliferation within the TEB. Based upon studies performed in transgenic and knockout mouse models, a functional role for Bcl-2 family members, but not for p53, in regulating endbud apoptosis was demonstrated. These studies have demonstrated that the TEB is a dynamic structure exhibiting the highest levels of proliferation and apoptosis observed to date during normal mammary gland development.

The regulation of the Wnt and Fgf growth factor families by steroid hormones appears to play an important role in mammary tumorigenesis and breast cancer. We have studied steroid hormone regulation of Wnt gene expression in intact and progesterone-receptor knockout (PRKO) mice. Wnt-2 gene expression is maximal in the mammary stroma of 4-6 week old mice and is repressed by estrogen, while Wnt-5b is expressed in lobuloalveolar cells and is dependent upon the presence of intact PR in the epithelium. These local growth factors may provide a more sensitive marker than mammary gland morphology assessed solely by histological methods in order to study the protective effects of low doses of steroid hormones in mammary carcinogenesis.

Differential expression of p190-B during mammary gland development, involution and carcinogenesis. Chakravarty, G., Roy, D., Zhong, L., Rosen , J.M. Baylor College of Medicine, Department of Cell Biology,One Baylor Plaza, Houston, TX 77030

Ductal morphogenesis in virgin mammary gland occurs when a highly proliferative structure called the Terminal End Bud (TEB) penetrates the fat pad. Studies of carcinogen induced tumor formation in rats have suggested that these cells are targets for neoplastic transformation. In an attempt to characterize genes that are differentially expressed in TEBs in the virgin mammary gland, differential display -PCR (DD-PCR) was performed on RNA isolated from TEB, mid gland and stromal tissue fractions from nulliparous Wistar-Furth rats. Differentially expressed transcripts were cloned and analysed. Interestingly, one of the clones had 87% homology to p190-B, a new member of the Rho-GAP family of proteins. We demonstrate here that although p190-B is expressed in both TEBs and alveolar buds, its transcription is downregulated during late pregnancy and involution. It is expressed in a variety of mammary tumors and its overexpression correlates with more aggressive tumor phenotype. In addition, confocal analysis of the virgin mammary gland revealed nuclear localization of the protein. Our results suggest that p190-B may be under estrogenic regulation during virgin mammary gland development and may contribute to the tumorigenic phenotype by alteration in this regulation or through co-operative interaction with other ras signal transducing proteins.

This work was supported by the U.S. Army Medical Research and Materiel Command under DAMD17-94-J-4253.

Table 1

Clone	Primers	Size (b.p.)	Identity
EDD-G5	AP-7, T1 1-G	257	LR11 Low Density Lipoprotein Receptor; 90%
EDD-G6	AP-2, T1 1-G	183	
EDD-G7	AP-2, T1 1-G	230	
EDD-C2	AP-7, T1 1-C	241	p190B Rho GAP; 87%
EDD-C3	AP-7, T1 1-C	204	yy55h09.s1; cDNA clone 277505; human ovary; 80%
EDD-C6	AP-1, T1 1-C	122	yf99a06.r1; cDNA clone 30458; human infant brain; 81%
EDD-C11	AP-8, T1 1-C	92	Calcium Binding Protein Cab45; 86%
EDD-C12	AP-8, T1 1-C	108	Adrenomedullin; 100%
EDD-C13	AP-8, T1 1-C	125	
EDD-C14	AP-8, T1 1-C	132	yn84b02.s1; cDNA clone 175083; human adult brain; 78%
EDD-C15	AP-8, T1 1-C	145	yw25b09.s1; cDNA clone 253241; human fetal cochlea; 91%
EDD-C16	AP-8, T1 1-C	151	rat mitochondrial rRNA; 98%
EDD-C17	AP-8, T1 1-C	181	rat cytochrome C oxidase; 99%
EDD-C18	AP-8, T1 1-C	422	